Electrotactile Feedback for Sensory Restoration: Modelling and Application

Kairu Li

School of Computing

University of Portsmouth

The thesis is submitted for the degree of
Doctor of Philosophy

September 2018

Whilst registered as a candidate for the above degree, I have not been registered for any other research award. The results and conclusions embodied in this thesis are the work of the named candidate and have not been submitted for any other academic award.

Dedicated to my parents, Ping and Lihua.

Acknowledgements

Foremost, I would like to express my sincere gratitude to my supervisors, Prof. Honghai Liu and Dr. JiaCheng Tan, for their continual guidance and support. During working with them for the last three years, I have learnt a lot, which I believe will benefit my future career and life. A special thanks to my first supervisor, Prof. Honghai Liu, who always believes in me, encourages me and gives me the moral support during the tough time. I would also like to thank Dr. Yinfeng Fang and Dr. Zhaojie Ju for their valuable advice, discussions and care.

My sincere and warm thanks go to all the members of the Intelligent Systems and Biomedical Robotics Group, for sharing knowledge, participating in my experiments and especially all the happy time we spent together. Your kindness and friendship give me a lot of strength.

Lastly, my heartfelt thanks go to my loving parents for their love and support all the time.

Abstract

An ideal upper-extremity prosthesis is expected to simultaneously decode users' intentions and deliver artificial somatosensory feedback. Among all the feasible feedback modalities, electrotactile stimulation remains the most promising solution due to its advantages of light weight, little noise and low power consumption. This thesis further enhances the existing electrotactile feedback strategies by proposing a haptics model, developing a portable electrotactile stimulation (ETS) system and establishing a virtual hand rehabilitation platform for implementation and evaluation.

Firstly, a Gaussian distribution based haptics model is proposed to characterise the human fingertip's biomechanics, including a prediction model to estimate the contact force according to the fingertip deformation and a probabilistic model to describe force uncertainty. Experiments results reveal the non-linearity, dispersion and individual difference of the fingertip's mechanical behaviour. Secondly, a potable 16-channel ETS system with a wireless mode for transmission is developed to provide electrotactile feedback for clinical use. The proposed ETS system can generate stable current output with programmable stimulation parameters, including amplitude, frequency and pulse width. The ETS output waveforms and stability were evaluated by capability tests. Thirdly, a virtual hand rehabilitation platform is established to investigate the effect of electrotactile feedback on user training of hand grasping tasks. The platform consists of a surface electromyography (sEMG) acquisition module, a virtual grasping environment, and an ETS module. Experiments were conducted to evaluate the impact of electrotactile feedback on a closed-loop grasping control in comparison with the visual feedback and no feedback. The quantitative results show that the integration of electrotactile feedback can

both reduce the duration of rehabilitation and improve the virtual grasping success rate in comparison with the no feedback condition while possessing a better practicality over visual feedback.

In summary, the proposed electrotactile feedback centred research is validated in facilitating the user training and improving the rehabilitation performance. Despite the initial motivation of this thesis driven by the upper-extremity prostheses, the verified success of electrical stimulation is not confined to the hand rehabilitation scenarios but potentially applicable to a wider spectrum of applications, such as biomedical engineering and virtual reality.

Contents

List of Figures

List of Tables

List of Abbreviations

AC Amplifying Circuit

BC Bridge Circuit

BM Bluetooth Module

CCSC Constant-Current Source Circuit

DAC Digital-to-Analogue Converter

DoaA Duration of an Attempt

DoF Degrees of Freedom

DoT Duration of Training

EEG Electroencephalography

EF Electrotactile Feedback

EMG Electromyography

ESM Electronic Switch Module

ESOM Electrical Stimulation Output Module

ETS Electrotactile Stimulation

FA Fast Adapting

FE Finite Element

FES Functional Electrical Stimulation

GMM Gaussian Mixture Model

GMR Gaussian Mixture Regression

GUI Graphical User Interface

LC Level Control

LED Light Emitting Diode

MCU Micro Controller Unit

MEMS Microelectromechanical System

MIS Minimally Invasive Surgery

MOSFET Metal-Oxide-Semiconductor Field-Effect Transistor

MRI Magnetic Resonant Imaging

NF None Feedback

NoA Number of Attempts

PDF Probability Density Function

PMF Probability Mass Function

PNS Peripheral Nervous System

PSM Power Supply Module

PVDF Polyvinylidene Fluoride

PWM Pulse Width Modulation

RMSE Root Mean Square Error

SA Slow Adapting

SC Switch Circuitry

SCI Spinal Cord Injury

sEMG Surface Electromyography

SR Success Rate

TENS Transcutaneous Electrical Nerve Stimulation

USART Universal Synchronous and Asynchronous Receiver-Transmitter

VF Visual Feedback

ZnO Zinc Oxide

Chapter 1

Introduction

1.1 Background

The human hand is a dexterous effector to accomplish a variety of daily tasks and a sophisticated sensing instrument to interact with the external environment. However, for people with amputation or congenital limb deficiency a large part of manipulation capability is lost. In this case, an upper-extremity prosthesis can be a substitute to restore the body appearance and hand capability.

An ideal hand prosthesis should provide satisfying functionality based on reliable decoding of the user's intentions and deliver tactile feedback in a natural manner. Most of the current prosthesis manufacturers focus on improving the mechanical structure to achieve dexterity and human-like appearance, while few of them provide efficient tactile feedback for better user experience and manipulation performance. It is reported that the unsatisfactory manipulation performance and the absence of tactile sensation feedback impedes the efficient use of prostheses. These deficiencies are also highlighted as the major factors resulting in the rejection from prosthesis users. In recent decades, studies about tactile sensation restoration have been boosted by advancements in sensor fabrication techniques. However, these research are not well implemented in current hand prostheses due to technical difficulties and the complicated nature of human sensory system. Thus, it is worthwhile devoting considerable effort in the research on tactile sensation restoration for clinical use.

1.2 Open Issues and Challenges

Sensing and reacting to the external world by hand is an instinctive and effortless task for physically capable individuals in daily life. However, it remains an ongoing challenge to restore similar abilities for users of hand prostheses. The realisation of artificial tactile sensation includes tactile sensing and tactile stimulation feedback. To restore the sense of touch for amputees in practice, the following issues and challenges need to be addressed.

- To mimic and restore a natural tactile sensation, it is essential to have a comprehensive and quantitative description of the human fingertip's mechanical behaviour related to tactile properties. However, most existing studies focus on investigating the neural reaction under the fingertip skin from a microscopically structural point of view. In addition, the experiments are only conducted under a small indentation depth of less than 2.5 mm (Kumar *et al.*, 2015)(Serina *et al.*, 1997), while the skin reaction under larger deformations which may occur in the context of hand manipulation is not taken into consideration. Thus, there is a lack of a theoretical model to quantitatively characterise the mechanism of human tactile perception.

- The sensory function of hand prostheses is not implemented as well as the development of their mechanical structure. Dominant commercial hand prostheses have successfully manufactured anthropomorphic prostheses with multiple degrees of freedom, which enable users to accomplish fundamental tasks in daily life. However, they are still unable to make users aware of the tactile information without continuous visual or auditory attention. Apart from the complexity of the human tactile sensing mechanism, the absence of wearable tactile stimulation devices is also an important factor that restricts the prosthesis development and rehabilitation performance.

- Existing studies about the effectiveness of tactile feedback on the performance of hand prostheses are still controversial. Most experiments concluded that the integration of tactile feedback improved the performance of prosthesis manipulation, while some others showing an improvement only in certain conditions

(Saunders & Vijayakumar, 2011) and users (Chatterjee *et al.*, 2008), or even little difference when compared with the non-feedback condition. Further research is needed to investigate how the tactile feedback affect the prosthesis performance and the rehabilitation process.

- A process of user training is necessary for amputees before they can master their prostheses in daily life. Traditional rehabilitation methods are usually time-consuming, tedious and unfriendly to individual differences. Thus, it is expected to have an interactive and enjoyable platform which can encourage the user's involvement and perceptive ability for a better rehabilitation performance.

1.3 Motivations and Objectives

The absence of tactile sensation leads to unreliable prosthetic manipulation performance and a high rejection rate of prosthetic hands from customers (Wijk & Carlsson, 2015)(Peerdeman *et al.*, 2011)(Østlie *et al.*, 2012), which not only substantially constrains hand prostheses from being commercially viable but also make amputees suffer from the loss of hand sensory functions.

There are more than 0.54 million people living in the U.S. and 2.26 million people in China with the loss of an upper limb (Ziegler-Graham *et al.*, 2008)(Chai *et al.*, 2014). The loss of a hand will inevitably deteriorate the quality of life and make an individual feel less capable and more dependent (Schofield *et al.*, 2014). It is a huge challenge for prosthetic hand replacement due to the complexity of rich sensing capabilities and dexterous functions, although the utilisation of an upper-extremity prosthesis can compensate a part of the lost functions. The mechanical structure of hand prosthesis has been gradually improved from body-powered hands to myoelectric hands, from simple hooks to anthropomorphic dexterous hands and soft robotic hands as shown in Fig. 1.1. However, the attention to the implementation of sensory feedback is still not enough, which limits the functionality and efficiency of dexterous hand prostheses (Wijk & Carlsson, 2015)(Peerdeman *et al.*, 2011)(Østlie *et al.*, 2012).

The research about prosthesis sensory functions has been expanding in recent years. Reports propose that amputees can benefit from the integration of tactile feedback with

(a) Body-powered prosthetic hand (Ottobock, 2018a)

(b) Hook hand (Ottobock, 2018b)

(c) Myoelectric prosthetic hand (Cordella *et al.*, 2016)

(d) Soft prosthetic hand (Zhao *et al.*, 2016)

Figure 1.1: Development of hand prostheses

prostheses in many aspects, such as improving manipulation performance and self-embodiment. In terms of manipulation performance, the integration is suggested to prevent slip (Silvera-Tawil *et al.*, 2015)(Girão *et al.*, 2013) and significantly increase the success rate of applying correct grasping forces (Witteveen *et al.*, 2014). Also, tactile feedback can help to alleviate phantom pain, muscle fatigue and enhance a sense of body ownership for prosthesis users (Wijk & Carlsson, 2015)(Dietrich *et al.*, 2012). As a result, the acceptance of hand prosthesis and rehabilitation may be promoted by the implementation of tactile feedback.

Therefore, the motivation for this research is to improve the user experience and functional performance of hand prostheses by providing tactile feedback during the rehabilitation process or for practical use.Among various tactile sensations, force is mostly selected as the feedback variable in closed-loop prosthesis systems. It critically influences the manipulation performance and cannot be directly observed by vision (Dosen *et al.*, 2016). Electrotactile feedback, as one of the dominant tactile feedback techniques, is adopted in this research to feed back the contact force due to its advantages such as the portable size and lower power consumption. Thus, the prosthesis users can estimate the contact force applied on their prosthetic hands according to the feedback of electrotactile stimulations acting on their residual body. This may improve the user's capability to undertake basic tasks like grasping or even sophisticated manipulation such as handicraft, playing an instrument, and so on.

On the basis of the motivation, this thesis aims to investigate how the integration of tactile feedback have effects on hand rehabilitation performance and efficiency. Fur-

ther studies, such as the haptics model establishment, development of the electrical stimulation system and the integration of electrotactile feedback with the hand rehabilitation platform are the main objectives of this thesis. A detailed description of each objective is presented as follows.

- To define and characterise tactile-related properties of the human fingertip to bridge the gap between the human's sensory capability and the artificial side.
- To develop a portable and parameter-adjustable electrotactile stimulation (ETS) system for the provision of tactile feedback.
- To establish a closed-loop rehabilitation platform, which will be the test platform to evaluate the effectiveness of electrotactile feedback.
- To evaluate the effectiveness of electrotactile feedback and investigate how it influences the hand rehabilitation performance.

1.4 Thesis Outline and Contributions

The structure of this thesis with a list of contributions is given as follows.

Chapter 2: Literature Review. In this chapter, the physiology of the human tactile sensing system is introduced. A review of existing literature about tactile sensing and stimulation techniques is provided, followed by an overview of major research topics in the context of tactile feedback for upper extremity prostheses.

Chapter 3: Probability-based Haptics Model. In this chapter, a haptics model is derived based on Gaussian distribution and non-linear regression models to characterise the biomechanics of the human fingertip. It is tested by practical data and a demonstration of the model establishment is also provided.

The contributions of this chapter are listed as follows:

- A novel probability-based haptics model is proposed to quantitatively characterise the human fingertip's biomechanical reaction to physical contact. The haptics model includes two parts: a force prediction model to estimate the most possible contact force according to the fingertip deformation and a probabilistic model based on Gaussian distribution to describe the force uncertainty.

- A dataset of the applied force corresponding to a wide range of the fingertip indentation depth is established by in vivo experiments. It is used to finalise the structure of the haptics model and evaluate its prediction performance.

Chapter 4: Development of the Electrotactile Stimulation System. In this chapter, the development of a multi-channel ETS system is presented with an introduction of the theoretical background, followed by illustrations of the system framework and the circuits of each component. Tests are conducted to evaluate the stimulator's output capability.

The contributions of this chapter are listed as follows:

- The multi-channel ETS system with adjustable parameters including amplitude, frequency, pulse width and channels is developed. Its potability allow it to be applicable to hand prostheses and rehabilitation platforms.
- The output capability of the ETS system, including the symmetrical/asymmetrical square wave outputs and the stability of current output, is evaluated by practical tests. Accordingly, effective measures are taken to improve the reliability and stability of the output signals.

Chapter 5: Evaluation of Electrotactile Feedback on a Virtual Hand Rehabilitation Platform. In this chapter, a virtual hand rehabilitation platform is established with the integration of the haptics model and the ETS system proposed in Chapter 3 and Chapter 4, respectively. The platform design and working principles are introduced. Then, experiments are conducted to investigate the impact of electrotactile feedback on the rehabilitation burden and performance, followed by a discussion of the results.

The contributions of this chapter are listed as follows:

- The virtual hand rehabilitation platform is developed by the integration of a surface electromyography (sEMG) acquisition module, a virtual grasping environment and the proposed ETS sysmtem, where a closed loop is formed. Thanks to the flexibility of virtual environment, the rehabilitation platform as an interactive and enjoyable therapeutic tool can be extended to a wide spectrum of hand function rehabilitation applications.

- Electrotactile feedback is implemented for grasping control on the virtual platform and compared with visual feedback and no feedback. Experiment results show that electrotactile feedback is effective to observably alleviate rehabilitation burden and improve the task success rate by comparing with no feedback. Despite that visual feedback shows a superior performance among three feedbacks, it is restricted to a laboratory environment for a non-perceptive nature. By contrast, electrotactile feedback is an applicable and promising feedback method, considering its feasibility in reality and the comparable performance with visual feedback.

Chapter 6: Conclusions and Future Work. In this chapter, a summary of this thesis with an overview of the future research topics in this area is provided.

Chapter 2

Literature Review

The study of sensory feedback attracts great interest across a wide range of research areas, such as robotics (Silvera-Tawil *et al.*, 2015)(Girão *et al.*, 2013)(Yousef *et al.*, 2011), biomedical engineering (Lucarotti *et al.*, 2013)(Tiwana *et al.*, 2012), and virtual reality. Among corresponding applications, the study of tactile restoration for hand prostheses has been gradually expanding in recent decades. This chapter provides an overview of related literature on tactile feedback for hand prostheses and corresponding technologies, which mainly include tactile sensing and stimulation feedback (Li *et al.*, 2017). The rest of this chapter is organised as follows. In Section 2.1, the physiology of human skin is presented. The dominant technologies of tactile sensing and stimulation are introduced in Section 2.2. A survey of tactile feedback to prostheses and particularly electrotactile feedback to users are respectively presented in Section 2.3 and Section 2.4, followed by a summary.

2.1 Physiology of Human Skin

The human skin is a somatosensory system that senses and reacts to external stimuli, such as mechanical stimulation, heat and pain. This section primarily focuses on the physiology of reactions to mechanical stimulation, corresponding to tactile sensations of force, shape, texture, stiffness, etc. For example, when an external contact force deforms the surface of a fingertip, it causes a strain distribution in the underlying soft tissues and subsequently stimulates mechanoreceptors, which are the sensory units

distributed in human skin to detect mechanical stimulations such as force, pressure and vibration. The activated mechanoreceptor generates a sequence of voltage pulses transmitting through neurons to the brain, where the information is processed. Thus, the awareness of tactile sensation for humans is accomplish by sensing and transmitting which are conducted by mechanoreceptors and the neural system, respectively.

There are four types of mechanoreceptors in the human glabrous skin: Merkel cells, Meissner corpuscles, Ruffini endings and Pacinian corpuscles. They are responsible for the detection of different stimulations. If classified by the adaptation rate, four types of mechanoreceptors can be categorised into two classes: fast adapting (FA) units and slow adapting (SA) units. If classified by the receptive fields, each class is divided into two groups: I and II. SA I and FA I receptors have a small receptive field with a sharp border, while SA II and FA II receptors have a large receptive field with a diffuse border, as shown in Fig. 2.1 (Aoyagi *et al.*, 2006)(Dargahi & Najarian, 2004).

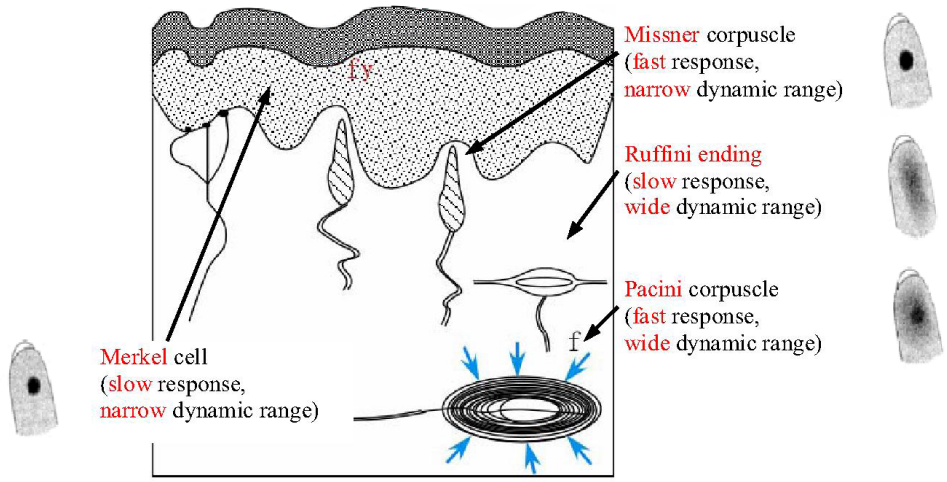

Figure 2.1: Four types of mechanoreceptors in human hands (Aoyagi *et al.*, 2006) and their receptive fields (Dargahi & Najarian, 2004)

Table 2.1 summarises the properties of the four types of mechanoreceptors with regards to the receptive speed, the receptive field and the perceptive function. In terms of the receptive speed, Meissner corpuscles and Pacinian corpuscles are mainly responsible for rapid or dynamic stimulation, while Merkel cells and Ruffini endings respond to sustained stimulation. Meissner corpuscles are sensitive to light touch, while Pacinian

corpuscles tend to detect deep pressure touch and high frequency vibration. Merkel cells are sensitive to low frequency vibration, while Ruffini endings usually respond to the stretching of the skin. In terms of the location and the receptive field, Meissner corpuscles and Merkel cells concentrate in the outer layer of the skin on fingertips and have small receptive fields. Conversely, Pacinian corpuscles and Ruffini endings are distributed more uniformly in deep layers of the skin on fingers and the palm. In terms of the function of perception, Merkel cells and Pacinian corpuscles can detect the sensation of stiffness. Merkel cells and Ruffini endings could detect slip and shape due to their response to steady pressure and skin stretch. Besides, Meissner corpuscles and Pacinian corpuscles contribute to the perception of texture, such as surface roughness, because they are sensitive to rapid vibration which is too small to activate the other two types of mechanoreceptors (Dargahi & Najarian, 2004). Additionally, the spatial resolution is the smallest distance for a person to distinguish two-point touch and this varies across the body. It is as close as 0.5 mm on fingertips while 7 mm on the palm.

The human skin can be an ideal model for artificial tactile sensors given its good performance of tactile sensing. Consequently, artificial sensors are expected to demonstrate small resolution, high sensitivity, low hysteresis, fast and linear response, wide dynamic range and high reliability. A spatial resolution of 5-40 mm could be high enough in practice. Typically, 20-60 Hz would be fine for the sampling rate in common tasks, while for special tasks, such as texture recognition, a higher sampling rate approximately 1-2.5 kHz is necessary (Silvera-Tawil *et al.*, 2015). A force sensitivity range of 0.3-10 N is required. For human-like skin or sensors, robust, flexible, stretchable and soft materials are desired to be embedded on various 3D structures. Additionally, low cost, low power consumption and scalability are also important for manufacture and implementation.

2.2 Technologies for Tactile Feedback

2.2.1 Tactile Sensing

Tactile sensing, based on different transduction techniques, aims to detect and measure a given property of an object through contact (Lee & Nicholls, 1999). This is usually

Table 2.1: Properties of four types of mechanoreceptors in human skin (summarized from (Silvera-Tawil *et al.*, 2015)(Dahiya *et al.*, 2010)(Lucarotti *et al.*, 2013)(Dargahi & Najarian, 2004))

	Meissner corpuscles	Pacinian corpuscles	Merkel cells	Ruffini endings
Classification	FA I	FA II	SA I	SA II
Adaptation rate	Fast	Fast	Slow	Slow
Receptive field	Small and sharp	Large and diffuse	Small and sharp	Large and diffuse
Density (units/cm^2)	140	20	70	10
Spatial resolution (mm)	3-4	10+	0.5	7+
Stimuli frequency (Hz)	5-50	40-500+	0.4-40	<7
Sensory function	High frequency vibration detection. Temporal changes in skin deformation.	High frequency vibration detection; Temporal changes in skin deformation. Tool use.	Low frequency vibration detection (static force); Pattern/form detection; Texture perception; Tactile flow perception.	Low frequency vibration detection (static force); Finger position; Stable grasp; Tangential force/ skin stretch.

conducted by tactile sensors attached on fingertips or palms of prosthetic hands, such as force sensors or artificial skin covering the whole hand.

As the first step in the restoration of tactile sensation, the increasing demand for tactile feedback inspires the exploration of transduction techniques (Harmon, 1980)(Lee, 2000)(Tiwana *et al.*, 2012) and their applications in various systems, such as upper limb prostheses (Osborn *et al.*, 2014)(Cranny *et al.*, 2005), virtual reality systems (Wang *et al.*, 2006)(Dede *et al.*, 2009), remote operation in dangerous environments (Gupta & O'Malley, 2006), minimally invasive surgery (MIS) (Payandeh & Li, 2003), nanometerscale operations (Rubio-Sierra *et al.*, 2003)(Jobin *et al.*, 2005), surgical training (Coles *et al.*, 2011), touch screens (Kim *et al.*, 2011) and robotic hands (Romano *et al.*, 2011)(Yousef *et al.*, 2011)(Ulmen & Cutkosky, 2010). The study of tactile sensing in upper limb prostheses is not as mature as that in other fields, but their achievements could be adopted into this field. Given that grasping is one of the major functions of hands, most studies of prosthesis tactile sensing focus on grasp force or pressure to prevent slip and achieve a stable grasp. The measured characteristics of touch, however, can be not only force and pressure but also stiffness, texture or shape. Thus, different transduction techniques are desired to be synthesized to realize a human-like tactile sensing system. This section presents available tactile sensing techniques which have potential to be applied in hand prostheses, namely, resistive sensors (strain gauges and piezoresistors), capacitive sensors, piezoelectric sensors, optical sensors and artificial skins. Characteristics of various tactile sensors are summarized in Table 2.2 and detailed in the following subsections.

2.2.1.1 Resistive Sensors

Resistive sensors measure the applied force according to the variation of resistance. There are two main types of resistive sensors, including strain gauges and piezoresistors.

- **Strain gauges**

  A strain gauge is a device adhered on the surface of an object to measure the strain caused by external pressure. Most strain gauges are based on a resistive foil pattern which is mounted on a backing material and both the foil and the

backing material are attached by different glues depending on the required lifetime. The resistance of the foil changes with the stress applied to it.

Strain gauges are more suitable for measuring dynamic strains rather than static ones (Najarian *et al.*, 2009) because of high temperature and humidity sensitivities. Wheatstone bridge configurations are usually introduced to compensate environmental changes (Tiwana *et al.*, 2012). Strain gauges also exhibit nonlinear response. Generally, the smaller a strain gauge is, the higher the accuracy that can be achieved because the measured strain is the average strain over the gauge length. Also, sensors of a smaller size are flexible and robust enough to be applied over dexterous surfaces, such as prostheses, robots and medical devices (Engel *et al.*, 2003). Micromachined strain gauges based on metal and semiconductor have been realized with the development of manufacturing technologies, although it is not easy to fabricate and handle tiny gauges (Najarian *et al.*, 2009)(da Silva *et al.*, 2002). Metal-based and semiconductor-based strain gauges exhibit many advantages, such as high spatial resolution and high strain sensitivity. For example, a nanofibre-based strain gauge, which can detect pressure, shear and torsion, was proposed to be flexible and sensitive even to human heartbeats (Pang *et al.*, 2012). Strain gauges have been popularly used in various sensors, such as pressure sensors, torque sensors and position sensors, which indicates a major advantage of strain gauges in terms of their well-established fabrication techniques and applications.

Da Silva *et al.* proposed a finger-mounted tactile sensor based on the strain gauge which presented a linear response, a wide force sensitivity of 0-100 N with a resolution of 0.3 N and a low hysteresis of 1.7% (da Silva *et al.*, 2002). As shown in Fig. 2.2, another flexible strain gauge sensor was fabricated for the detection of normal and shear force, which could be measured by the voltage drop in strain gauges (Hwang *et al.*, 2007). This sensor had a simple structure, but it was less sensitive to small forces.

- **Piezoresistors**

Piezoresistive tactile sensors are also resistive sensors. Its resistance varies with the deformation caused by the applied force on it, so the force can be obtained by the measurement in a piezoresistor's resistance. Piezoresistors are

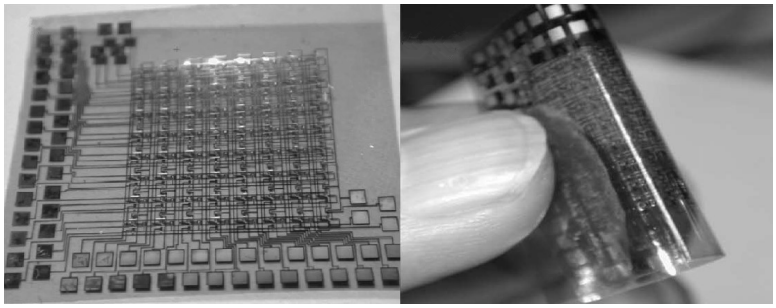

Figure 2.2: Flexible tactile sensor based on strain gauges (Hwang *et al.*, 2007)

made of silicon, metals and semiconductors. Due to the easy measurement of resistance, piezoresistive tactile sensors are suitable to be connected to electronic devices. They exhibit good sensitivity and are less susceptible to interference (Tiwana *et al.*, 2012). Another advantage is the ease in which they can be implemented in microelectromechanical systems (MEMSs) or integrated with printed circuit boards (Stassi *et al.*, 2014). Despite the mentioned advantages, piezoresistors suffer from hysteresis, temperature sensitivity, fragility, rigidity and high cost (Stassi *et al.*, 2014). Some efforts have been made to overcome the problem of fracture by embedding piezoresistors in flexible thin films (Wisitsoraat *et al.*, 2007) or polymers (Park *et al.*, 2009)(Ahmed *et al.*, 2013).

Jorgovanovic *et al.* presented the static and dynamic characterization of piezoresistive sensors used for detecting the positions of prosthetic finger joints (Orengo *et al.*, 2009). The feasibility of wireless communication between sensors and a receiving device, to reduce wires, was also discussed. Kane *et al.* proposed a piezoresistive stress sensor array with high spatial resolution comparable with human dermis ($\approx$300 μm) (Kane *et al.*, 2000). It exhibited high potential for dexterous manipulation applications. Various applications with piezoresistive tactile sensors can also be found in stress and force measurement (Noda *et al.*, 2006)(Mei *et al.*, 2000), stiffness of soft tissues detection (Kalantari *et al.*, 2011), fingertip sensing (Koiva *et al.*, 2013), etc.

2.2.1.2 Capacitive Sensors

A capacitive sensor is among the most sensitive sensors for detecting small force changes. It generally consists of two parallel conductive layers which are separated by dielectric materials. When force is applied on the capacitors, the capacitance between the layers varies with the reduced distance between layers and the deformation of the middle dielectric material as well (Schmitz *et al.*, 2008). A capacitive sensor exhibits high sensitivity, robust performance, a large dynamic range (Pritchard *et al.*, 2008), lower temperature sensitivity and low power consumption (Muhammad *et al.*, 2011). It can be used for both dynamic and static force measurement (Nafari *et al.*, 2007). In order to accurately measure the change in capacitance, the size of the capacitors should not be too small, because the small size may limit their spatial resolution (Pritchard *et al.*, 2008). Additionally, their sensitivity to noise leads to relatively complex electronics required for noise filtration. Capacitive sensors are considered as effective sensing elements and have been applied to multi-axis force measurement for gripping and objects manipulation (da Rocha *et al.*, 2009), texture recognition (Muhammad *et al.*, 2011), touch screen application (Kim *et al.*, 2011), etc.

A capacitive sensor for shear sensing was proposed with a size of 4 N (Tiwana *et al.*, 2011). It showed a high repeatability and approximately linear output within ± 2 N, however, its dimension (3.5 mm$\times$1.6 mm$\times$1.6 mm) was a point to be considered in practical applications. Another capacitive tactile sensor was presented for gripping force measurement with a sensor range of 0-3000 mN (Wang *et al.*, 2014). It was tested on a prosthetic hand as shown in Fig. 2.3.

2.2.1.3 Piezoelectric Sensors

Piezoelectric effect is the ability of certain materials to generate an electrical charge in response to external mechanical stress. A piezoelectric tactile sensor is a device based on the piezoelectric effect to measure changes, such as force, by converting them to an electrical voltage. Measurement in voltage mode is the simplest way to obtain the applied force. Besides, current measurement and shock wave measurement can be utilized as well (Ueberschlag, 2001).

Piezoelectric sensing is one of the few sensing techniques that do not require power supply, which is considered as an outstanding advantage. Besides, it also exhibits high

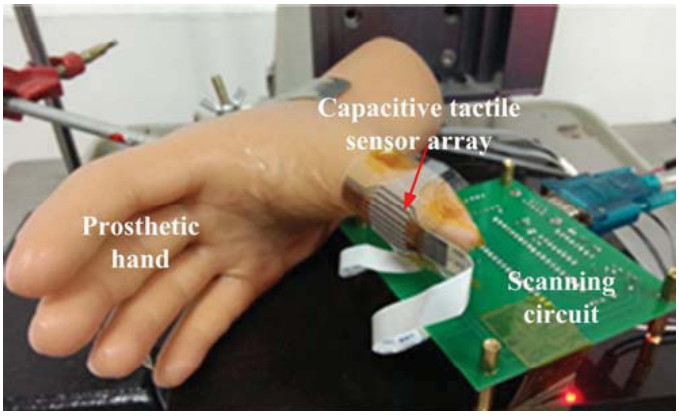

Figure 2.3: Capacitive tactile sensor array integrated with the thumb of a prosthetic hand (Wang *et al.*, 2014)

sensitivity, reliability and fast dynamic response. A wide response range of 0 to 1 kHz enables it to be a good choice for vibrations measurement (Seminara *et al.*, 2011). However, due to the decrease of the output voltage, piezoelectric sensors are unsuitable for measuring static force and show low spatial resolution and poor temperature stability (Pritchard *et al.*, 2008)(Seminara *et al.*, 2011).

Various piezoelectric materials can be used for constructing piezoelectric tactile sensors. One of the most widely used is polyvinylidene fluoride (PVDF). PVDF is a semicrystalline polymer consisting of long chain molecules with repeated unit CF-CH. Its strong piezoelectricity is attributed to the high electronegativity of fluoride atoms compared with carbon atoms, which leads to a large dipole movement (Dargahi, 2000). PVDF has many advantages (Lang & Muensit, 2006)(Li *et al.*, 2008): mechanical flexibility, dimensional stability, high piezoelectric coefficients, low weight, formability into very thin sheets (5 μm) and a relatively low price. Another promising piezoelectric material is zinc oxide (ZnO) nanotransducer because of its high flexibility and bio-compatibility (Marino *et al.*, 2016). Also, its ability to generate electrical power when subjected to mechanical vibration leads to various potential applications, including wearable and self-power medical devices (Dakua & Afzulpurkar, 2013). ZnO is proposed to be a good candidate material, for a pressure and temperature sensor, to be applied to prosthetic limbs (Lee *et al.*, 2015). During the past years, piezoelectric sensors have been used in prosthetic hands for the detection of slip (Cotton *et al.*, 2007), texture (Takamuku *et al.*, 2007) and stiffness (Omata & Terunuma, 1992)

2.2.1.4 Optical Sensors

An optical fibre force sensor generally consists of a light source, a transduction medium and an optical detector, which is often a vision sensor or a photodiode. The light generated by the light source, usually light emitting diodes (LEDs), passes through the transduction medium, which includes optical fibres and a modulator, and finally reaches the detector (Maekawa *et al.*, 1993)(Puangmali *et al.*, 2008). Then the detector circuit converts the light signal into an electrical signal to be further processed. The intensity or the spectrum of the modulated light changes according to the variation of the applied force, which is the working principle of optical sensors.

Many electronics-based sensing techniques cannot be applied in magnetic environments because of the electromagnetic interference, however, optical sensing is one of few techniques that are immune to electromagnetic field (Heo *et al.*, 2008). This major advantage enables optical sensors to be used in minimally invasive surgeries (MISs) where magnetic resonant imaging (MRI) is widely used to provide high quality images of living organs (Maekawa *et al.*, 1993)(Yamada *et al.*, 2005). In addition, optical sensors have s simple and compact structure and high spatial resolution (Ataollahi *et al.*, 2010).

Despite of the aforementioned attractive characteristics, there are several limitations in optical sensors. Most optical fibres are fragile and not as flexible as electric wires due to their rigidity. Also, their complexity and relatively large size is another problem to be considered in dexterous hand applications. Some solutions have been proposed (Ohka *et al.*, 1995)(Massaro *et al.*, 2011). For example, plastic optical fibres were used to overcome the rigidity problem and prevent the damage of optical sensors (Ascari *et al.*, 2007). Efforts were also made to reduce the size of optical sensors by using only one LED matrices instead of two as both the light source and detector (Rossiter & Mukai, 2005). Additionally, optical sensors were applied in a scalable tactile sensor skin to cover the whole body of a robot, which demonstrated that the sensors could be made with high flexibility and compliance (Ohmura *et al.*, 2006). An LED-based optical sensor prototype was mounted between the fingers of a prosthetic hand as shown in Fig. 2.4 (Sani & Meek, 2011). It was tested on surfaces with different properties which included roughness, curvature and stiffness for slip detection.

It failed to detect any motion for transparency surface (e.g. glass) and highly reflective surface (such as a front silvered mirror and CD). However, this problem could be overcome by a laser-based optical sensor.

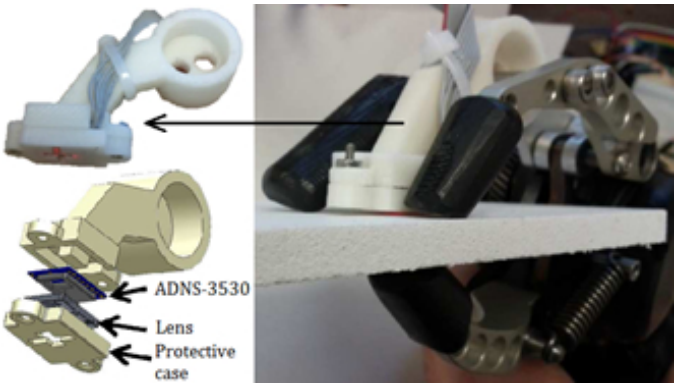

Figure 2.4: Prototype of an optical sensor applied with a prosthetic hand (Sani & Meek, 2011)

2.2.1.5 Artificial Skins

In addition to various tactile sensors, efforts have also been made in studies of artificial skin through sensor fusion and the imitation of mechanoreceptors in the skin.

A stretchable artificial skin, as shown in Fig. 2.5 (Kim *et al.*, 2014), assembled pressure, temperature and humidity sensor arrays and was fabricated within ultrathin single crystalline silicon nanoribbons. It also integrated with electroresistive heaters which could be warmed to 36.5 °C to facilitate native skin perception. Furthermore, researchers connected the smart skin's sensors to a rat's peripheral nerves. The results showed that the sensory signal was successfully transferred to the rat's brain which indicated that this research could provide opportunities for PNS interfaces and enable amputees to feel various external stimulations. With regard to the imitation of mechanoreceptors in human skin, (Aoyagi *et al.*, 2006) proposed a four-layer arrayed capacitive sensor by reference to the four types of mechanoreceptors in human skin. Also, a power-efficient piezoresistive sensor was employed to mimic the SA mechanoreceptors for static pressure feedback (Tee *et al.*, 2015). The output of the sensors was used to stimulate somatosensory neurons through an optical/neural interface for pressure feedback. This study paved the way for the design and use of

Table 2.2: Characteristics of tactile sensors based on different transduction techniques

Tactile sensors	Working principle	Advantage	Disadvantage
Strain gauges	Its resistance varies with the applied stress.	High spatial resolution; High strain sensitivity; Widely used, well developed; Low cost.	Non-linear; Sensitive to temperature and humidity; Inability to sense stable value.
Piezoresistors	Its resistance varies with the deformation caused by applied force.	Simple electronics; High sensitivity; Ease of integrating in MEMS; Resistant to interference.	Hysteresis; Temperature sensitivity; Fragile and rigid; High cost.
Capacitive sensors	Its capacitance varies with the deformation caused by applied force.	Sensitivity of small force change; Reliability; Large dynamic range, suitable for both dynamic and static force measurement; Low temperature sensitivity; Low power consumption.	Limited spatial resolution; Noise sensitivity; Complex electronics.
Piezoelectric sensors	An electric voltage will be produced when a force applied to it.	No need for power supply; High reliability; Fast dynamic response, able to measure vibration.	Low spatial resolution; High temperature sensitivity; Inability to sense static value.
Optical sensors	The intensity or the spectrum of light varies with the applied force.	Immune to electromagnetic field; High spatial resolution.	Fragile and rigid; Large size; Inability to transparency and highly reflective surface.

large-area organic electronic skins with tactile feedback for limb prostheses, although it was based on direct neural stimulation.

Figure 2.5: Artificial skin (Kim *et al.*, 2014)

2.2.2 Tactile Stimulation

Tactile stimulation feedback is used to send tactile information detected by tactile sensors, to a user's residual body for perceptual interpretation and is usually conducted by stimulation techniques. Depending on whether the stimulation electrodes are implanted into the skin, tactile stimulation can be classified as invasive (e.g. direct neural stimulation) and non-invasive (surface stimulation). Compared with direct neural stimulation, non-invasive tactile stimulation is safer and easier to be installed with hand prostheses and applied onto users' body, although it may not generate the tactile sensation as naturally as the invasive stimulation does. In this section, the direct neural stimulation and dominant non-invasive stimulation techniques, including electrotactile stimulation, vibrotactile stimulation, mechanotactile stimulation and contactless techniques applied for prosthetic hands are introduced.

2.2.2.1 Invasive tactile stimulation

In theory, invasive stimulation with neural electrodes implanted in the peripheral nervous system (PNS) may potentially generate natural tactile feelings. Preliminary success has been achieved in studies, although there remain great challenges to achieve the full restoration of tactile sensation for hand prostheses users.

An invasive tactile system with 20 stimulation channels was recently tested on self-controlled prostheses. It could generate feelings of pulsing pressure, constant pressure, tapping, 2 types of texture and objects moving at 19 small places on a subject's hand, such as their palm, wrist and fingertips (Tan *et al.*, 2014)(Tyler, 2016). Further studies are expected to restore natural feeling over the whole hand.

However, invasive stimulation suffers from risks of infection and rejection, poor knowledge of neural decoding, technical issues of surgery, electrode replacement and so on. Given the above scenarios, this thesis gives priority to non-invasive stimulation feedback. For direct neural stimulation, please refer to (Nghiem *et al.*, 2015)(Gasson *et al.*, 2005)(Tan *et al.*, 2014)(Tyler, 2016).

2.2.2.2 Electrotactile Stimulation

Electrotactile stimulation provides sensations by passing a local electric current to stimulate afferent nerves in the skin using surface electrodes. The modulated parameters include frequency, amplitude, pulse width and so on. Mulvey *et al.* proposed that transcutaneous electrical nerve stimulation (TENS) could generate a sensation on human skin by directing electrical pulses across the skin surface (Mulvey *et al.*, 2009). It is mostly used to reduce phantom pain and stump pain (Mulvey *et al.*, 2010). Initial experiments were conducted to support that TENS could be projected into a prosthetic hand and could enhance its sense of perceptual embodiment (Mulvey *et al.*, 2012). A recent study revealed that TENS could generate a strong sensation, although its effect on perceptual embodiment was modest (Mulvey *et al.*, 2014). It was tested to generate tactile sensation on the residual limbs of 11 amputees with their eyes covered as shown in Fig. 2.6 (Chai *et al.*, 2015). However, most research is still based on able-bodied participants and vision feedback is still a major factor for perceptual embodiment. More clinical tests are expected for evaluation in further experiments.

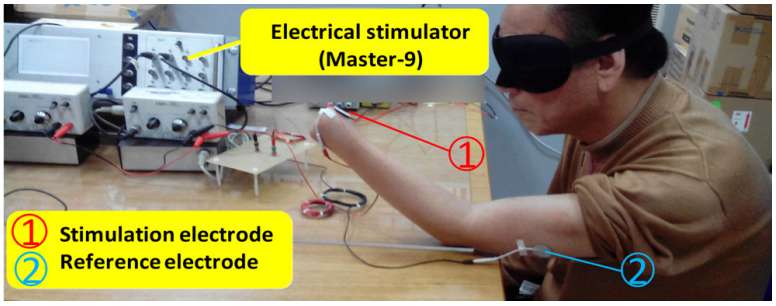

Figure 2.6: Experimental setup for TENS: electrodes on the residual limb of the amputee (Chai *et al.*, 2015)

Electrotactile feedback is a direct way to stimulate PNS and is potential to generate natural tactile perception. Due to no mechanical parts, electrotactile stimulation has advantages of lower power consumption, light weight and little noise compared with other tactile feedback techniques (Antfolk *et al.*, 2013). Despite many advantages, some unexpected feelings, such as burning pain, may result from electrotactile stimulation, which can be ameliorated by voltage-regulated stimulation and large electrodes. Additionally, another major drawback of electrotactile stimulation is its interference with electromyography (EMG) signal and electroencephalography (EEG) signal, although there are cases which tested electrotactile stimulation with EMG-based and EEG-based rehabilitation system (Xu *et al.*, 2016)(Bhattacharyya *et al.*, 2016a). Studies about how to eliminate the interference when applied with myoelectric prostheses and EEG-based prostheses are discussed in Section 2.4.2.

2.2.2.3 Vibrotactile Stimulation

Vibrotactile stimulation is generated by mechanical vibration which is transverse or normal to the skin surface to convey tactile information through modulating vibration frequency, amplitude, duration, etc. (Meek *et al.*, 1989). It was first applied with prosthetic hands in 1953 (Antfolk *et al.*, 2013)(Conzelman Jr John *et al.*, 1953) and is considered to be suitable for myoelectric prostheses (Rombokas *et al.*, 2013) and EEG-based prostheses (Chatterjee *et al.*, 2007) because of no interference with electric signals. The sensitivity to vibrotactile stimulation varies with the age and physical condition of subjects together with the stimulation positions and frequency. Generally,

the frequency ranges from 50 Hz to 300 Hz (Cincotti *et al.*, 2007). Currently, vibrotactile stimulation is widely used in cell phones and devices to assist deaf or blind people (Schätzle & Weber, 2015)(Chang *et al.*, 2002). A vibrotactile stimulation system applied with a myoelectric prosthetic hand is illustrated in Fig. 2.7 (Cipriani *et al.*, 2008).

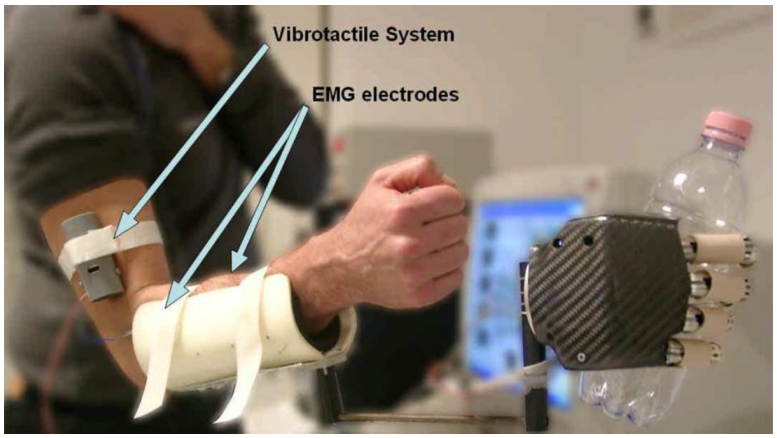

Figure 2.7: Vibrotactile stimulation system applied with a myoelectric prosthetic hand (Cipriani *et al.*, 2008)

2.2.2.4 Mechanotactile Stimulation

Mechanotactile stimulation is to provide users with a force/pressure or position feedback when users move their prostheses. Compared with electrotactile stimulation and vibrotactile stimulation, mechanotactile stimulation is able to generate a natural feeling of force/pressure, but the generated stimulation is applied in a different area (the residual body of the subject) from the original stimulus. As shown in Fig. 2.8 (Casini *et al.*, 2015), a wearable mechanotactile stimulator is demonstrated to provide pressure and skin stretch information to the subject's residual limb. Current mechanotactile devices still have a relatively large size, weight and high energy consumption when compared with vibrotactile or electrotactile devices (Schofield *et al.*, 2014). Thus, further minimization is desired for mechanotactile stimulation devices.

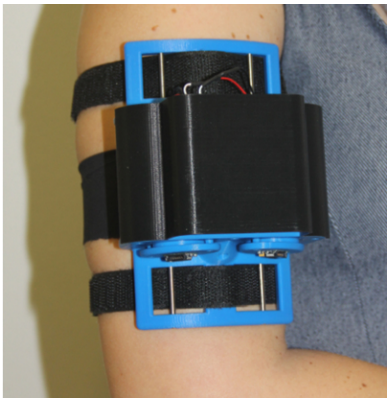

Figure 2.8: Mechanotactile stimulator (Casini *et al.*, 2015)

2.2.2.5 Others

Some contactless techniques were also utilized for tactile feedback, such as magnetic-field (Hollis, 2013), air-jet, airborne ultrasound (Arafsha *et al.*, 2015) and infrared (Kutilek *et al.*, 2012). These studies are still at the laboratory stage and are not adopted as widely as aforementioned stimulations. Their bulky dimension might be a challenge in daily use for upper extremity prostheses but, with the development of technologies, they have potential to be applied in rehabilitation, virtual reality and so on.

2.3 Tactile Feedback to Hand Prostheses

Presently, neither commercial nor laboratory prosthetic hands provide satisfactory tactile sensation for users, although limited tactile feedback is available as shown in a few studies. Taking dominant commercial hand prostheses for example, such as i-Limb by Touch Bionics (Bionics, 2018), Myohand and Michelangelo hand by Ottobock (Ottobock, 2018c), and the Bebionic hand by steeper (Bebionic, 2018)(Liu, 2011), their multiple degrees of freedom (DoFs) enable users to accomplish fundamental tasks in daily life, however, they are unable to make users aware of the tactile information without visual feedback. VINCENTevolution 2 might be the only commercialized hand prosthesis with a stimulation system for force feedback (VincentSystems, 2018), but no customer reviews are found to confirm the effectiveness of its feedback performance presently.

Available laboratory artificial hands are integrated with various sensors. For example, force/pressure sensors and torque sensors are utilized in DLR-HIT hand (DLR, 2018), Southampton Hand (Kyberd *et al.*, 2001)(Kyberd *et al.*, 2009), LUKE hand (MOBIUSbionics, 2018) and Cyerhand (Carrozza *et al.*, 2003) for slip prevention and finger position feedback. Southampton hand and Shadow hand (Shadow, 2018) are integrated with temperature sensors. Also, micro-vibration sensors are optional on Shadow hand. However, the tactile information acquired by sensors is only fed back to prostheses themselves to pursue a stable control performance, instead of providing tactile feedback to users.

Encouragingly, a 20-channel invasive tactile system was recently tested on self-controlled prostheses users to provide limited tactile feedback (Tan *et al.*, 2014)(Tyler, 2016). The invasive tactile feedback system could generate feelings of pulsing pressure, constant pressure, tapping, 2 types of texture and objects moving at 19 small places on a subject's hand, such as their palm, wrist, and fingertips. Further studies are expected to restore natural feelings over the whole hand. However, the invasive stimulation suffers from risks of infection and rejection, poor knowledge of neural decoding, technical issues of surgery and electrode replacement. Thus, there remains great challenges of a full restoration of tactile sensation for hand prostheses and a portable device to provide tactile feedback for the users, although preliminary success has been achieved.

2.4 Electrotactile Feedback to Users

Electrotactile stimulation might be the most promising way to provide tactile feedback for prostheses, so this section gives a further review of its state-of-the-art studies. In comparison with other tactile feedback techniques mentioned above, electrotactile stimulation has the advantages of lower power consumption, light weight and little noise, which makes it suitable to be installed on upper-extremity prostheses. Meanwhile, an electric signal acts as the carrier of neural information in the human neural system, so electrotactile stimulation is a direct way to stimulate human PNS by transferring electric signals into the skin and has the potential to generate natural tactile perception. Thus, considerable attention has been paid to electrotactile feedback in the area of sensory restoration.

2.4.1 Role of Tactile Sensation Integration

To position tactile feedback in the field of prosthetic control, studies mainly focus on its impact on functionality improvement and body ownership enhancement. Usually, tactile sensation is expected by prosthesis users in practical use, although there is not a consensus of its effectiveness on performance improvement in academia. Whether integrating tactile sensation would improve the functionality performance of prostheses is still a matter of some controversy. Some reported that the success rate of grasp increased with tactile sensation feedback, while some others pointed out that there was not much difference of the task performances compared with non-feedback control. In order to objectively evaluate the role of tactile sensation in prosthetic control, Jorgovanovic *et al.* conducted virtual grasping experiments in which the feedback of grasping force was given by electrotactile stimulation and the visual and auditory feedback were eliminated (Jorgovanovic *et al.*, 2014). The outcome confirmed the benefits of tactile sensation in prosthesis force control. In another study, tactile sensation was proposed to build up and update an internal model of feed forward control (Dosen *et al.*, 2015). Thus, tactile sensation has the potential to improve and facilitate prosthetic control with less effort for the users.

2.4.2 Influence Prevention

Many studies about prosthetic control and tactile stimulation feedback are based on myoelectric prostheses and EEG-based prostheses. As mentioned in Section 2.2.2.2, myoelectric signals and EEG signals are tiny electric signals. they will be contaminated by electrotactile stimulation, if the signal recording and electrotactile stimulation work on the same body part simultaneously without special processing. Thus, it is necessary to eliminate such influence in practical use.

Various methods were applied to reduce the influence of electrotactile stimulation on myoelectric signals. They can be categorized into two groups: software-based solutions, such as signal processing algorithms; hardware-based solutions, such as blanking/blocking window (Widjaja *et al.*, 2009). Filter-based signal processing algorithms are a common way to restore the performance of myoelectric control, such as the Butterworth filter used in (Peruzzini *et al.*, 2012), and an adaptive filter based on least mean square (LMS) used in (Jiang *et al.*, 2014). Regarding hardware-based solutions, time

windows were applied between the recording period and stimulating period to avoid the overlapping of the myoelectric signal and stimulation signal (Dosen *et al.*, 2014). Similarly, a method of artificial blanking with three data segmentation approaches was proposed and proved to be an effective way to eliminate the influence of stimulation signal on EMG pattern recognition (Hartmann *et al.*, 2015). Additionally, optimization of stimulation waveform and the electrode design may also help to reduce the interaction of those two electric signals (Jiang *et al.*, 2014).

Apart from above methods, novel prostheses based on non-electric signal are expected to avoid signal interaction from the very root. For example, sonomyography-based technology has potential to be applied to hand prosthesis (Akhlaghi *et al.*, 2016). Ultrasound is able to detect changes in muscle thickness in real time and has no interaction with electric stimulation signals (Fang *et al.*, 2015a). However, there must be a long way to go before a novel technology can be applied in practice.

2.4.3 Modality Coding

Natural sensation might be achieved by invasive electrodes (Tyler, 2016), while surface electrodes usually generate needle-like, buzz or numb feelings instead. In this case, modality coding is adopted by non-invasive stimulations to provide sensation feedback. Modality coding is used to map various stimulation modes on the subject's body to represent different tactile sensations.

With regard to electrotactile stimulation, adjustable signal parameters include frequency, amplitude, pulse width and wave form. For multi-channel stimulation, the allocation and combination of electrodes can also be taken into consideration. Difference between low frequency ($<$30 Hz) stimulation and high (50-100 Hz) frequency stimulation can be recognised by subjects effectively (Arieta *et al.*, 2005)(Paredes *et al.*, 2015). Amplitude and wave width are generally used to represent intensity difference such as force feedback. Square wave is commonly used in electrotactile feedback experiments (Arieta *et al.*, 2005), while few comparisons of the impact of different stimulation wave forms can be found in literature at the current time. Spatial coding is usually adopted by multi-channel systems in which the allocation and combination of electrodes are utilized to form different modes and subjects can achieve tactile information by recognizing the stimulation area of the working electrode(s) from among

all the distributed electrodes (Isaković *et al.*, 2016). Moreover, mixed coding is applied in tactile sensation restoration and encouraging outcomes were achieved (Dosen *et al.*, 2016). It should be noticed that most of the stimulations applied are for force feedback, only a few of the studies are concerned with other tactile sensations, such as texture and shape. Despite the significance of force feedback for grasp tasks, the restoration of other kinds of tactile sensations is also important because recognizing an object's properties without visual monitoring can enhance a feeling of body ownership and improve the quality of life for people who suffer from hand loss (Raspopovic *et al.*, 2014).

2.4.4 Hybrid Feedback

Considering the characteristics of different feedback interfaces, attempts have been made to apply more than one type of feedback for sensation delivery. For example, Marco D'Alonzo *et al.* proposed a hybrid vibro-electrotactile (HyVE) approach which combined vibrotactile stimulator and electrotactile stimulator together to provide sensory feedback and the experimental outcome was better or comparable to single stimulation (D'Alonzo *et al.*, 2014a)(D'Alonzo *et al.*, 2014b).

2.5 Summary

Few existing prosthetic hands provide effective tactile sensation feedback to users, which impedes their performance and acceptance. Some tactile feedback techniques and devices have been proposed to address the issue but with limited success in clinical use. To have a comprehensive understanding of the whole process of tactile sensation restoration for prosthetic hands, this chapter presents the physiology of the human sensory system, followed by a review of available tactile sensing and non-invasive stimulation techniques with their working principles, applications, and properties. Then, existing studies of tactile feedback and especially electrotactile stimulation are also reviewed.

Chapter 3

Probability-based Haptics Model

To artificially mimic and restore the tactile feedback for hand prosthesis users, it is fundamental to have a quantitative description of the human skin's biomechanics, especially the haptics-related mechanism of the fingertip where hand-object contacts mostly happen (Gonzalez *et al.*, 2014). Mechanical changes of the human fingertip, such as deformation, may activate mechanoreceptors to detect and generate tactile sensation as introduced in Section 2.1. Therefore, this chapter proposes a novel probability-based haptics model to characterise the relation between the contact force and the deformation of the human fingertip. The remainder of this chapter is organised as follows. Section 3.1 gives an introduction and a literature review in the fingertip modelling field. The experimental methods, materials and data recording are described in Section 3.2. Section 3.3 presents the theoretical foundation of the haptics model and a demonstration of the model establishment process, followed by a summary in Section 3.4.

3.1 Introduction and Related Work

Hand manipulation heavily relies on the intuitively sensory feedback during human-object interaction and environment exploration. An investigation of the human fingertip's biomechanics may facilitate the sensory feedback and broaden the research perspectives in the field of biomechanical engineering and robotics. Related studies have gained increasing attention not only to tactile sensation rehabilitation for hand

prostheses but also to a wide range of applications, such as artificial fingertip/skin development (Shao *et al.*, 2009), finger model establishment in virtual reality (Ciocarlie *et al.*, 2007), and ergonomic design (Pawluk & Howe, 1999).

Existing studies of the human fingertip's biomechanics and the model establishment mainly aimed at the neural reaction properties of the mechanoreceptors under the fingertip's skin by investigating the physical response of the human fingertip under various load conditions. The final acheivements of these studies were mathematical models or simulation models targeting at the relation between the contact force/pressure and the fingertip skin deformation, despite different experimental setups and modelling methods.

Researchers employed various shape of indenters to press the fingertip for the deformation generation and retrieval, such as the point load (Wu *et al.*, 2004), line load (Srinivasan, 1989)(Dandekar *et al.*, 2003a)(Wu *et al.*, 2006), and flat load (Serina *et al.*, 1998)(Serina *et al.*, 1997)(Wu *et al.*, 2006). To test multiple indenters may help to achieve a comprehensive understanding of the fingertip's biomechanics, because the force-deformation relation may be subject to the conditions of the contact surface. In these studies, experimental data used for modelling can be categorised into 3 classes, including the measurement of force-displacement data (Wiertlewski & Hayward, 2012), force-contact area data (Wang *et al.*, 2012), and pressure-deformation data (Xydas & Kao, 1999)(D'Angelo *et al.*, 2017).

Regarding the methods used for the establishment of the haptics model, some research, from a structural and experiment-based point of view, simplified the human fingertip as one or multiple layers of membranes (Srinivasan, 1989); while others, in the sight of physical character analysis, built physical-mathematical models according to the viscoelasticity analysis of the fingertip soft tissue. Taking a structure-based model for example, by simplifying the fingertip as an incompressible fluid-filled elastic membrane, Srinivasan proposed a "waterbed" model which predicted the fingertip deflection profile under line loads and the model was validated on humans and monkeys in vivo (Srinivasan, 1989). The model was created under many simplifications and assumptions, such as neglecting the viscoelastic effects and assuming the membrane to be linearly elastic, so the accuracy was inevitably sacrificed. Then, non-linear models were proposed to describe the relation between the normal force and the radius of contact area for soft-finger materials (Xydas & Kao, 1999)(Kao & Yang, 2004). In

some research, only soft materials such as rubber and silicone were employed in experiments instead of human fingers. However, to reveal the actual biomechanics of the human fingertip, in vivo tests are necessary. After achieving a deeper understanding of human fingertip characters, more complex models based on the analysis of fingertip viscoelasticity were proposed. Jindrich *et al.* presented a non-linear viscoelastic model to describe the fingertip force-displacement relation and concluded that the non-linear model could predict the fingertip force according to the fingertip pulp compression during dynamic tapping (Jindrich *et al.*, 2003). Duchemin G. *et al.* conducted in vivo test and proposed a model to reflect the soft finger and the underlying tissue's behaviour and properties, which took into account the influence of motion velocity and lubrication (Duchemin *et al.*, 2005).

Additionally, to investigate the microscopic sensing process of the human finger, 2D/3D finite element (FE) models were established based on the numerical models to simulate human finger sensing characteristics. Wu *et al.* proposed a two-dimensional (2D) structural fingertip model which could predict the stress and strain distributions within the soft tissue, and simulate the deflection profiles of a fingertip under a line load, a one-point load and a two-point load with a small indentation depth of 1mm (Wu *et al.*, 2004). Three-dimensional (3D) models were also proposed under a flat load, a sharp wedge (Wu *et al.*, 2006), and a line load (Dandekar *et al.*, 2003b). For example, a 3D FE model was developed to predict the temporal force response of fingertip under both a line load and a cylinder load surface deflection (Kumar *et al.*, 2015).

The modelling of human fingertip's biomechanics has not been accomplished and still requires further research. First, most biomechanical models of human fingertips are established from a microcosmic point of view mainly concerning the mechanoreceptors response to external tactile stimulation with a small indentation depth of 0-0.2 mm to 0.8-2.5 mm (Kumar *et al.*, 2015)(Serina *et al.*, 1997). However, large deformations that may also occur in the context of hand manipulation should also be involved in the model. Also, assumptions and simplifications in the models based on either the anatomical structure or the physical characterisations of human fingertip are the main limitations of the models' accuracy of theoretical models compared with statistical models. Additionally, obvious intersubject skin difference and the force uncertainty on the same subject have been observed from the related literature, which should be

taken into consideration as well. So far, no studies have been conducted yet to address these issues. It is necessary to establish a quantitative model from an external and macroscopic perspective to reveal the fingertip behaviour under a larger indentation depth, which will serve applications related to the process of hand manipulation. Also, a probabilistic haptics model instead of a deterministic one is expected to characterise the force uncertainty, considering that the haptics information may varies even under the same physical deformation condition. A probabilistic model will facilitate to improve the robust of hand control in virtual or practical applications.

3.2 Data Collection

This section presents an experimental paradigm to collect the data related to the biomechanics of human fingertip, including the experimental setup, procedure and results.

3.2.1 Experimental Setup

The experimental setup as shown in Fig. 3.1(a) comprised a Finger Tactile Pressure Sensing (FingerTPS) system and an indenting test bracket. FingerTPS is a commercial system designed to collect high-quality data of force/pressure exerted on human hand. It consisted of a calibration force sensor, wearable fingertip force sensors, a Chameleon Visualization and Data Acquisition Software which collects and displays the force data through the interface. In this study, we employed this system to measure the contact force varying with the indentation depth on the fingertip in real time. The indenting test bracket with a cone-shape probe was fixed on the edge of a table and was used to press the fingertip to different indentation depths. A vertical view of the indenting bracket with the fingertip is illustrated as Fig. 3.1(b). The backboard attached to the table side helped to fix the fingertip during the experiment. The probe was adjusted by a screw which has 7 rounds of adjustable whorls and the screw's vertical length changed 1 mm per round, so the indentation depths of the skin deformation could range from 0 mm to 7 mm.

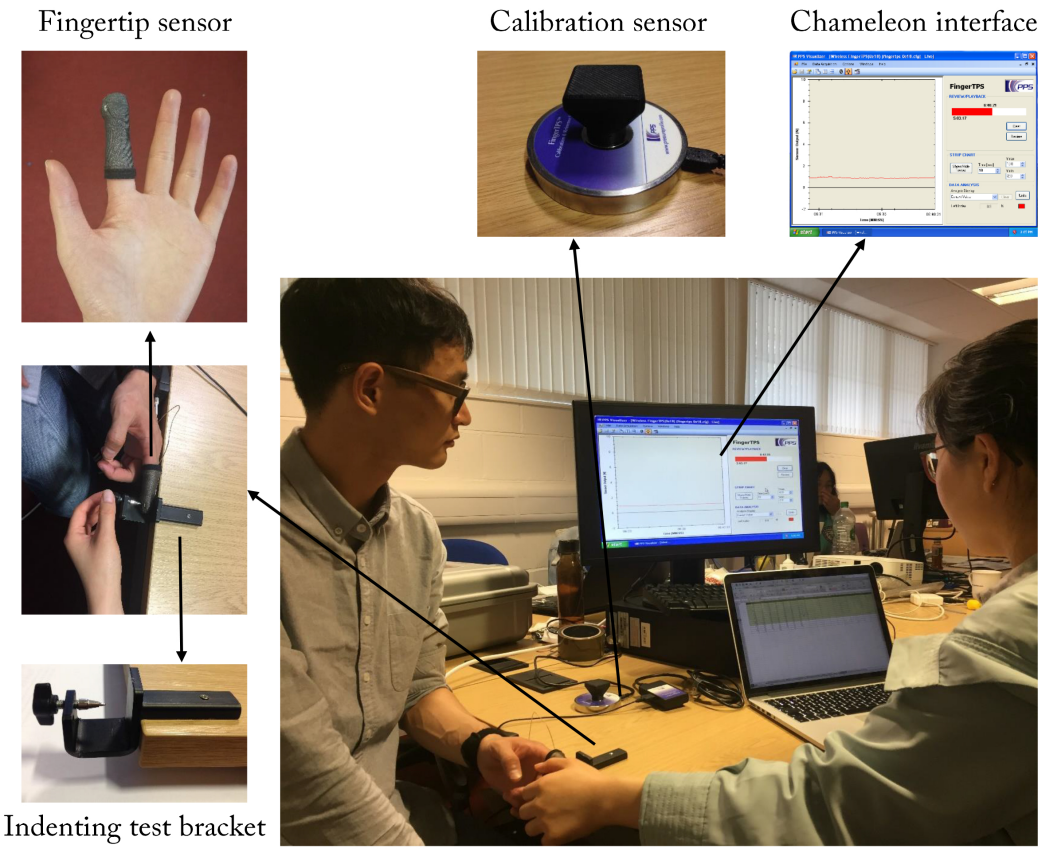

(a) Data collection system

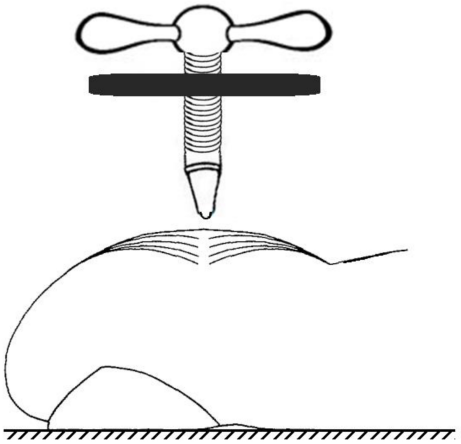

(b) Vertical view of the indenting bracket

Figure 3.1: Experimental setup for the haptics data collection

3.2.2 Experimental Procedure

Six subjects (23-31 years old, 2 females and 4 males) participated in the experiment. None of them reported any skin or finger injury.

During the experiment, the subject was comfortably seated in an armchair with his/her body-side towards the table where the indenting bracket was fixed. Fig. 3.1(a) presented the indenting and recording scene of the experiment. In preparation, the subject needed to wear a fingertip force sensor on their left index fingertip and press the finger on the reference sensor for calibration according to the instruction of the FingerTPS system. Then the subject was asked to put the tested finger into the indenting test bracket with the middle point of the fingertip pulp directly towards the cone top of the screw as shown in Fig. 3.1(b). Initially, the cone top of the screw was adjusted to be detached from the fingertip. It should be noted that there would be a tiny but measurable force to the fingertip force sensor and be observed from the Chameleon Visualization and Data Acquisition Software without indentation because of the pressure between the sensor and the fingertip. To eliminate the interference, the force was set to 0.0 N as a measurement baseline and maintained throughout the experiment of the same subject. After then, the subject was reminded to keep the tested finger as stable as possible to make sure that the indentations of all the experiment sessions were within the same region of the finger pulp to avoid measurement error.

At first, the probe was screwed to lightly touch the fingertip but not cause any pressure and deformation, which was considered as the starting point of each test session. Then, the probe was screwed to indent 0.5 mm deeper every time until it reached the max indentation depth of 7 mm or the subject reported discomfort. The indenting process from 0.0 mm to the final indentation depth was viewed as one session. During a single session, the contact force corresponding to different indentation depths ranging from 0.0 mm to 7.0 mm were recorded, so a maximum of 15 values of force were recorded in each session. At the end of each session, the researcher would screw the probe back to its starting point. To collect enough data to verify the experiment's repeatability, the indentation tests were repeated 20 times on each subject. The duration of the whole experiment lasted about 40 minutes and slightly varied with individuals.

3.2.3 Data Recording

The experiment data collected from subject 1 to 6 are recorded as shown in Fig. 3.2. According to the experiment results, the maximum indentation depth that all the subjects could endure is 5 mm, so the description and analysis in the following sections will only consider the data ranging from 0 mm to 5 mm.

Taking the data of subject 2 as shown in Fig. 3.2(b) for example, there are 11 measured indentation depth $d(d = 0, 0.5, ..., 4.5, 5mm)$, and each of them corresponds to 20 measured contact forces. The contact force increases monotonically and non-linearly with the indentation depth. The slope becomes bigger during the large indentation than the small indentation and the turning point appears when the indentation depth is around 3 mm, although it is not obvious. Meanwhile, the data dispersion becomes more obvious with the increase of the indentation depth. The data of the other five subjects also share the same features—monotonically increasing, non-linear, and increasing dispersion. Additionally, we can see that the changing range and changing speed of the contact force are different among the subjects, although they show a similar trend. For example, the average contact forces of subject 1, 4 and 5 range between 0-2 N, while subject 2, 3 and 6 show a larger range of about 0-2.5 N. The force dispersion of subject 3 and subject 5 is obviously larger than that of the other subjects, especially subject 1 and 6. Thus, the skin conditions of fingertip exactly varies with individuals, although there are also several fundamental features in common for general human skin.

3.3 Development of Haptics Model based on Gaussian Distribution

This section proposes the haptics model to characterise the haptics-related biomechanics of human fingertip, which can be described by the relation between the contact force and the skin deformation. According to features of the data collected in Section 3.2.3, a deterministic model with certain parameter values may not reflect the specific state of every subject and the force uncertainty during the skin deformation. Consequently, a probability model, Gaussian distribution, is introduced to describe the individual difference and force uncertainty. Thus, this section will firstly present the

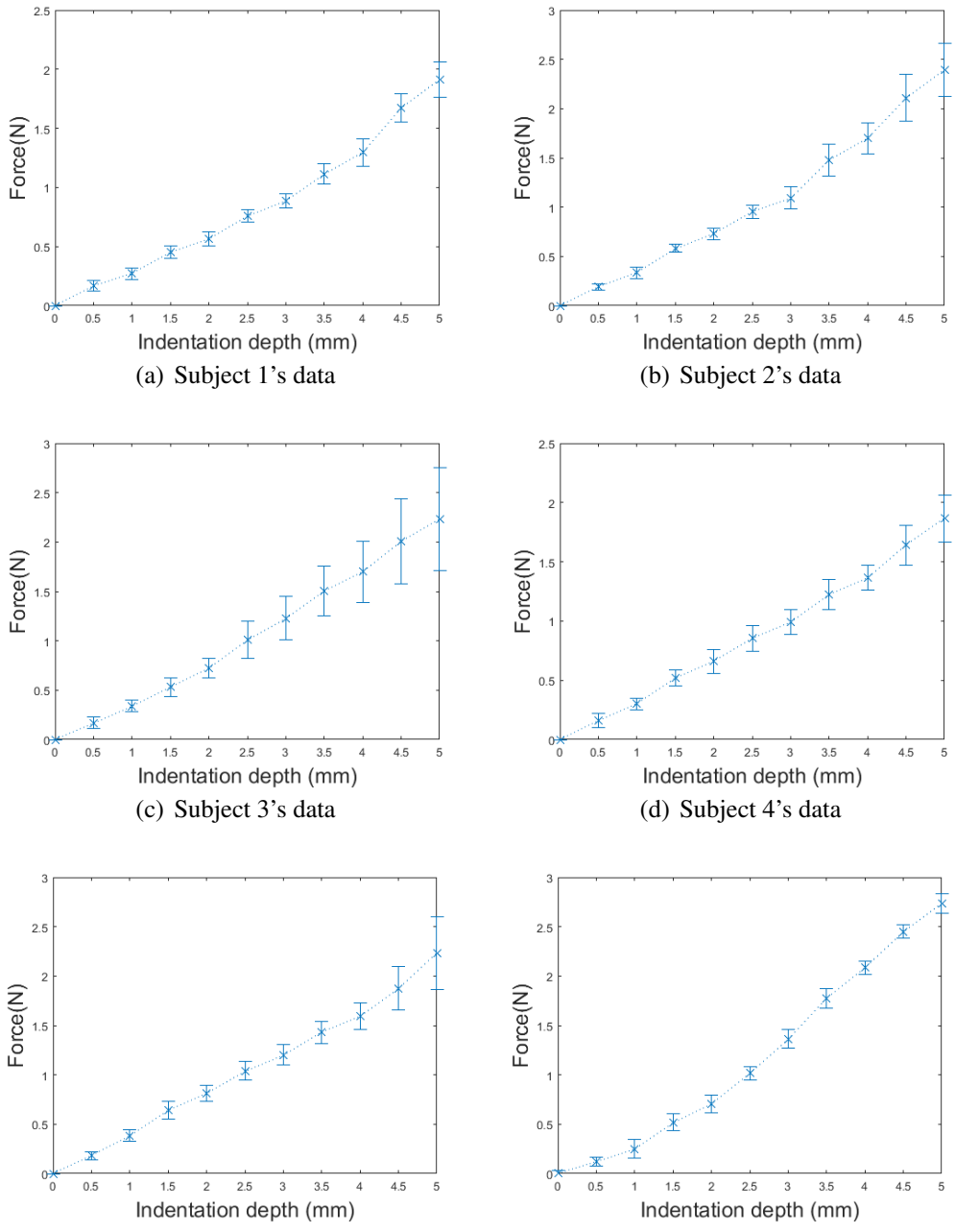

(a) Subject 1's data (b) Subject 2's data

(c) Subject 3's data (d) Subject 4's data

(e) Subject 5's data (f) Subject 6's data

Figure 3.2: 20 sessions of the measured forces at discrete indentation depth ranging from 0 mm to 5 mm on 6 subjects. At different indentation depths, the mean forces are depicted as points, and the corresponding maximum and minimum measured forces are presented by bars.

background knowledge of probability models, followed by a theoretical derivation of the haptics model. Finally, a demonstration of the model establishment and validation with practical data is provided.

3.3.1 Theoretical Background of Probability Model

In statistics, probability describes the relative frequency of outcomes of random phenomena over the long term, such as a coin flip, weather or gambling. A probability model is a mathematical representation of a random phenomenon to predict probabilities associated with each outcome. The outcome with uncertain values is also called a random variable. According to the feature of random variables, probability models can be divided into discrete distribution and continuous distribution. A discrete distribution is used to describe a phenomenon with finite and discrete possible outcomes, such as a coin flip or a dice toss. In contrast, a continuous distribution characterises phenomena with uncountable and continuous outcomes, such as weather.

A discrete distribution can be defined by a probability mass function (PMF), which gives an exact value of a discrete random variable. It applies when the number of trails is fixed, each trail is independent, and the possibility of success is always the same. Common discrete distributions include Bernoulli distribution, binomial distribution, geometric distribution and Poisson distribution. They are introduced respectively as follows.

- Bernoulli distribution

  A Bernoulli distribution is a binary probability model of a random variable taking binary outputs $x \in \{0, 1\}$ when a single trial is conducted. It is a basic discrete probability distribution abstracted from the coin flip and is usually applied in clinical trials, polling, etc. The PMF of the Bernoulli distribution is as shown in Eq. 3.1.

  $$P(x) = \begin{cases} 1-p, & x = 0 \\ p, & x = 1 \end{cases} \tag{3.1}$$

  where p, ($p \in (0, 1)$) is the probability when $x = 1$.

- Binomial distribution

A binomial distribution can be viewed as the probability model of a series of Bernoulli trial which is repeated n, ($n \in N$) times, such as flipping a coin for many times or statistical results of questionnaires. It becomes a Bernoulli distribution when $n = 1$. In a single trail, the success probability is always p, ($p \in (0, 1)$), while the failure probability is $1 - p$. Then the probability $p(k)$ of obtaining k successes among all the n trails can be calculated by Eq. 3.2 which is the PMF of the Binomial distribution.

$$p(k) = C_n^k p^k (1-p)^{n-k} \tag{3.2}$$

- Geometric distribution

  The geometric distribution and the binomial distribution are applied on the same type of experiment which consists of n, ($n \in N$) trails with a single trail either success or failure. The only difference is that the geometric distribution cares about the probability $p(k)$ of the first success after k, ($k = 0, 1, 2, ..., N$) trails. The corresponding PMF is shown in Eq. 3.3.

$$p(k) = (1-p)^{k-1} p \tag{3.3}$$

- Poisson distribution

  A Poisson distribution is used to predict the probability of a given number k of events happening in a fixed interval of time. It is usually employed in business to forecast the demand during a certain period, so that the supply can be adjusted accordingly. If during the fixed time interval, an event x happens μ times on average and the probability keeps unchanged, then the probability $p(k)$ of the event happening k times during the given interval can be calculated according to Eq. 3.4.

$$p(k) = \frac{\mu^k e^{-\mu}}{k!} \tag{3.4}$$

As for a continuous distribution, the probability of a random variable taking on any particular value is 0 due to the infinite number of possible outcomes. As a result, we can only use the probability of some interval (a, b) to describe the possibility distribution of a continuous random variable, which is defined as a probability density function (PDF). Common continuous distributions include uniform distribution, normal distribution (also called Gaussian distribution) and exponential distribution.

- Uniform distribution

  The uniform distribution describes a situation where the possibility of outcomes remain the same in a certain domain. However, only a few processes in reality have this form of distribution. A representative implementation is to generate pseudo-random values in computer programming. Its PDF is shown as Eq. 3.5.

$$f(x) = \begin{cases} \frac{1}{b-a}, & a < x < b \\ 0, & else \end{cases} \tag{3.5}$$

- Normal/Gaussian distribution

  The normal distribution, also called Gaussian distribution, is one of the most important distribution in statistics. The corresponding PDF is defined as Eq. 3.6.

$$f(x|\mu, \sigma^2) = \frac{1}{\sqrt{2\pi} \cdot \sigma} \cdot e^{-\frac{(x-\mu)^2}{2\sigma^2}} \tag{3.6}$$

  where μ and σ are the mean and the standard deviation of the distribution, respectively. When $\mu = 0$ and $\sigma = 1$, it becomes a standard normal distribution as shown in Fig. 3.3. Normal distributions differs in mean and standard deviation, but they all appear like "bell" curves with a symmetric shape around the mean and with a distribution denser in the center and less dense in the tails. The distribution pattern occurs in many situations, such as the product quality, IQ scores, blood pressure, heights of people and salaries, which makes the normal distribution a widely used statistical tool in business, social sciences, etc.

- Exponential distribution

  An exponential distribution is a probability distribution that usually describes time between events in a Poisson process. A Poisson process can predict when the random events will possibly happen, while the exponential distribution can be used to predict the waiting time between two events. Consequently, the exponential distribution is usually applied in the test of product reliability, lifetime distribution, etc. The corresponding PDF is shown as Eq. 3.7.

$$f(x, \lambda) = \begin{cases} 1 - e^{-\lambda x}, & x \geq 0 \\ 0, & x < 1 \end{cases} \tag{3.7}$$

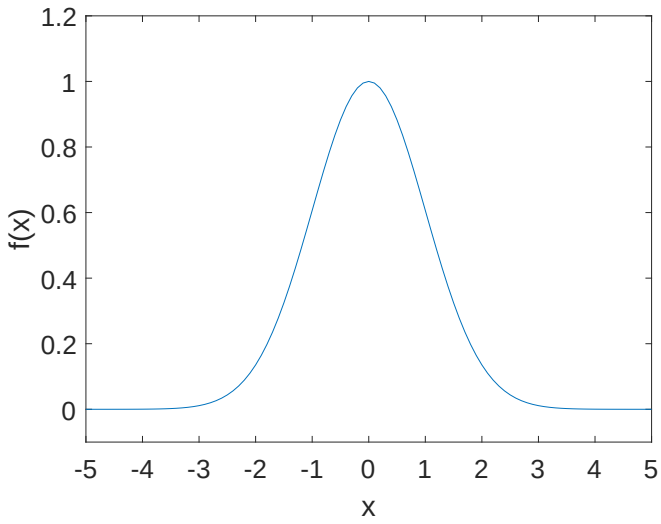

Figure 3.3: Standard normal distribution

3.3.2 Haptics Modelling

The haptics model aims to characterise the haptics-related biomechanics of human fingertip, which can be described by the relation between the contact force and the skin deformation. However, a model with certain parameter values may not reflect the specific state and requirement of every subject. Experience indicates that the data, i.e. the biomechanics of the fingertip, varies with individuals, and uncertainty exists during skin deformation. Consequently, an individual-dependent probabilistic model is expected to reflect the individual difference and force variation. Given that the fingertip's mechanical behaviour is a continuous procedure, the model should be based on a continuous distribution. A preliminary test was conducted to compare the goodness of fit among common continuous distributions based on a sample group of the experimental data. Gaussian distribution is finally chosen to describe the force variation because it outerperforms the uniform distribution and exponential distribution. It also has several advantages, such as a simple mathematical form, fewer parameters and the association with the Central Limit Theorem, which makes it a good choice in many cases and easy to implement (Robert, 2014). Thus, the haptics model proposed in this study will include a force prediction part and an uncertainty description part to characterise the

fingertip biomechanics under physical contact as shown in Eq. 3.8.

$$\begin{cases} \overline{f} = F(d) \\ P = p\left(f \mid d\right) \end{cases} \tag{3.8}$$

where $\overline{f}$ is the most possible contact force under a certain indentation depth d ($d > 0$). P is a probability density distribution of the contact force f and d.

The force prediction model $F(d)$ aims to predict $\overline{f}$ according to d. $\overline{f}$ can be estimated by the mean of the measured forces under a certain indentation depth, as Eq. 3.9.

$$\overline{f} \mid_d = \frac{\sum_{i=1}^{n} f_i}{n} \mid_d \tag{3.9}$$

where n is the repeated times of the measurements under the same indentation depth d, and f_i is the force of the ith measurement.

The dots in Fig. 3.4 represent typical measurement results of $\overline{f}$ under different d. By applying proper regression methods, a prediction model of $\overline{f}$ can be obtained. Eq. 3.10 presents the fitted result of $F(d)$ based on Fourier series model. The selection of the regression model will be explained in Section 3.3.3. The fitting performance is also shown in Fig. 3.4.

$$F(d) = a_0 + a_1 \cdot \cos(\omega \cdot d) + b_1 \cdot \sin(\omega \cdot d) \tag{3.10}$$

where a_0, a_1, b_1 and ω are the fitted coefficients.

On the other hand, considering the force variation even under the same indentation depth, it is assumed that the probability density distribution of the contact force f at a certain indentation depth d follow the Gaussian distribution as Eq. 3.11 due to the skin/force uncertainty:

$$P \mid_d = G(f) = \frac{1}{\sqrt{2\pi} \cdot \sigma} \cdot \mathrm{e}^{-\frac{(f-\mu)^2}{2\sigma^2}} \tag{3.11}$$

where μ and σ are two coefficients of Gaussian distribution, namely its mean and standard deviation. When $d = 0$, f is always equal to 0, so it is not included in this distribution model.

The mean of the measured forces at a certain indentation depth $\mu \mid_d$ can be easily estimated according to Eq. 3.9 and Eq. 3.12.

$$\mu \mid_d = \overline{f} \mid_d \tag{3.12}$$

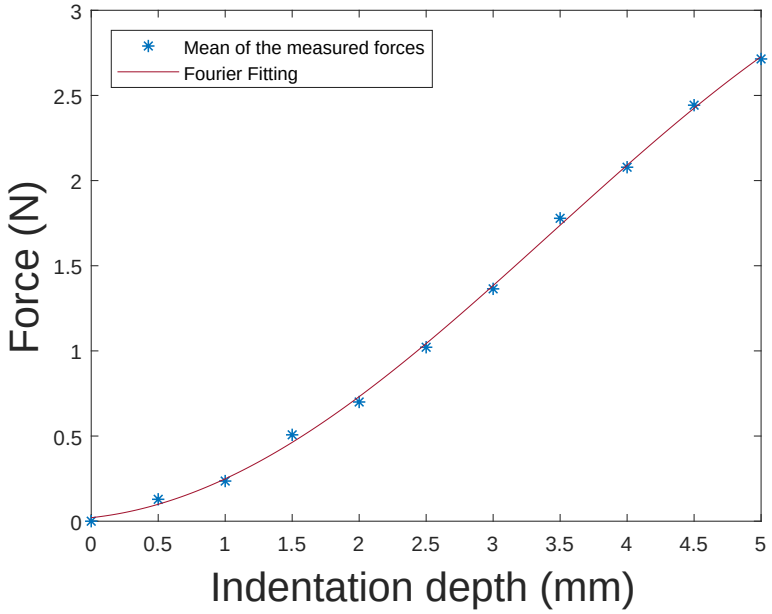

Figure 3.4: $\overline{f} - d$ fitting performance based on Fourier series regression

Next, the standard deviation of the measured force $\sigma \mid_d$ can be estimated according to Eq. 3.13. A typical measurement result is presented as dots in Fig. 3.5.

$$\sigma \mid_d = \sqrt{\frac{\sum_{i=1}^{n}(f_i - \mu)^2}{n-1}} \mid_d \tag{3.13}$$

The exponential model is selected to fit the data, and the fitting performance is shown as the curve in Fig. 3.5. The selection of exponential model will be explained in Section 3.3.3. A continuous model of $\sigma - d$ can be achieved as Eq. 3.14.

$$\sigma = S(d) = a \cdot e^{b \cdot d} \tag{3.14}$$

where a and b are the fitted coefficients.

Then, the possibility distribution at a certain indentation depth $P \mid_d$ can be obtained by introducing $\sigma \mid_d$ and $\mu \mid_d$ to Eq. 3.11, and the result is visualized as Fig. 3.6.

A generalised model of the probability distribution $p(f \mid d)$ can be obtained by introducing Eq. 3.10 and Eq. 3.14 to Eq. 3.11, as shown in Eq. 3.15.

$$p(f \mid d) = \frac{1}{\sqrt{2\pi} \cdot a \cdot e^{b \cdot d}} \cdot e^{-\frac{[f - a_0 - a_1 \cdot \cos(\omega \cdot d) - b_1 \cdot \sin(\omega \cdot d)]^2}{2a^2 \cdot e^{2b \cdot d}}} \tag{3.15}$$

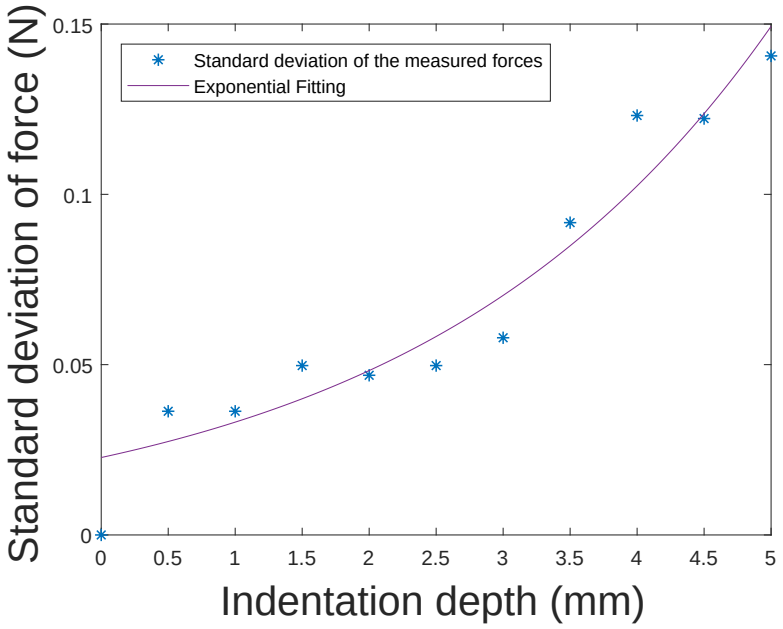

Figure 3.5: $\sigma - d$ fitting performance based on exponential regression

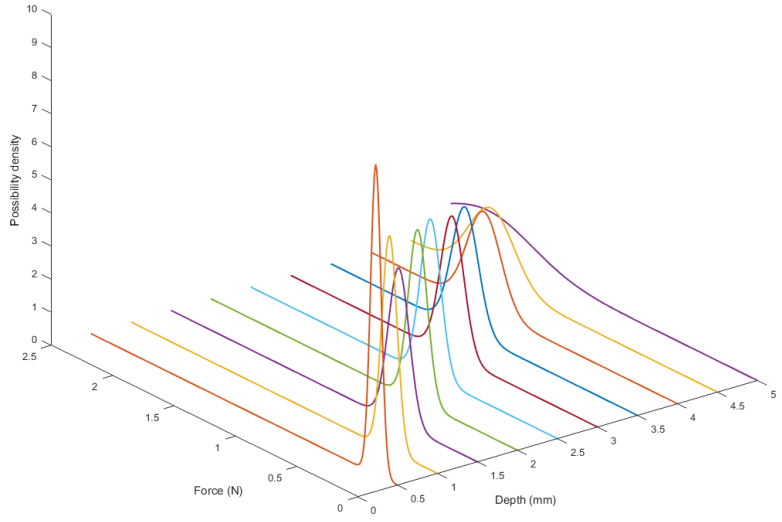

Figure 3.6: Force probability density distribution at discrete indentation depths

In summary, the whole haptics model is finalised as Eq. 3.16.

$$\begin{cases} F(d) = a_0 + a_1 \cdot \cos(\omega \cdot d) + b_1 \cdot \sin(\omega \cdot d) \\ p(f \mid d) = \frac{1}{\sqrt{2\pi} \cdot a \cdot e^{b \cdot d}} \cdot e^{-\frac{[f - a_0 - a_1 \cdot \cos(\omega \cdot d) - b_1 \cdot \sin(\omega \cdot d)]^2}{2a^2 \cdot e^{2b \cdot d}}} \end{cases} \tag{3.16}$$

3.3.3 Demonstration and Model Validation

This section demonstrates a detailed modelling process based on a subject's data, including model training, validation, and test. The main evaluation measure of the haptics model is the root mean square errors (RMSE) between the actual forces and the model's fitting outputs to evaluate the accuracy and precision of the haptics model.

3.3.3.1 Training

Taking subject 1's data for example, the 14 sessions of training data are presented as dots in Fig. 3.7. There is a non-linear relation between the contact force f and the indentation depth d. To predict the most likely force $\overline{f}$ (also the force's mean/expectation) based on the indentation depth d, several common-used non-linear regression models—-Fourier series model (Eq. 3.17), Gaussian model (Eq. 3.18), polynomial model (Eq. 3.19) and exponential model (Eq. 3.20) were applied to fit the data, where $a_0, a_1, b_1, a, b, c, k_1, k_2, k_3, a$ and b are the fitted coefficients.

$$y = a_0 + a_1 \cdot \cos(\omega \cdot x) + b_1 \cdot \sin(\omega \cdot x) \tag{3.17}$$

$$y = p \cdot \mathrm{e}^{-\left(\frac{x-q}{c}\right)^2} \tag{3.18}$$

$$y = k_1 \cdot x^2 + k_2 \cdot x + k_3 \tag{3.19}$$

$$y = a \cdot \mathrm{e}^{b \cdot x} \tag{3.20}$$

The fitting performance of different regression models based on the data of subject 1 were compared as curves in Fig. 3.7 where their respective root mean square errors (RMSE) were also displayed. The polynomial model presented the least RMSE, which indicated that it seemed to be the most suitable fitting model for subject 1 to predict

$\overline{f}$ according to d. In spite of this, Fourier model was chosen to fit the relation of $\overline{f}$-d. One consideration is its comparable RMSE to that of Polynomial model. Another consideration will be further explained in Section 3.3.3.2. Thus, the first part of the haptics model for the relation between $\overline{f}$ and d of subject 1 was fitted to be Eq. 3.21.

$$\overline{f}' = 1.694 + 0.1971 \cdot \sin(0.4228d) - 1.673 \cdot \cos(0.4228d) \tag{3.21}$$

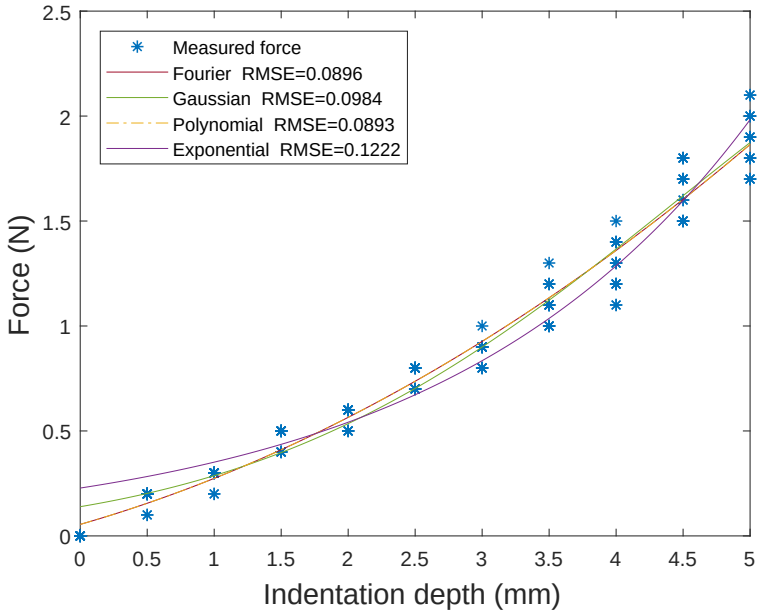

Figure 3.7: Training data of subject 1 and the fitting performance of various regression models

Likewise, a suitable model to predict the non-linear relation between the standard deviation of force σ and the depths d was also selected among the above regression models (Eq. 3.17, Eq. 3.18, Eq. 3.19, Eq. 3.20). Their fitting performance with respective RMSE was presented in Fig. 3.8. Considering that exponential model had the smallest RMSE and less coefficients than other models, it was chosen to describe the $\sigma - d$ relation. Thus, the prediction model of $\sigma - d$ for subject 1 was achieved as Eq. 3.22. It should be noted that when $d = 0$, the contact force f is always 0 and there is $\sigma = 0$. Consequently, the probability of $f = 0$ at $d = 0$ is 100% and the probability density $P\,|_{d=0}$ tends to positive infinite, so it is not necessary to discuss the probability

when $d = 0$.

$$\sigma' = 0.02272\mathrm{e}^{0.3766d} \tag{3.22}$$

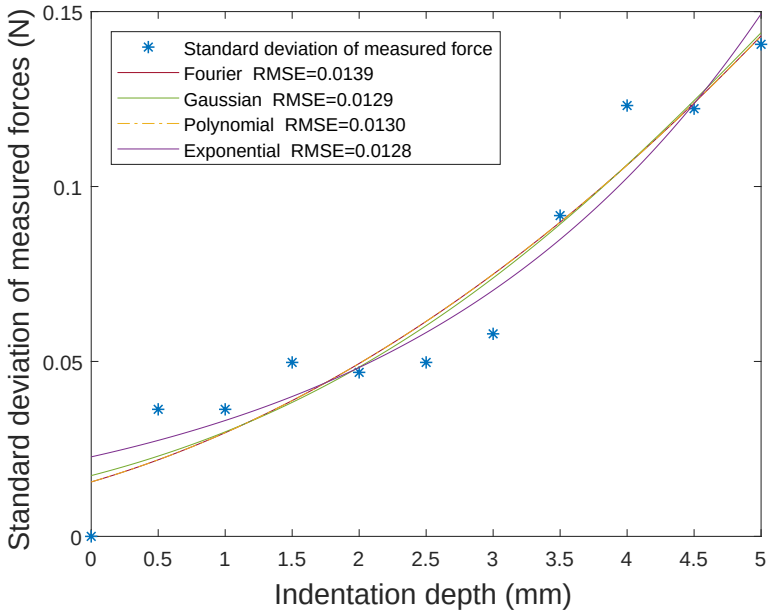

Figure 3.8: Fitting performance of experimental force's standards deviations

Then, by introducing Eq. 3.21 and Eq. 3.22 to Eq. 3.11, a continuous probability density distribution of the contact force f and indentation depth d for subject 1 was obtained as Eq. 3.23 and depicted as Fig. 3.9.

$$P' = \frac{1}{0.057\mathrm{e}^{0.3766d}} \cdot \mathrm{e}^{-\frac{[f-1.694-0.1971\cdot\sin(0.4228d)+1.673\cdot\cos(0.4228d)]^2}{1.032\times10^{-3}\mathrm{e}^{0.7532d}}} \tag{3.23}$$

Above all, the whole haptics model for subject 1 was achieved as Eq. 3.24.

$$\begin{cases} \overline{f}' = 1.694 + 0.1971 \cdot \sin(0.4228d) - 1.673 \cdot \cos(0.4228d) \\ P' = \frac{1}{0.057\mathrm{e}^{0.3766d}} \cdot \mathrm{e}^{-\frac{[f-1.694-0.1971\cdot\sin(0.4228d)+1.673\cdot\cos(0.4228d)]^2}{1.032\times10^{-3}\mathrm{e}^{0.7532d}}} \end{cases} \tag{3.24}$$

Similarly, the haptics models for other subjects can be obtained in the same way. Table 3.1 and Table 3.2 list 4 regression models' RMSEs based on all the 6 subjects' experimental data, with the smallest RMSE value for each subject marked in bold.

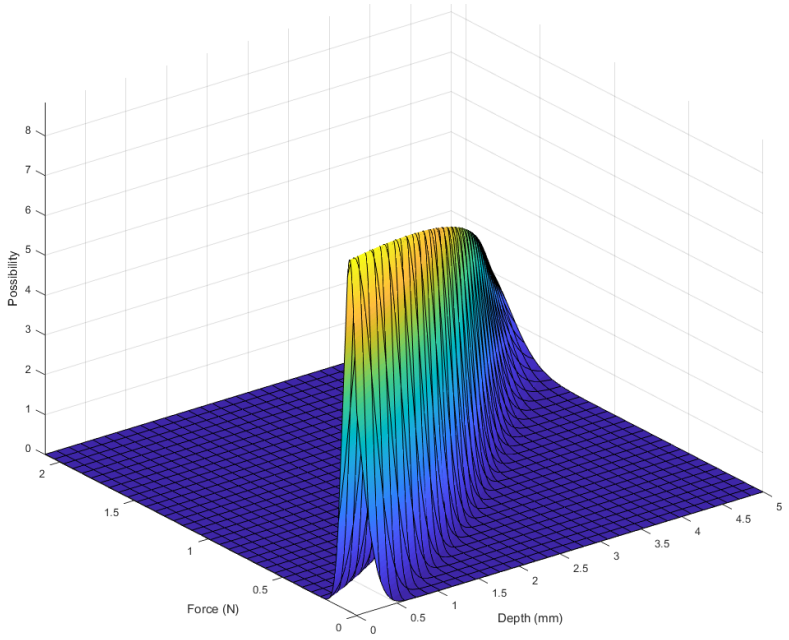

Figure 3.9: Continuous probability density distribution of $f - d$

In Table 3.1, the Fourier series model outperforms the other three models for subject 6, while for other subjects polynomial model presents the least RMSEs. In spite of this, Fourier series model shows the least RMSE on average, and its RMSEs for each subject are comparable with the least RMSEs which are fitted by polynomial model. In Table 3.2, the exponential model exhibits the least RMSE on most subjects and on average, which indicates it can be a good choice for $\sigma - d$'s fitting.

3.3.3.2 Validation

Considering the consistency of the fitting performance of above regression models on different subjects, it may not be necessary to test various regression models for each subject every time. If Fourier series model/polynomial model and Exponential model keep demonstrating good performance on some new data for validation, they can be set as the default models to fit $\overline{f} - d$ and $\sigma - d$. Then, there can be a unified structure of the haptics model, while only its parameters need to be adjusted according to each subject's condition.

Table 3.1: RMSE of different $\overline{f} - d$ regression models for different subjects based on 14 sessions of experimental data

RMSE	FS	GM	PM	EM
Subject 1	0.0896	0.0984	**0.0893**	0.1222
Subject 2	0.1253	0.1358	**0.1249**	0.1759
Subject 3	0.2503	0.2553	**0.2500**	0.2971
Subject 4	0.0805	0.0969	**0.0803**	0.1420
Subject 5	0.1466	0.1682	**0.1461**	0.2064
Subject 6	**0.0616**	0.0706	0.0822	0.2110
Average RMSE	**0.1257**	0.1375	0.1288	0.1924

Table 3.2: RMSE of different $\sigma - d$ regression models for different subjects based on 14 sessions of experimental data

RMSE	FS	GM	PM	EM
Subject 1	0.0139	0.0129	0.0130	**0.0128**
Subject 2	0.0238	0.0214	0.0222	**0.0203**
Subject 3	0.0294	**0.0241**	0.0275	**0.0241**
Subject 4	0.0189	0.0175	0.0177	**0.0165**
Subject 5	0.0470	0.0369	0.0440	**0.0348**
Subject 6	0.0144	0.0144	**0.0135**	0.0151
Average RMSE	0.0246	0.0212	0.0230	**0.0206**

Another two sessions of data are used for validation. To choose a proper regression model among the Fourier series model, Gaussian model, polynomial model, and an exponential model for the fitting of $\overline{f} - d$ and $\sigma - d$, RMSE of each model's fitting performance $\overline{f} - d$ based on the validation data of all the 6 subjects are presented in Table 3.3, Table 3.2 and Table 3.4 with the smallest values marked in bold. Fourier series model obtains the least RMSE on the validation data of all the subjects, and as mentioned in Section 3.3.3.1, it also obtains the least average RMSE on training data. Given the close results of the fitting models with the best and the second best RMSE respectively, the model selection does not limit to one option. In this study, Fourier model is selected to fit the relation between $\overline{f}$ and d because of its consistent and outstanding fitting performance. As for the coefficient σ, it needs to be calculated based on multiple and enough sessions of data instead of one or two sessions. Hence we decided to compare the RMSE of different models based on the training data (14 sessions, as Table 3.2) and all the experimental data (18 sessions in total, as Table 3.4). On both training and validating data sets, the exponential model shows the least average RMSE and presents the best fitting performance on 83.3% of subjects among all the tested regression models, so it should be the most suitable model to fit the relation of $\sigma - d$. Therefore, the haptics model for subject 1 is finalised to be Eq. 3.24. Also, a unified structure of the probability-based haptics model can be decided as Eq. 3.8.

Table 3.3: RMSE of different $\overline{f} - d$ regression models for different subjects based on 2 sessions of experimental data

RMSE	FS	GM	PM	EM
Subject 1	**0.1034**	0.1092	**0.1034**	0.1373
Subject 2	**0.1077**	0.1243	**0.1077**	0.1714
Subject 3	**0.1923**	0.2031	0.1928	0.2542
Subject 4	**0.1676**	0.1857	**0.1676**	0.2225
Subject 5	**0.0829**	0.1250	**0.0829**	0.1856
Subject 6	**0.0861**	0.0919	0.0943	0.2022
Average RMSE	**0.1233**	0.1399	0.1248	0.1955

Table 3.4: RMSE of different $\sigma - d$ regression models for different subjects basd on 18 sessions of data

RMSE	FS	GM	PM	EM
Subject 1	0.0164	0.0148	0.0153	**0.0139**
Subject 2	0.0216	0.0186	0.0202	**0.0175**
Subject 3	0.0287	0.0222	0.0269	**0.0213**
Subject 4	0.0235	0.0226	0.0220	**0.0215**
Subject 5	0.0438	0.0346	0.0410	**0.0326**
Subject 6	0.0134	0.0138	**0.0126**	0.0152
Average RMSE	0.0246	0.0211	0.0230	**0.0203**

3.3.3.3 Testing

The rest 2 sessions of data are used for testing by comparing the model's predictive results based on Eq. 3.21 with experimental data. The RMSE of $\overline{f} - d$ are presented in Table 3.5.

Table 3.5: RMSE of $\overline{f}$ and error percentage of 2 sessions of testing data

	RMSE of f	f_error%
Subject 1	0.0710	8.54%
Subject 2	0.1931	20.13%
Subject 3	0.1907	18.99%
Subject 4	0.2008	20.64%
Subject 5	0.1620	15.23%
Subject 6	0.0776	6.54%
Average	0.1492	15.01%

3.4 Summary

The Gaussian distribution based haptics model was proposed in this chapter to reflect the relation of force and the fingertip indentation depth ranging from 0 mm to 5 mm.

Experiments were conducted to collect in vivo data for analysis. The results revealed the non-linearity of the fingertip's mechanical characteristics. With the increase of indentation depth, the contact force's dispersion became large and its rising speed became fast, which might be attributed to the influence of the bone. Based on statistical methods and non-linear regression models, a force prediction model and a force probability distribution model were derived and form the whole haptics model. Thus, the haptics model can not only predict the most possible force under a certain contact deformation but also cover a reasonable level of force variation.

Chapter 4

Development of the Electrotactile Stimulation System

The lack of a well-designed wearable device is a main factor that restricts the clinical applications of tactile feedback in hand prostheses and rehabilitation systems. To fill this gap, this chapter develops a portable multi-channel electrotactile stimulation system for clinical use. The chapter is organised as follows. Section 4.1 gives an general description of the electrical stimulation's application in biomedical engineering, especially the sensory and motor function rehabilitation area. Section 4.2 introduces the background and basic principles of a typical electrotactile stimulation (ETS) system. The integral design framework and the main functional modules of the multi-channel ETS system are presented in details in Section 4.3. To evaluate the output capability of the proposed ETS system, Section 4.4 provides the test results of different stimulation waveforms and the stability of output currents. This chapter ends with a summary in Section 4.5.

4.1 Introduction and Related Work

Electrical stimulation has been studied for decades in the area of sensory and motor function restoration for amputees and patients with spinal cord injury (SCI), because a local electrical current is believed to pass through the skin and directly stimulates afferent neurons (Kaczmarek *et al.*, 1991)(Snyder-Mackler *et al.*, 1995). According

to the stimulation intensity, it has two main applications in the rehabilitation area, electrotactile stimulation (ETS) with lower intensity output and functional electrical stimulation (FES) with higher intensity output. Both of them function by modulating the current parameters, such as amplitude, frequency and pulse width.

As introduced in Section 2.2.2.2, ETS evokes tactile sensations by passing a low-intensity current to the skin through surface electrodes. Commercial stimulators are available, but they are usually with bulk size (KINETICS, 2018)(TENSPROS, 2018) (BIOPAC, 2018) or with limited numbers of output channels (Tens+, 2018). The clinical applications of ETS in rehabilitation is still limited, although some efforts have been devoted to the device development (Farina *et al.*, 2014)(Takeda *et al.*, 2017)(Cornman *et al.*, 2017)(Onesti *et al.*, 1989). Further study and development are expected in this field.

As for FES, it is used for motor recovery by generating relatively strong electrical current to activate the skeletal muscle of the paralyzed patients to complete desired motions (Lynch & Popovic, 2008)(Quandt & Hummel, 2014)(Bhattacharyya *et al.*, 2016b). FES has become one of the most important and effective treatments for stroke rehabilitation, since it was first used for foot drop rehabilitation (Liberson, 1961)(Popović, 2014). For lower limb rehabilitation, FES has been applied in treatments for knee joint position control (Chang *et al.*, 1997), unsupported standing (Matjacic & Bajd, 1998)(Holderbaum *et al.*, 2002), gait training (Thrasher *et al.*, 2006)(Popovic *et al.*, 1999) and cycling (Hunt *et al.*, 2004)(Donaldson *et al.*, 2000). Also, it is reported that FES may effectively improve the upper limb function rehabilitation efficacy during early stroke (Alon *et al.*, 2007).

The expected features of electrical stimulators include adjustable parameters, stable stimulation signals, multiple output channels and portable size, which are applicable for both ETS devices and FES devices, although their operative intensities are different. A flexible stimulator can be easily customised to fit different individuals. A stable output ensures a consistent tactile perception or motor function for the users. Multi-channel output may facilitate multi-sensation feedback by ETS and complex motions' generation for FES by activating more muscles compared with single-channel stimulator. As for ETS, multi-channel output can enable spatial coding which is intuitive and can be easily perceived by users. Furthermore, a small and light stimulator is more suitable for prosthesis integration or take-home use.

4.2 Theoretical Background of Electrical Stimulators

4.2.1 Typical Design Structure of Electrical Stimulators

Safety, portability and ease of use are three main concerns of the design of an ETS system. Most available electrical stimulation systems follow the circuit structure proposed by Ilic *et al.* (Ilic *et al.*, 1994), consisting of a control module, stimulation output module, sensor interface, power management module and a human-machine interface. Fig. 4.1 is a schematic diagram of a typical ETS system's structure (Broderick *et al.*, 2008). The digital-to-analogue converter (DAC) in the microcontroller provides the input for the level control (LC) module to control the amplitude of the outout current or voltage of the electrical stimulation. The timing signals control the switch circuitry (SC) module to adjust the stimulation parameters, such as frequency and pulse width.

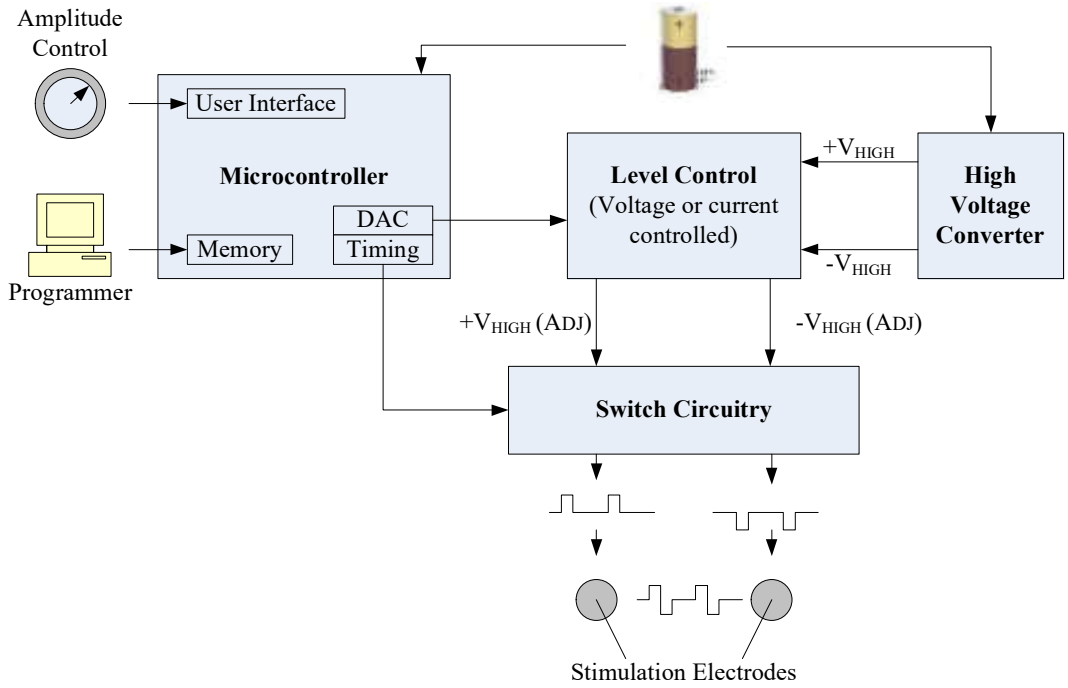

Figure 4.1: Schematic diagram of a typical ETS system's structure, consisting of the digital-to-analogue converter (DAC), level control (LC) and switch circuitry (SC) (Broderick *et al.*, 2008).

4.2.2 Output Modes of Electrical Stimulation

The output modes of an electrical stimulator can be classified into three types: constant-current output, constant-voltage output and a hybrid form (Broderick *et al.*, 2008). The constant-voltage output mode presents an advantage of safety that the amplitude of stimulation current decreases with the increase of skin resistance, which indicates less potential for tissue damage. However, the variation of the stimulation signal leads to inconsistent motor response. In the constant current output mode, the amplitude of the stimulation current remains unchanged, while the amplitude of the stimulating voltage increases with the increase of skin resistance. This mode has a better performance in the control of the stimulating intensity (Sheffler & Chae, 2007), so it is adopted in the design of most electrical stimulators, The intensity of electrical stimulation can be adjusted by changing the amplitude, pulse width, and frequency of the output signals. For an ETS system, the stimulation frequency is usually adjusted to be less than 100 Hz and the amplitude is less than 10 mA, because a strong electrical stimulation can easily cause muscle fatigue (Baker *et al.*, 1993)(Lynch & Popovic, 2008). If the intensity of electrical stimulation is high enough (20-50 mA), it will work as FES which may lead to unexpected passive muscle contraction or even motor responses.

4.2.3 Waveforms of Electrical Stimulation Output

Three typical output waveforms of the ETS, monophasic pulses, symmetric biphasic square pulses, and asymmetric biphasic square pulses, are shown in Fig. 4.2. Biphasic pulses can reach the sensation thresholds of the stimulated area with lower intensity compared with monophasic pulses. As for biphasic pulses, the area of positive pulses is generally equal to that of negative pulses, because the negative pulses can neutralize the charge accumulation and polarization effect caused by the positive pulses on the skin and prevent the tissue damage (Baker *et al.*, 1993). Biphasic pulses are generally used in FES, given its high intensity of the stimulation signal. As for ETS, both monophasic pulses and biphasic pulses can be applied because of its relatively low stimulation intensity.

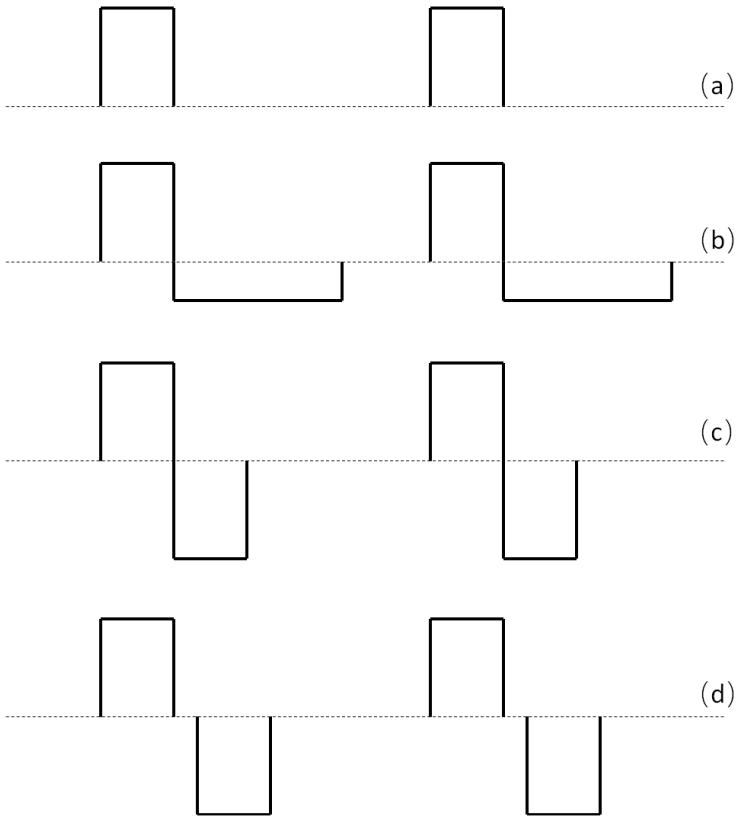

Figure 4.2: Typical electrical stimulation pulses: (a) Monophasic pulse; (b) Asymmetric biphasic square pulse; (c) Symmetric biphasic square pulse; (d) Symmetric biphasic square pulse with interval.

4.3 Design of the Multi-channel ETS System

4.3.1 Framework of the Multi-channel ETS System

This research aims to develop an electrical stimulator for the provision of ETS. The design framework of the proposed ETS system is illustrated in Fig. 4.3, consisting of 6 parts: power supply module (PSM), micro controller unit (MCU), electrical stimulation output module (ESOM), electronic switch module (ESM), Bluetooth module (BM), graphical user interface (GUI), and the corresponding hardware prototype and GUI design are shown in Fig. 4.4(a). Fig. 4.5 presents an industrial design of the ETS stimulator. The following sections will provide a detailed description of the circuit design of different modules.

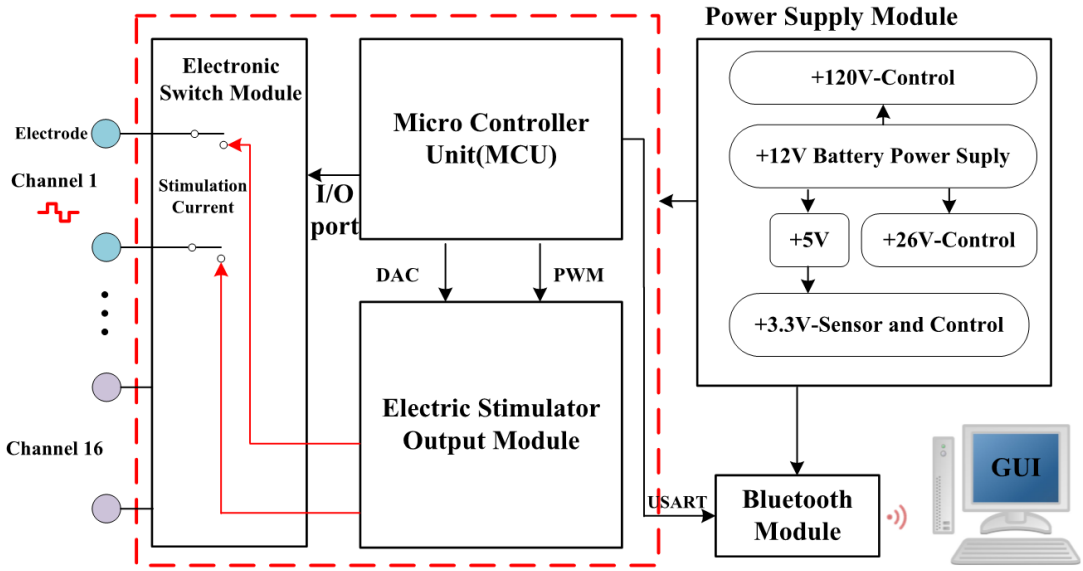

Figure 4.3: Design framework of the multi-channel ETS system

4.3.2 Power Supply Module

In the power supply module (PSM) as shown in Fig. 4.3, an independent +12V DC battery is employed to drive the electrotactile stimulator. Constant-current output mode is

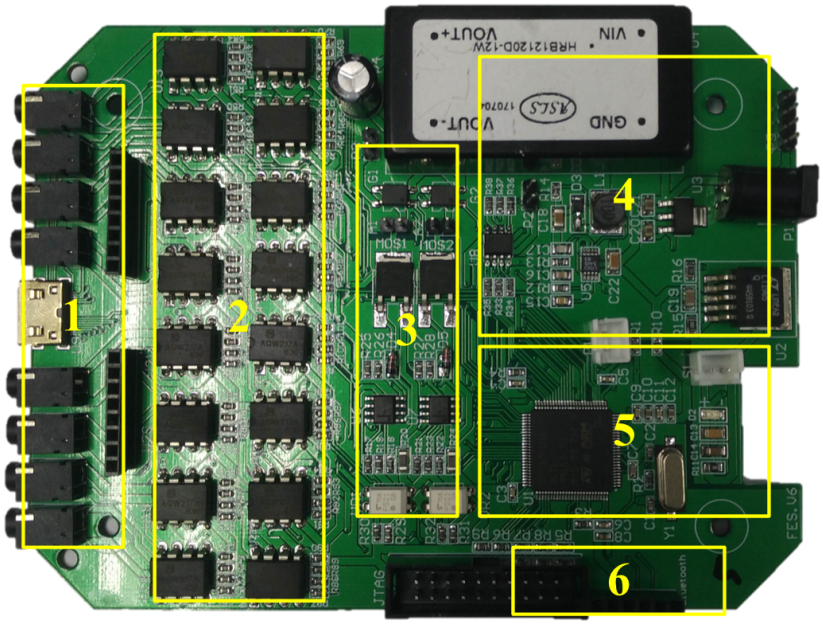

(a) Hardware design of the ETS syste: (1) The output ports; (2) The ESM; (3) The ESOM; (4) The PSM; (5) The MCU; (6) The Bluetooth interface.

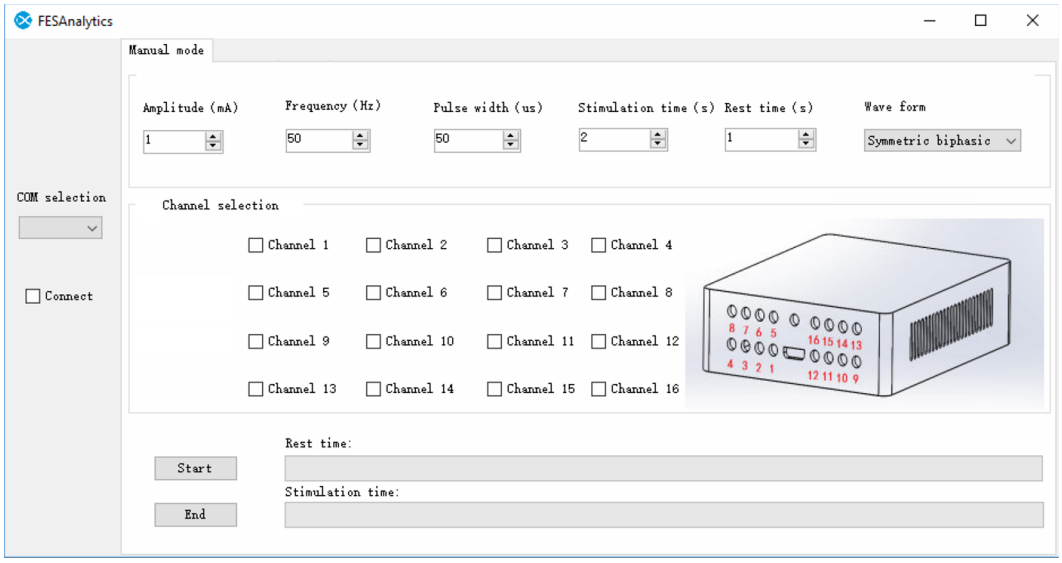

(b) Graphical user interface (GUI) design of the ETS system

Figure 4.4: Design of the multi-channel ETS system

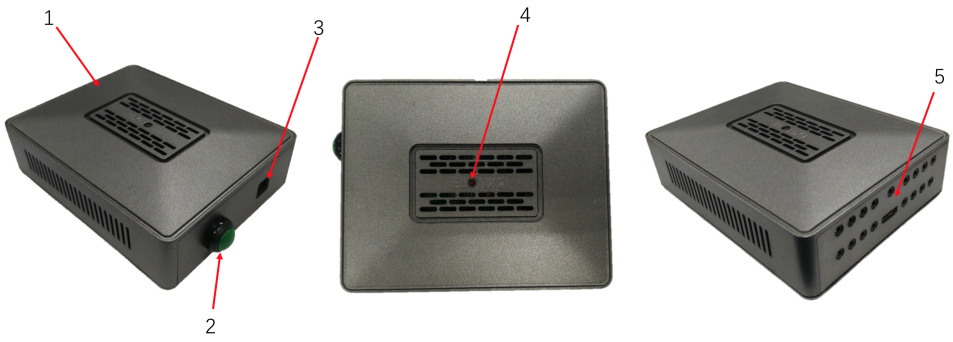

Figure 4.5: Industrial design of the multi-channel stimulator: (1) The shell; (2) The power switch; (3) The LED for power; (4) The output ports

employed in the ETS system. To ensure a stable and constant stimulation output under different load, the voltage is boosted from +12V to +120V by a DC-to-DC converter to supply the following constant current module. Meanwhile, the power is also converted by a voltage regulator to +5V to supply the BM. Then, the +5V is converted to +3.3V by a voltage regulator to supply the MCU. Additionally, the +12V is also boosted to +26V by a voltage regulator to supply the operational amplifier for constant current generation.

4.3.3 Micro Controller Unit

The micro controller unit (MCU) performs a vital role in the ETS system to decode control commands from the host computer and then to adjust and control the output of the stimulation current. STM32F103VCT6 (STMicroelectronics) is selected to be the MCU chip, which is equipped with ARM Cortex-M3, 32-bit RISC core, frequency up to 64 MHz, 8 timers, 2 DAC output, etc. As illustrated in Fig. 4.3, such hardware configuration can meet the requirements of the stimulator's communication ports, including 32 I/O ports (for the 16-channel output control), 4 ports of pulse width modulation (PWM) control signals (for the control of the stimulation frequency and pulse width), and 2 ports of the reference voltages (for the control of the stimulation intensity). The MCU can communicate with the host computer wirelessly via the BM, which is connected with the MCU through a serial port (universal synchronous and asynchronous receiver-transmitter, USART).

4.3.4 Electrical Stimulation Output Module

As stated in Section 4.2.2, the constant-voltage output mode has an advantage of safety, while the constant-current output mode can provide stable output current regardless of the load resistance's variation. Considering the low intensity of the stimulation for electrotactile feedback, constant-current mode is applied to the ETS in this research. The output square pulses are generated by the cooperation of the electrical stimulation output module (ESOM), MCU, PSM and ESM. The output voltage of I/O port controls the optocoupler relay (AQW217) in the ESM to enable or disable the stimulation channels and switch among channels. Fig. 4.6 shows the schematic diagram of the square constant-current generation modules. The ESOM consists of three components: the amplifying circuit (AC), constant-current source circuit (CCSC) and the bridge circuit (BC).

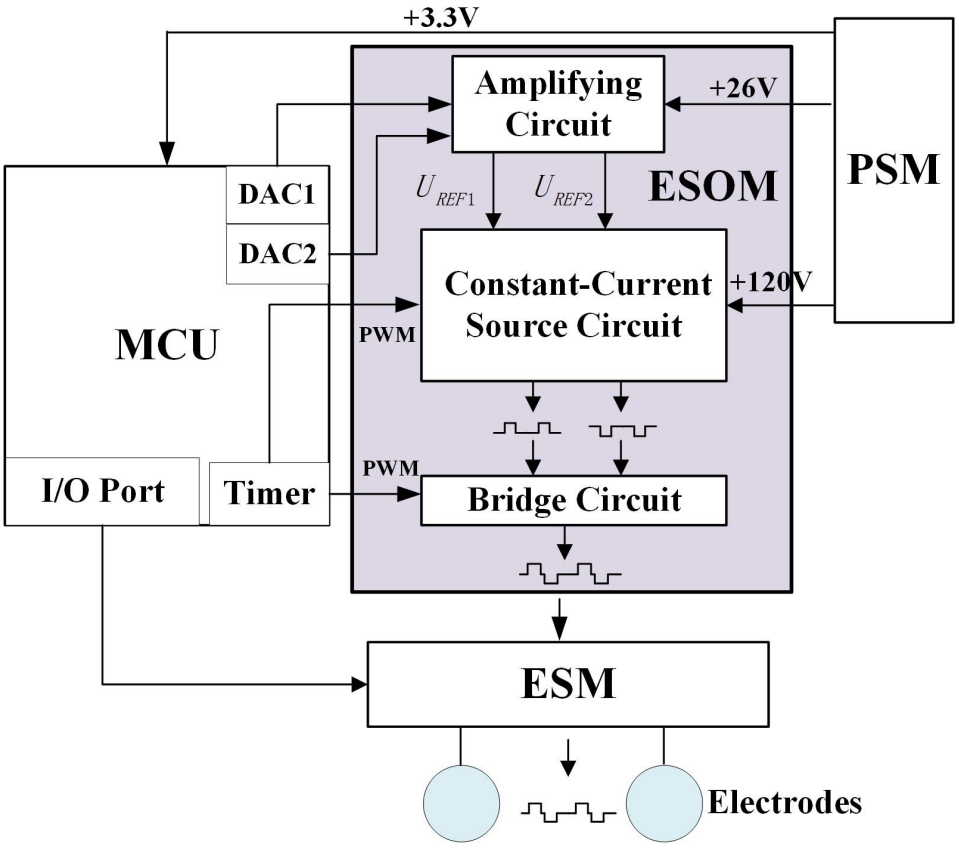

Figure 4.6: Schematic diagram of the electrical stimulation output module (ESOM)

4.3.4.1 Amplifying Circuit

The amplifying circuit (AC) is used to provide the reference voltage for the control of the positive and negative phase of the current's amplitude, based on the DACs' output converting from the MCU. However, the voltage of the DACs ranges from 0 V to +3.3 V, which is too small to be the reference voltage for the CCSC. To solve the problem, the AC is applied to boost the DACs' output voltage to an high enough level to drive the CCSC. The AC is a non-inverting operational amplifier circuit based on the operational amplifier LM358 (Texas Instruments). A circuit schematic is shown in Fig. 4.7. The voltage can be calculated by Eq. 4.1.

$$u_0 = \left(1 + \frac{R_F}{R_1}\right) \cdot u_i \tag{4.1}$$

where u_0 and u_i are the output voltage and the input voltage, respectively.

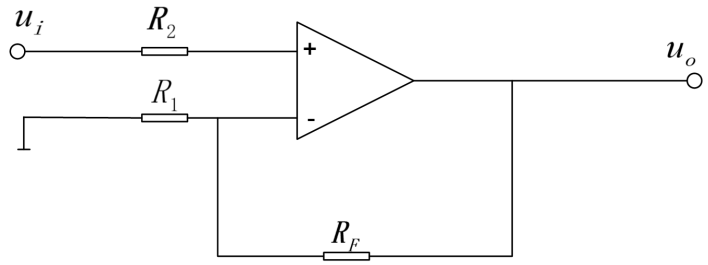

Figure 4.7: Circuit schematic of the amplifying circuit (AC)

4.3.4.2 Constant-Current Source Circuit

The constant-current source circuit (CCSC) is designed to generate the ETS current. It is made up of two constant-current sources which can generate monophasic pulses, one for positive pulses generation and the other for negative pulses. The circuit diagram of a constant-current source is shown in Fig. 4.8, which is based on the operational amplifier (LM358, Texas Instruments) and the MOSFET (metal-oxide-semiconductor field-effect transistor, FDD3N50NZ, Fairchild).

The two operational amplifiers form a current feedback network and compare with the control voltage U_{REF} by detecting and feeding back the current through the resistance R_S, thereby maintaining the drain and source current of the MOSFET at a

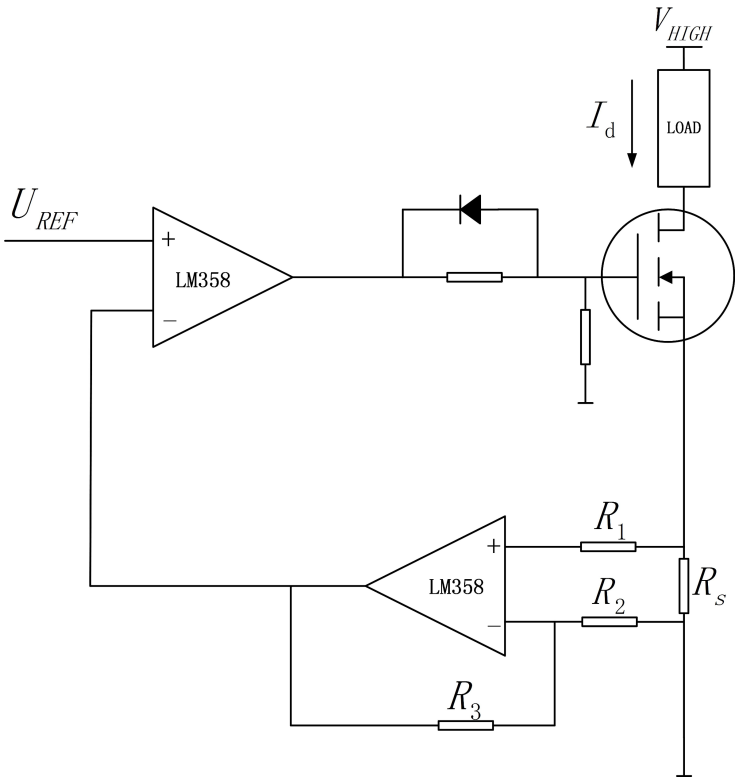

Figure 4.8: Circuit schematic of the constant-current source circuit (CCSC)

constant magnitude. The magnitude of the stimulation current can be calculated by Eq. 4.2.

$$I_d = \frac{R_2 U_{REF}}{(R_2 + R_3)\, R_S} \tag{4.2}$$

where I_d is the stimulation current applied to the skin which is represented by the "LOAD" in Fig. 4.8, U_{REF} is the amplified output from the DAC, and R_s is the sampling resistance to capture the stimulation magnitude of current in real time.

4.3.4.3 Bridge Circuit

The bridge circuit (BC) is applied to generate and regulate biphasic square stimulation pulses. Under the control of the PWM signals controlled by the timers in the MCU, the CCSC cooperates with the BC to realize biphasic pulses with the desired frequency and duration as shown in Fig. 4.9. The PWM signals control the optocoupler 1 and optocoupler 2 (TLP188, Toshiba) to switch on and switch off in turn, so the constant +120V is converted to a PWM-shaped square wave whose amplitude remains +120V, while the pulse width and frequency are consistent with the PWM signals. Similarly, the constant voltage U_{REF1} and U_{REF2} are converted to square waves $U^{'}_{REF1}$ and $U^{'}_{REF2}$ by optocoupler 3 and optocoupler 4 (TLP521, Toshiba), respectively. Thus, when optocoupler 1 and optocoupler 4 are switched on at the same time, the circuit from the power supply +120V to the reference voltage $U^{'}_{REF2}$ is closed. Then, the constant-current source 2 starts working and generates the positive phase of the stimulation current I+. Similarly, when optocoupler 2 and optocoupler 3 are switched on, the constant-current source 1 generates the negative phase of the stimulation current I- in the same way. Finally, the alternating I+ and I- make up the biphasic stimulation current whose amplitude is determined by the reference voltage, while the pulse width and frequency are determined by the PWM signals.

In this study, the optocouplers act as not only the switches for biphasic current generation but also the isolator between the timing signals and the analog circuit of the stimulation current because of the huge voltage difference between them. Optocoupler 1 and optocoupler 2 separate the battery voltage-boosted power supply (+120 V) from the constant current source. Similarly, optocoupler 3 and optocoupler 4 separate the reference voltages and the constant-current sources.

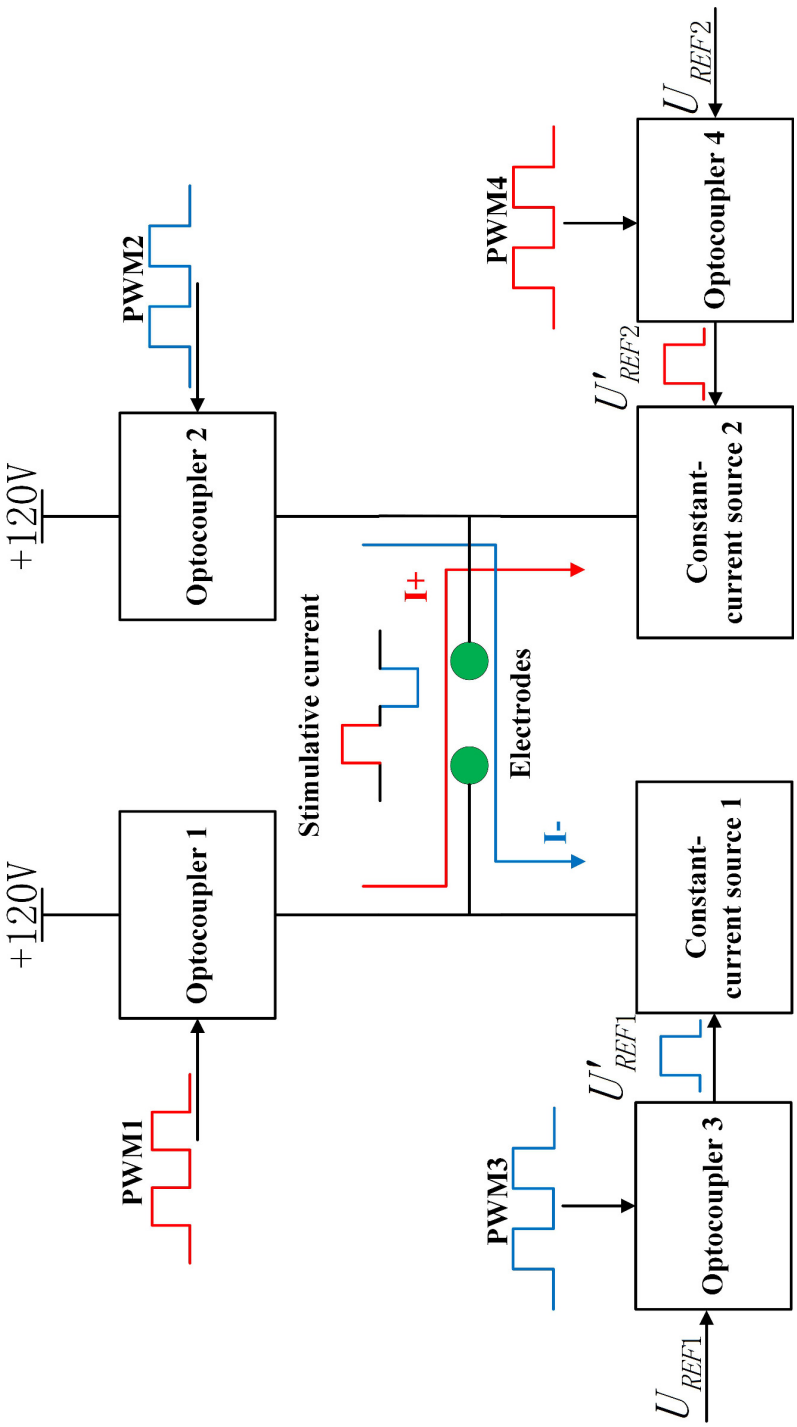

Figure 4.9: Design of the Bridge circuit (BC) module

4.3.5 Stimulation Timing Sequence Design

The adjustment of the stimulation parameters is realised by the PWM signals generated from the timers in the MCU. As presented in Fig. 4.9, PWM1, PWM2, PWM3 and PWM4 control the on-off state of optocoupler 1 to optocoupler 4, respectively. The timing sequence for the biphasic stimulation current generation, including the control signals, reference voltages and the current waveform, is illustrated in Fig. 4.10. The overlapping parts of the high level between PWM1 and PWM4 mean that the optocoupler 1 and optocoupler 4 are being switched on at the same time, which determines the pulse width of the positive phase current. Meanwhile, $U_{REF2}^{'}$ is kept equal to U_{REF2} to determine the amplitude of the current. As for the negative phase, the pulse width is determined by the overlapping parts of the high level between PWM2 and PWM3, and the amplitude is determined by $U_{REF1}^{'}$ when its level is equal to U_{REF1}. All the PWM signals are running in the same frequency which is also the frequency of the stimulation current. When the pulse width of PWM3 and PWM4 are the same and the high level of $U_{REF1}^{'}$ and $U_{REF2}^{'}$ are equal in value, the symmetric biphasic pulse current is realized. Conversely, the asymmetric biphasic pulse current is realized when the pulse width of PWM3 and PWM4 are different, and meanwhile, the high level of $U_{REF1}^{'}$ and $U_{REF2}^{'}$ are not equal. Finally, the monophasic stimulation currents generated from the CCSC are integrated and converted to be a biphasic stimulation current by a proper timing control.

It is worth to be noted that the area of the negative phase should always be equal to that of the positive phase whether it is symmetric biphasic pulses or asymmetric biphasic pulses, because the negative phase plays an important role in eliminating the charge accumulation in the skin and avoiding tissue damage. Besides, to avoid the two constant-current sources working at the same time which may cause the stimulation current into confusion, a short interval time (IT, 100 μs) is set between PWM3 and PWM4, which ensures a separation between the positive phase and the negative phase. Additionally, a dead time (DT) is also inserted between the PWM signals. It is applied to reduce the unexpected current fluctuation or impulses when the high voltage power supply is added to the constant-current source, which will be further explained in Section 4.4.1.

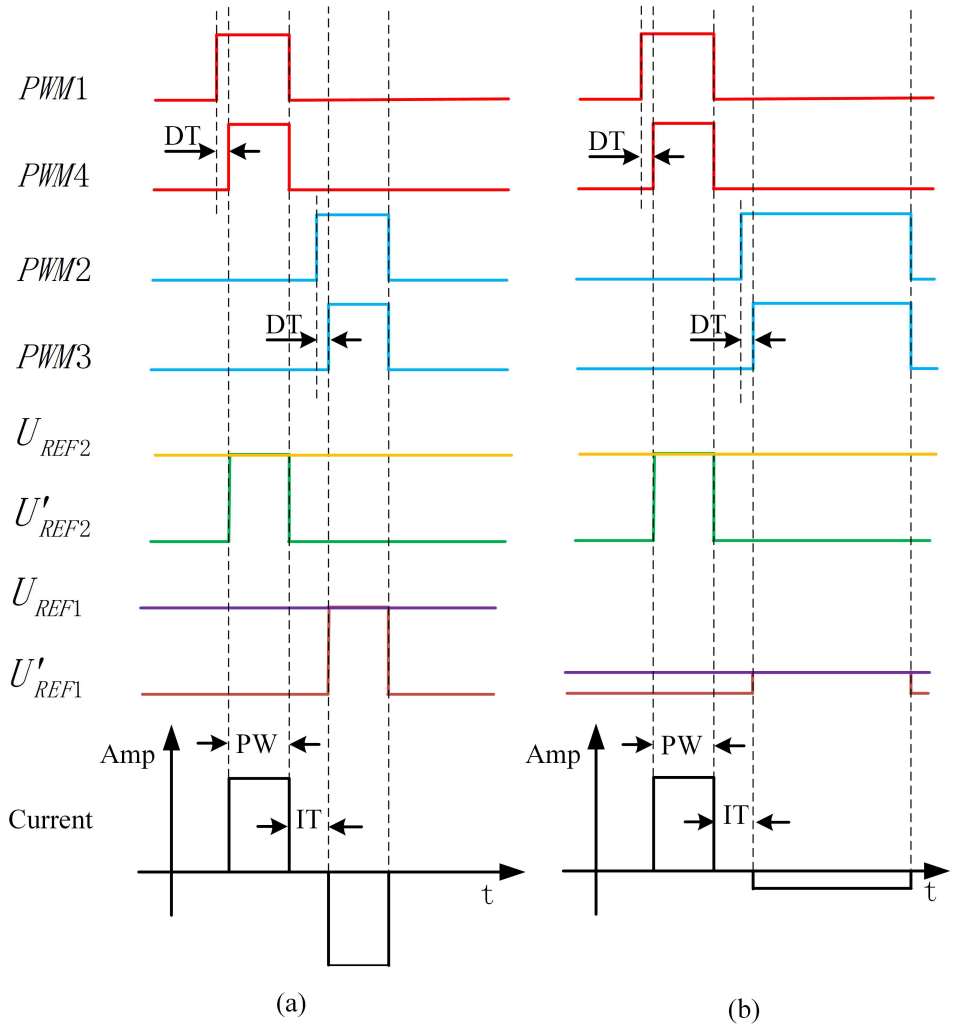

Figure 4.10: Timing sequence diagram of generating biphasic stimulation current in ESOM: (a) Symmetric biphasic; (b) Asymmetric biphasic. DT represents dead-time, PW represents pulse width, Amp represents the current amplitude and IT is the interval time. Note that the area of the positive pulse is equal to the area determined with the negative pulse in both types of the current waveform.

4.4 ETS Output Capability Test

4.4.1 Test of the Stimulation Waveform

The ETS system is expected to output stable stimulation current regardless of the variation of load resistance, The stimulation parameters of all the output channels, including the amplitude, pulse width and frequency, are required to be adjustable. Stimulation capability tests were conducted to test the output performance of the ETS.

The stimulation waveforms of different parameters are recorded and compared in Fig. 4.11. Tests show that there were serious current fluctuation and impulses (pointed by the red arrows) at the rising edges of the amplitude which was the moment that the high voltage power supply was added to the constant-current source. A DT was inserted to reduce the current fluctuation as mentioned in Section 4.3.5. Fig. 4.11(b)- Fig. 4.11(f), show the waveform where a dead time (DT) was inserted between the positive pulse and the negative pulse, while no DT was added in Fig. 4.11(a). Comparing Fig. 4.11(a) and Fig. 4.11(b) which shared the same stimulation parameters, after inserting a DT to the PWM signals when generating the negative square wave as shown in Fig. 4.10, the impulses (pointed by the green arrow) in Fig. 4.11(b) became much smaller than that in Fig. 4.11(a). Furthermore, the DT was added to the start points of both the positive and negative pulses in Fig. 4.11(d), it was obvious that the amplitude of the impulse reduced significantly compared with that in Fig. 4.11(c) in which no DT was added. Thus, the insertion of DT among the PWM signals can effectively suppress the transient current fluctuation during the current switching, although there is still small fluctuation appearing upon the positive phase. The remain fluctuation, whose maximum amplitude and duration were reduced to 60 mA and 7 μs, took place when the DT was set as 30 μs. Besides, Fig. 14(a)- Fig. 4.11(d) were symmetric biphasic currents, while Fig. 4.11(e) and Fig. 4.11(f) were asymmetric biphasic currents, which demonstrates that the system can output both symmetric and asymmetric biphasic pulses.

4.4.2 Test of the Stimulation Current

The constant current output capability of the ETS was also evaluated in this study. Fig. 4.12 presents the performance of the constant-current output of the ETS system with

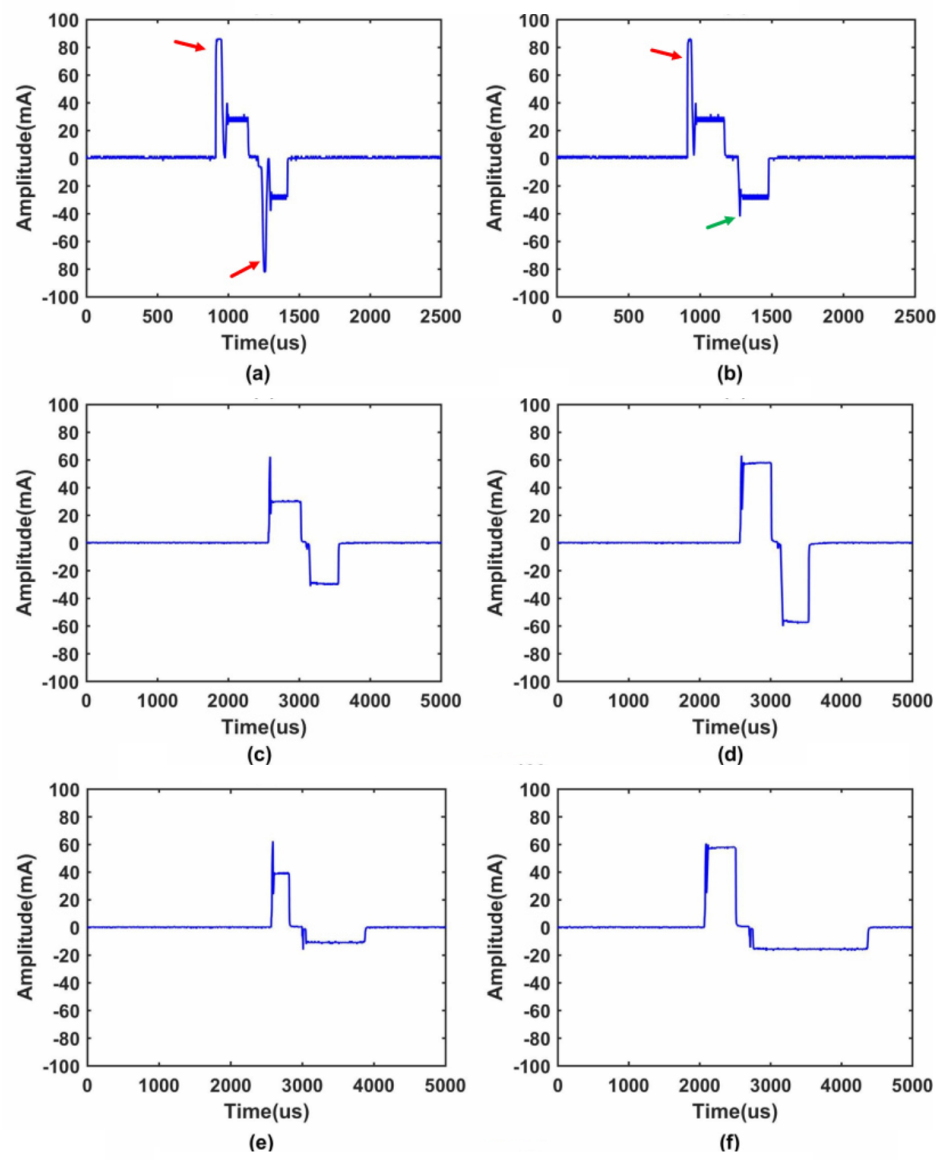

Figure 4.11: Waveform of stimulation current with different parameters: (a) and (b) Amplitude-30 mA, pulse-200 s, frequency-50 Hz; (c) Amplitude-30 mA, pulse-400 s, frequency-50 Hz; (d) Amplitude-60 mA, pulse-400 s, frequency-50 Hz; (e) Amplitude-40 mA, pulse-200 s(positive phase), frequency-50 Hz; (f) Amplitude-60 mA, pulse-400 s(positive phase),frequency-50 Hz. For (a), no DT was added to the control signals for generating the bipolar square wave; For (b), DT was only added to the control signals for generating the negative square wave; For (c)-(d), DT was added to the control signals for generating the bipolar square wave. (a)-(d) are symmetrical bipolar square wave while (e)-(f) are asymmetrical bipolar square wave.

the variation of the load resistance. The amplitudes of the voltage on load resistance were measured when the fixed stimulation current was going through it. The load resistance varied from 200 $\Omega \sim 3$ kΩ (metal-oxide film resistance, error $\pm 5\%$), and the average resistance of the human body is about 2 kΩ. The low current output of 4/8 mA and the high current output of 30/60 mA were tested, respectively. The theoretical output results were simulated according to $I \times R_{load}$.

As shown in Fig. 4.12(a), the ETS could maintain a constant output close to the simulated value when the current was set at low amplitutes such as 4 mA and 8 mA, as well as the 30 mA-output in Fig. 4.12(b). However, when the current went up to 60 mA, the output current could keep stable only if R_{load} <2 kΩ. When R_{load} >2 kΩ, the system could not maintain the 60 mA-output and the current decreased with the resistance increasing. It is because the load voltage could not reach +120 V due to the power loss in the system, although the maximum value of the voltage supply to the constant-current was +120 V. Table 4.1 compares the proposed ETS system with different commercial electrical stimulating systems. The proposed ETS system's parameter modulation is comparable with other systems, meets the requirements of ETS and FES, and it has advantages of the portable size and more output channels.

Table 4.1: Comparision of commercial electrical stimulation systems and the proposed ETS system

Device	Output channels	Amplitude (mA)	Frequency (Hz)	Pulse width (μs)	Dimensions (mm)	Company
RehaStim 2	8	0-130	2-220	0-500	$1200 \times 540 \times 600$	HASOMED, Germany
Quattro 2.5	4	0-100	0-249	30-400	$381 \times 267 \times 21$	Roscoe Medical, USA
Premier Plus	2	0-100	1-200	0-500	$120 \times 60 \times 3$	The TENS Company, UK
Proposed ETS	16	0-55	1-100	0-500	$138 \times 108 \times 35$	-

4.5 Summary

This chapter presented the system design of the multi-channel ETS system. The proposed ETS system has 16-channel outputs which exceed the channels of most portable

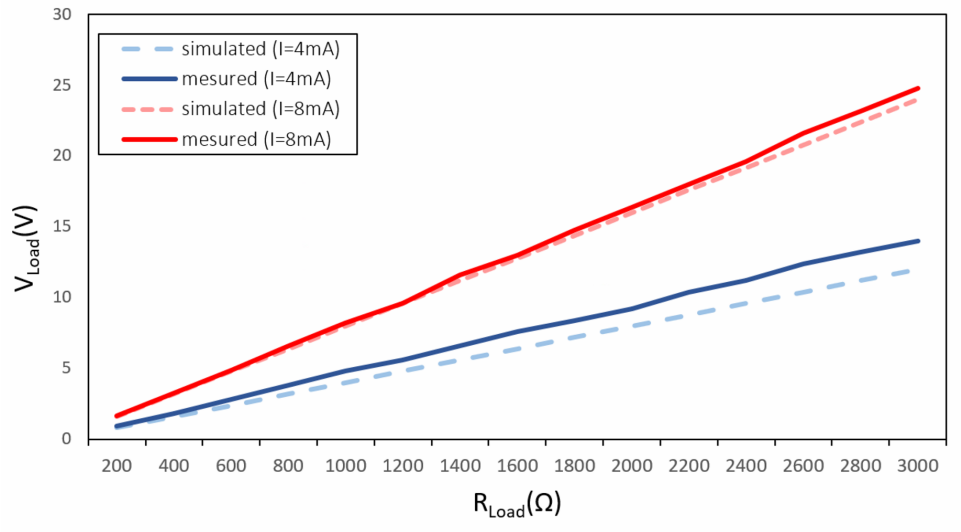

(a) Constant current output of 4 mA and 8 mA

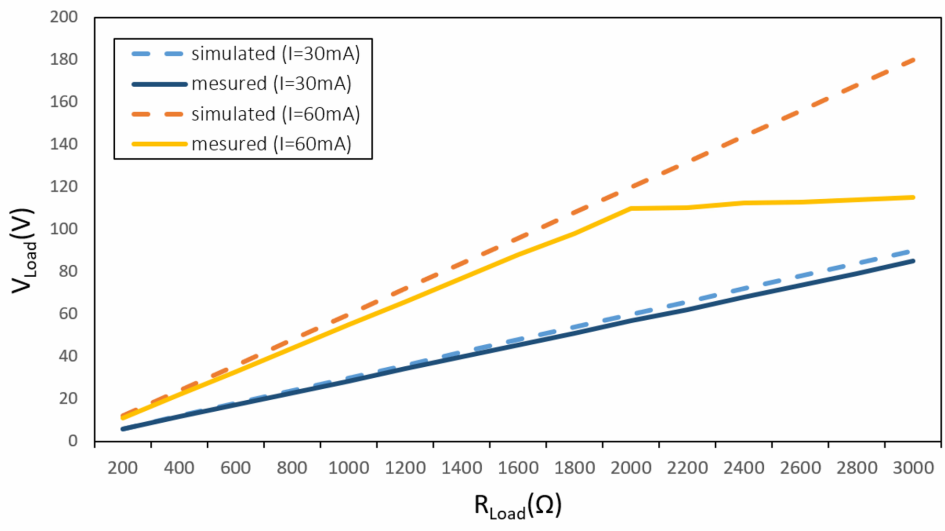

(b) Constant current output of 30 mA and 60 mA

Figure 4.12: Current output capability test

stimulators of a similar size and can be applied for both ETS and FES. Its multiple and adjustable outputs enable flexible coding schemes for electrotactile feedback. The constant current output mode is applied to generate a consistent tactile sensation by outputting stable stimulation current. The portable size and wireless communication mode make the proposed ETS potential to be integrated with hand prostheses. The proposed system can not only be used as a treatment for rehabilitation or daily use for amputees but also provide an extensible platform for future study.

Chapter 5

Evaluation of Electrotactile Feedback on a Virtual Hand Rehabilitation Platform

The absence of suitable tactile feedback leads to an inferior rehabilitation performance with a compromised usability and a huge burden of user training. It is challenging and essential to integrate a proper tactile feedback module with the existing hand rehabilitation systems to achieve a better control performance and accelerate the rehabilitation process. Thus, this chapter focuses on the implementation and evaluation of the elecrotactile feedback in the hand rehabilitation process. A virtual hand rehabilitation platform comprising multiple functional modules is proposed to conduct a closed-loop force control. Experiments of three different feedback conditions including visual feedback, electrotactile feedback and no feedback are conducted and compared based on the proposed platform. The remainder of this chapter is organised as follows. Section 5.1 review the implementatons of tactile feedback in both academia and practice together with a introduction of the virtual environment application in therapeutic training. Section 5.2 demonstrates the design of the virtual hand rehabilitation platform. The experimental setup, protocol and analysis criteria are described in Section 5.3. Experimental results are presented and discussed in Section 5.4 and Section 5.5, respectively. A summary of this chapter is provided in Section 5.6.

5.1 Introduction and Related Work

Tactile sensation of the human hand is important for the exploration and interaction with the environment in a large variety of tasks, ranging from basic grasps to complex operations of sophisticated instruments. For transradial amputees, the loss of sensations and motor functions due to the amputation can inevitably deteriorate quality of life and make an individual feel less capable and more dependent (Schofield *et al.*, 2014). Even if equipped with hand prostheses, transradial amputees still face to huge obstacles in the process of rehabilitation and some situations where fine-force control is necessary due to the absence of tactile feedback (Kuiken *et al.*, 2009). Thus, it is expected to apply closed-loop control in hand prostheses and the corresponding rehabilitation process by implementing tactile feedback to improve the user experience and prosthesis performance.

It is an important acdemic topic to close the loop of prosthesis control by tactile feedback in the area of upper-limb rehabilitation. Available studies mainly investigated the impacts of tactile feedback on the self-embodiment and prosthesis performance. On one hand, it was revealed that tactile feedback did help to generate a sense of body ownership and improve the user experience (Mulvey *et al.*, 2014)(Ackerley & Kavounoudias, 2015)(Tan *et al.*, 2014)(Tyler, 2016), and it was something that amputees wanted in their prostheses (Wijk & Carlsson, 2015)(Cordella *et al.*, 2016). On the other hand, the opinion of tactile feedback on improving prosthesis performance is still a matter of controversy. Most studies concluded that the integration of tactile feedback improved the performance of prosthesis manipulation (Walker *et al.*, 2015)(Jorgovanovic *et al.*, 2014)(Aboseria *et al.*, 2018), although there were some studies showing an improvement only with certain conditions or users, or even little difference when compared with the non-feedback condition (Saunders & Vijayakumar, 2011). In some cases, clinical therapists claimed that amputees with only visual and audio feedback could acquire comparable prosthetic grasping performance with the performance of a closed-loop condition if the rehabilitation/training process was adequate enough. However, the time-consuming rehabilitation/training process may cost several weeks, months or even more than one year (Miller *et al.*, 2008)(Cheesborough *et al.*, 2015) and also cause a great load of cognitive burden during not only the training stage but also in practical use.

Despite the intensive research on tactile feedback witnessed in academia, limited instances have been utilised in clinical scenarios. Few of the commercial hand prostheses provide tactile feedback, neither the rehabilitation system for their users. This is attributed to the lack of a deep insight into the usability of tactile stimulation and a wearable device for implementation. As a result, prosthesis users have to rely on non-intuitive cues (e.g. vision, motor sound, and the prosthesis velocity of closing) as an alternative solution instead of tactile feedback in the prosthesis manipulation (Wijk & Carlsson, 2015)(Ninu *et al.*, 2014), which requires continuous visual or auditory attention and a heavy cognitive burden. Regardless of some efforts devoted to the hardware development and mechanism understanding (Takeda *et al.*, 2017)(Onesti *et al.*, 1989), it is still challenging and timely to further explore the tactile feedback's impact on the reduction of user training and cognitive consumption in daily life usage.

Virtual environments, together with tactile feedback, can provide an enriched training environment and enhance the sense of interactivity (Pamungkas & Ward, 2016), which may boost the user's involvement and perceptive ability for a better rehabilitation performance. Especially for circumstances requiring fine-control, such as grasping eggs, people can practice in a virtual environment without creating any waste or causing any damage. As a promising therapeutic training tool, Virtual environments is potential to generate an immersive and enjoyable treatment display for upper limb rehabilitation (Levin *et al.*, 2015) and act as a flexible platform that can be customised to meet the individual needs (LeBlanc *et al.*, 2013).

Thus, this chapter establishes a virtual rehabilitation platform by integrating the aforementioned multi-channel electrotactile stimulation system and the haptics model with a virtual hand environment. Experiments are conducted on the platform to confirm the effectiveness of electrotactile feedback and investigate how it influences the hand rehabilitation performance and efficiency.

5.2 Design of the Virtual Hand Rehabilitation Platform

To validate the hypothesis of the tactile feedback's effectiveness on hand grasping rehabilitation, a novel integrated platform is established to support the experiment of virtual grasping in different feedback conditions.

5.2.1 Platform Construction

The schematic diagram of the virtual rehabilitation platform is presented in Fig. 5.1(a) with a detailed decomposition of the virtual environment in Fig. 5.1(b). According to Fig. 5.1(a), after being informed about the weight of the target object, the subject will try to conduct grasp gesture with an empty hand. Then the surface electromyography (sEMG) signal caused by the muscle contraction is detected and processed by an sEMG acquisition module. The output sEMG intensity is sent to a virtual environment where a virtual hand and object are set for grasping display. The rehabilitation process can be switched among three feedback conditions, none feedback (NF), visual feedback (VF) and electrotactile feedback (EF), where different feedback information will be provided to the subject for grasping force control.

Fig. 5.2 presents an experimental setup. Two pairs of sEMG electrodes are attached on a subject's forearm of the left arm. One channel is to extract sEMG signals for grasping force estimation, and the other one acts as a reference signal for noise filtering. The subject will contract arm muscles when he/she is told or presented an object with certain weight and force range of safe holding. Consequently, the sEMG signals generated by muscle contraction will be detected by the sEMG acquisition module, which output the intensity of sEMG signals to the following modules.

In the condition of NF, the subject will be asked to close eyes and complete grasps only based on experience. Regarding the VF condition, the subject is allowed to watch a real-time grasping animation and a force bar displayed via a virtual interface, so that the subject can adjust the muscle contraction accordingly to try for successful grasps. The principle of EF is similar to VF, but the subject receives force feedback according to the electrical stimulation instead of a visual display. Different levels of electrotactile stimulation will be generated by the electrotactile stimulator and delivered to the subject's right arm via three pairs of electrodes. Thus, either of VF or EF will close the loop of grasping force control for the rehabilitation platform.

The close-loop rehabilitation platform is realised by multiple functional modules with the details introduced in the following sections.

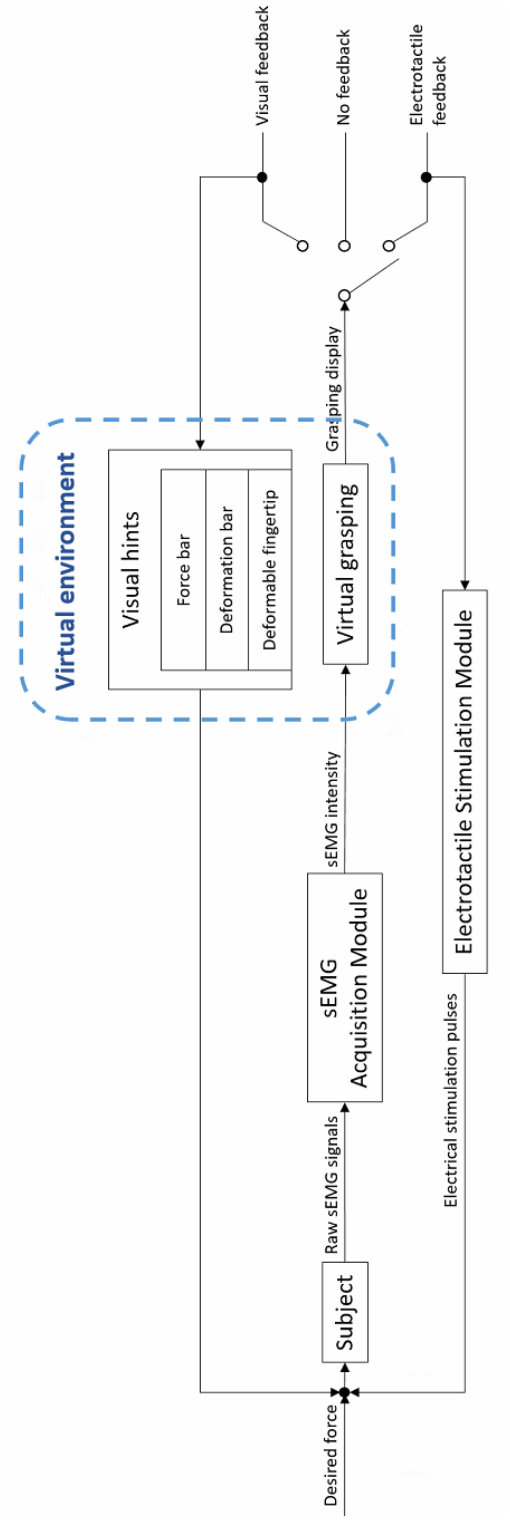

(a) Schematic diagram of the hand rehabilitation platform

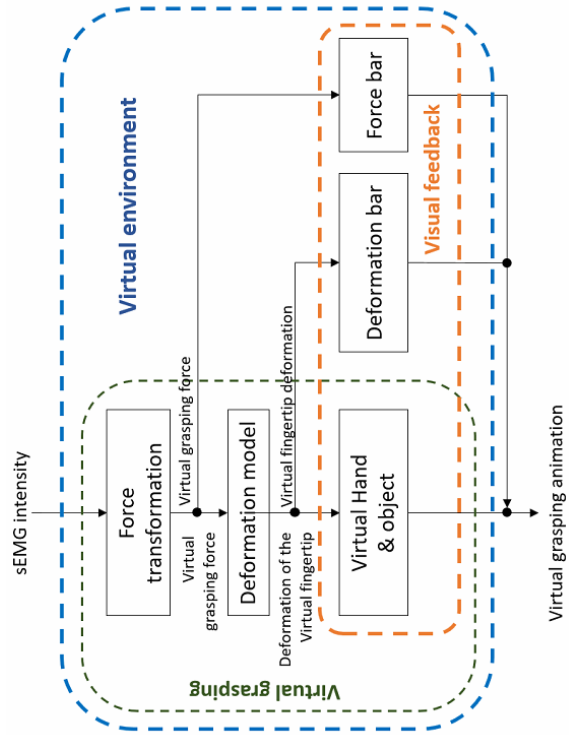

(b) Virtual environment

Figure 5.1: Platform construction

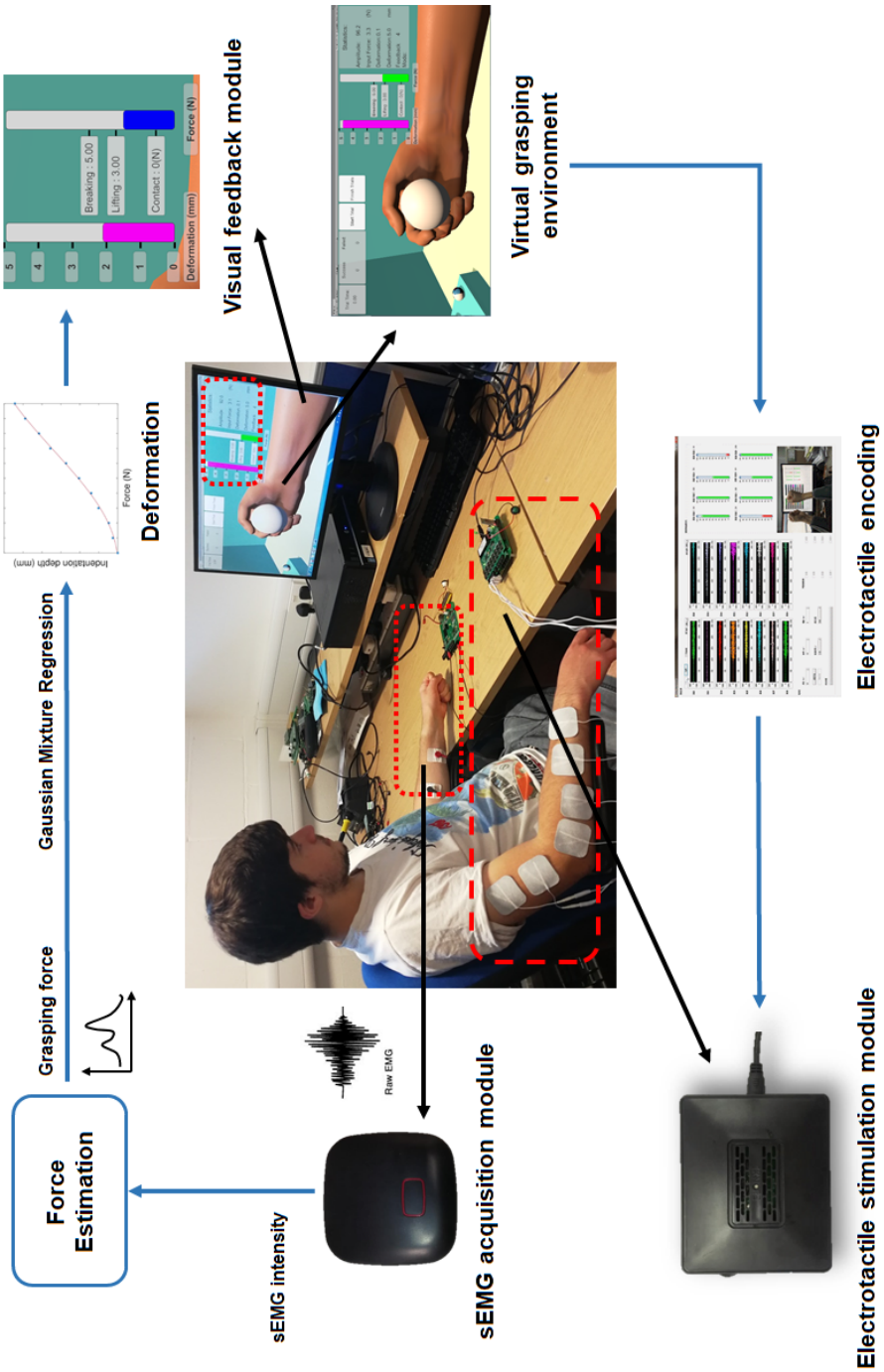

Figure 5.2: Experimental setup

5.2.2 Functional Module Description

The rehabilitation platform consists of an sEMG acquisition module, a virtual grasping environment where a fingertip deformation model is implemented, and an electrotactile stimulation module.

5.2.2.1 sEMG Acquisition Module

For myoelectric prosthesis users, the control of prostheses relys on the decoding of their residule limbs' sEMG signals, which are the electrical manifestation of the activity of muscle fibers and can be recorded by non-invasive electrodes attached on the human skin. The analysis and interpretation of the sEMG signal can be applied for hand motion recognition, control of smart prosthetic devices, and so on. To mimic the prosthesis control process of an amputee, sEMG signals of the subjects' arms are adopted to control the virtual hand and provide an intuitive interaction experience for subjects who conduct the virtual grasping.

In this study, a multi-channel sEMG acquisition system (Elonxi Ltd, UK) is utilised to detect the sEMG signal generated from the subjects' arms (Fang *et al.*, 2015b)(Fang *et al.*, 2017) for the virtual hand control and force estimation. The employed sEMG acquisition device as shown in Fig. 5.3 has up to 16 channels for sEMG signal collection which can be applied for gesture classification, neuromuscular disease diagnosis, etc. The sEMG signals are sampled at a frequency of 1 kHz. After the integrated signal processing, the sEMG acquisition module package and transmit the value of sEMG intensity to the host-computer via a wireless module. In this study, two channels were employed, because only the intensity of sEMG signal was needed and no complex tasks like gesture recognition were involved.

5.2.2.2 Electrotactile Stimulation Module

The ETS system proposed in Chapter 4 is employed to provide force feedback in the rehabilitation platform. The ETS module can deliver different waveforms of stimulation, while the symmetric biphasic square pulse is chosen as the output signal. In biphasic waves, negative pulses can neutralize the charge accumulation on the skin, polarization effect caused by positive pulses and prevent the tissue damage (Baker *et al.*, 1993).

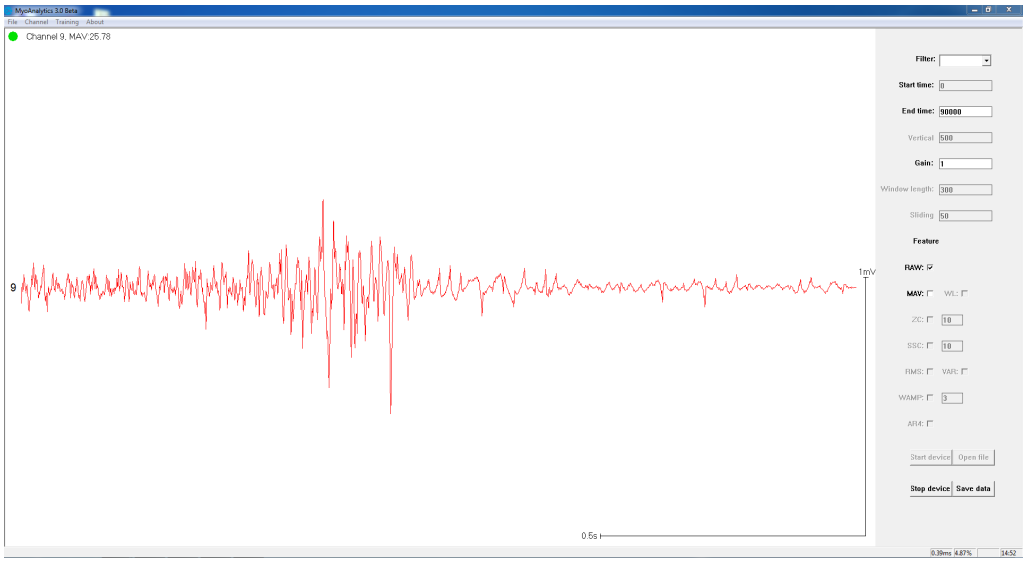

(a) Interface of the sEMG acquisition module

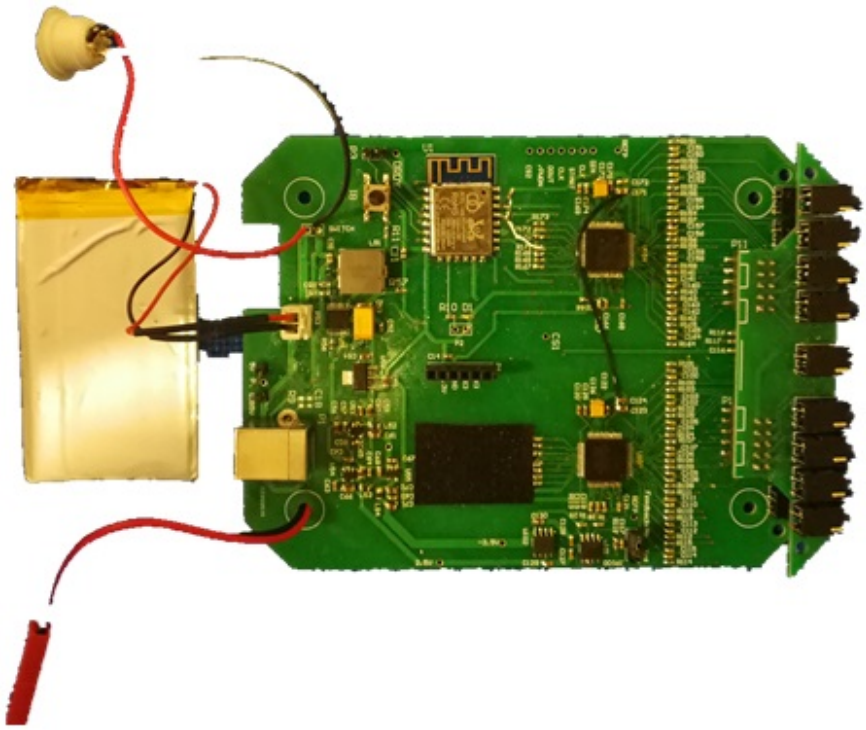

(b) Hardware of the sEMG acquisition module

Figure 5.3: sEMG acquisition module

From the 16-channel's outputs with adjustable parameters, three channels are used to present 9 levels of force intensity. The coding scheme will be detailed in Section 5.3.3.

5.2.2.3 Virtual Grasping Environment

A visual environment of the rehabilitation platform as shown in Fig. 5.4 is designed to conduct rehabilitation procedure with different feedback conditions by integrating the sEMG module and the ETS module. It also provides visual feedback by displaying a deformable virtual hand, a force bar and a deformation bar. A basic hand simulator was applied in the virtual environment (UnityAssetStore, 2018). It was developed into a human-like hand with deformable fingertips during grasping tasks. A ball with adjustable weight and rigidity is set as a grasped object for the practice of fine force control. A force bar shows the grasping force variation and three scales which are the thresholds of contacting, lifting and breaking points, while the deformation bar simultaneously presents the virtual fingertip's deformation depth. The trail results are displayed in the board of upper-left corner, while related statistics are listed in the right.

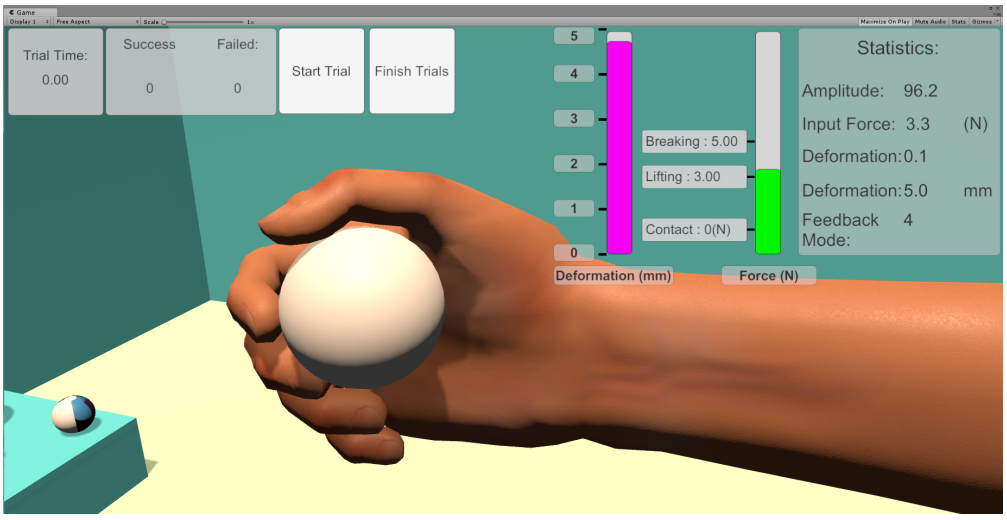

Figure 5.4: Virtual grasping environment

The hand pose, grasping force and the fingertip deformation of the virtual hand are controlled based on the intensity of sEMG signals output from the sEMG acquisition module in real time. With the continual increase of the grasping force, the fingertip deformation started to change accordingly within a range of 0-5 mm as mentioned in

Section 3.2.3. To mimic the human skin, when the fingertip skin was pressed to a certain level, the fingertip did not deform further, although the contact force kept increasing. A two-hierarchical feedback comprising both grasping force and fingertip deformation is applied. Specifically, the feedback strategy is realised in the form of visual feedback and integrated to the virtual platform. Grasping force estimation lies on the basis of force prediction in (Yang *et al.*, 2009), which utilises the sEMG signals to fit the exerted force. The model was tuned by the locally captured data of ten subjects.

The deformation model of the virtual fingertip is designed according to the human fingertip's biomechanics investigated in Chapter 3, which proposed a in vivo dataset of the human fingertip and a haptics model to predict the contacting force according to the fingertip deformation depth. The parameters of the haptics model needed to be customised individually. However, in this study, the deformation depth of the virtual fingertip needs to be calculated according to the virtual grasping force which is estimated based on sEMG signals. Additionally, a generalised model with extensive suitability is also expected for the application of the rehabilitation system. Thus, Gaussian mixture regression (GMR) is introduced to calculate the virtual fingertip's deformation.

GMR is a probabilistic regression method which can be applied based on the parameters of a Gaussian mixture model (GMM). GMM is a mixture of a sequence of Gaussian distributions. It is a popular approach to data approximation and allows for a proper trade-off between the variation of the training data and model complexity (Calinon *et al.*, 2007). A D-dimension Gaussian distribution of a vector $\boldsymbol{x} = (x_1, x_2, ..., x_D)^T$ is defined by Eq. 5.1.

$$p(\boldsymbol{x}) = \frac{1}{\sqrt{(2\pi)^D |\Sigma|}} \cdot e^{-\frac{1}{2}\left[(\boldsymbol{x}-\mu)^{\mathrm{T}}\Sigma^{-1}(\boldsymbol{x}-\mu)\right]} \tag{5.1}$$

where Σ and μ is the covariance matrix and the mean of the Gaussian distribution.

In this study, a GMM consists of K components of 2-dimension Gaussian distributions defined in Eq. 5.2 is used to characterise the variations and correlations across the variables of the aforementioned dataset $\xi_i = \left\{\xi_{f,i}, \xi_{d,i}\right\}_{i=1}^{N}$. The dataset includes N datapoints, and K is set to 3 given the feature of the dataset. ξ_f is the contacting force, ξ_d is the deformation depth of the fingertip, $\xi_{f,i}$ and $\xi_{d,i}$ are the corresponding

ith values.

$$p\left(\xi\right)=\sum_{k=1}^{K}\omega_k\cdot\frac{1}{2\pi\sqrt{\left|\Sigma_k\right|}}\cdot e^{-\frac{1}{2}\left[\left(\xi-\mu_k\right)^{\mathrm{T}}\Sigma_k^{-1}\left(\xi-\mu_k\right)\right]} \tag{5.2}$$

where ω_k is the prior probability (weight) of the kth Gaussian component, and there is $\sum_{k=1}^{K}\omega_k=1$.

To estimate the parameters of the GMM by maximising the log-likelihood, the k-means clustering method and the standard expectation-maximization (EM) algorithm are employed for initialization and iteration. Consequently, the mean μ and the covariance matrix Σ of the kth Gaussian component are obtained as Eq. 5.3.

$$\mu_k=\begin{Bmatrix}\mu_{f,k} & \mu_{d,k}\end{Bmatrix},\Sigma_k=\begin{pmatrix}\sigma_{f,k} & \sigma_{fd,k}\\ \sigma_{df,k} & \sigma_{d,k}\end{pmatrix} \tag{5.3}$$

Taking values of ξ_f as query data, the corresponding ξ_f values are estimated through GMR. The conditional expectation $\widehat{\mu}_{d|f,k}$ of $\xi_{d,k}$, given ξ_f, and the estimated conditional covariance $\widehat{\sigma}_{d,k}$ of $\xi_{d,k}$, given ξ_f, can be calculated by Eq. 5.4.

$$\begin{aligned}\widehat{\mu}_{d|f,k}&=\mu_{d,k}+\sigma_{dt,k}(\sigma_{f,k})^{-1}\left(\xi_f-\mu_{f,k}\right)\\ \widehat{\sigma}_{d|f,k}&=\sigma_{d,k}-\sigma_{df,k}(\sigma_{f,k})^{-1}\sigma_{fd,k}\end{aligned} \tag{5.4}$$

The responsibility λ_k of the kth Gaussian component for the estimation of ξ_f and ξ_d is defined as Eq. 5.5.

$$\lambda_k=\frac{p\left(\xi_f|k\right)}{\sum_{k=1}^{K}p\left(\xi_f|k\right)} \tag{5.5}$$

Based on Eq. 5.4 and Eq. 5.5, the conditional expectation $\widehat{\mu}_d$ of ξ_d, given $\widehat{\xi_f}$, and the conditional covariance $\widehat{\sigma}_d$ of ξ_d, given $\widehat{\xi_f}$, can be calculated by Eq. 5.6.

$$\widehat{\mu}_d=\sum_{k=1}^{K}\lambda_k\widehat{\xi}_{d,k}\quad\widehat{\sigma}_d=\sum_{k=1}^{K}\lambda_k^2\widehat{\sigma}_{d,k} \tag{5.6}$$

Thus, $\widehat{\mu}_d$ is viewed as the estimated value of the deformation of the virtual fingertip ξ_d in the condition of the virtual contact force ξ_f.

5.3 Experimental Setup and Methods

The experiment aims to evaluate the impact of electrotactile feedback on the rehabilitation process. Definitions of various virtual grasp results are given in this section. Then, experimental setups of different feedback conditions are presented, followed by a description of the experimental protocol and methods of data analysis.

5.3.1 Definition of Task Success and Failure

The fine control of different force levels was realised by setting different weights of the objects from light, medium to heavy. Each object was set with certain grasping threshold of lifting and breaking. Subjects needed to apply proper grasping forces to hold each object according to its weight.

A successful grasp trail required the subject to maintain the grasping force between the lifting and breaking points (safe holding range) for at least 2 s. Otherwise, it was considered as a failed trail. If the grasping force kept below the lifting threshold for more than 5 s, the subject failed because of a non-lift. If the force went beyond the safe range for more than 300 ms, such as exceeding the breaking threshold or dropping below the lifting threshold, the trail also failed because the object broke or dropped.

5.3.2 Visual Feedback Setup

The visual feedback (VF) was provided by the interface introduced in Section 5.2.2.3 and a typical illustration was shown in Fig. 5.4. At the beginning of each trial, the virtual hand kept at an open pose. It began to close and touch the ball when the virtual grasping force increased from a relaxed state to the contacting threshold. With the increase of the grasping force, the object was lifted, held or broke subsequently. Despite the realised function of visual fingertip deformation in the virtual environment, a more observable hint is desired for the purpose of user training. Thus, the hand-object interaction is also provided numerically by the deformation bar.

Subjects were asked to practice and conduct successful grasps as many as possible. They received VF by observing the force bar and deformation bar which rose or

dropped linearly to the virtual grasping force. Subjects could adjust their muscle contracting intensity to control the grasping force. After each trail, the system was set to an initial state with the virtual hand open and subjects relaxed arms.

5.3.3 Electrotactile Feedback Setup

Multi-channel electrotactile feedback (EF) was provided by discriminable modes of electrical stimulation in this study to feedback the virtual grasping force. Mixed coding scheme was employed by modulating multiple stimulation parameters, including amplitude, frequency, pulse width and a combination with spacial coding. The stimulation modes were divided to 1-9 levels corresponding to the intensity of sEMG signals/grasping force from light to strong. They were delivered by three pairs of electrodes attached on the subject's right arm. Each pair of electrodes delivered three levels of electrical stimulation from low intensity to high intensity. The stimulation parameters were modulated individually according to the subject's request before the experiment to ensure a comfortable and identifiable perception of each stimulation level. A typical coding scheme applied in the experiment will be provided in Section 5.4.1. During the experiment, subjects could to control the grasping force according to the stimulation levels by adjust their muscle contracting intensity.

5.3.4 Experimental Protocol

The experiment included three stages, preparation, training and testing. Before the experiment, the experimental aim and procedure were explained to the subjects, and then they signed the consent. Ten able-bodied subjects (24-29 years old) participated in the experiment. The study was approved by the local ethical committee.

5.3.4.1 Preparation

The goal of preparation was to get subjects familiar with the rehabilitation system and learn the coding scheme of the electrotactile stimulation. At the beginning, the subject was comfortably seated on an armchair and wore two pairs of sEMG electrodes and three pairs of eletrotactile stimulation electrodes on the left arm and right arm, respectively.

Firstly, the upper limit of sEMG signal intensity was set by asking the subject to contract the left forearm muscles as much as possible for three times. Sixty percent of the average intensity was regarded as the upper limit of the subject's sEMG signal.

Secondly, the stimulation parameters of 9 electrotactile stimulation levels were determined. An initial setting was tested on the subject's right arm. It was adjusted according to the subject's verbal feedback. If the subject reported any discomfort or difficulty in distinguishing stimulation levels, the stimulation parameters would be reduced or increased accordingly until the subject could identify all the stimulation levels without discomfort.

Finally, the subject had one minutes to experience the rehabilitation system and conduct virtual grasps freely with simultaneously VF and EF.

5.3.4.2 Training and Testing

The training and testing process were conducted in three feedback conditions, which included: a) feed-forward control with no feedback (NF); b) closed-loop control with visual feedback (VF); c) closed-loop control with electrotactile feedback (EF).

- **Feed-forward control with no feedback (NF)**

  During the training process, 3 objects of different weights were provided to a subject for virtual grasping in a sequence of object 1 (light), object 2 (medium) and object 3 (heavy). For each object, the subject had one minute to practice grasping by observing the force bar via the visual interface. Then, the subject was asked to close eyes and performed virtual grasping attempts based on practice experience. After each attempt, the subject was informed about the grasping result, whether the object dropped, broke or successfully held, so that the subject could adjust the arm contracting intensity of the arm in the next attempt. Finally, the subject would learn the fine control of force for the object. After the subject successfully grasped the object twice in a row, another object would be shown to the subject. The total number of attempts for each object in training process was recorded.

  In the testing stage, the subject was asked to grasp each object for 10 times. Different from the training process,the objects of different weights were presented randomly to the subjects during the testing stage. The experiment in the

condition of NF was completed when the subject accomplish the training and testing on all objects.

- **Closed-loop control with visual feedback (VF)**

  The procedure in this feedback condition was similar with that of the NF condition, but the subject was allowed to watch the visual interface. The subject could perform virtual grasping according to the force bar and observe the grasping results by himself/herself.

- **Closed-loop control with electrotactile feedback (EF)**

  Different from the other two conditions, a short preparation needed to be conducted before the training with EF. The stimulation parameters determined in the preparation stage were presented to the subject again. On one hand, it would make sure that the subject could identify each stimulation level and was happy with the settings. On the other hand, it would give the subject a second chance to adjust the parameters if necessary. After the finalisation of the stimulation parameters, the researcher stimulated the subject with different stimulation levels randomly and ask the subject to report the level numbers. The preparation process was accomplished until the subject correctly answered all the stimulation levels in a row.

  The training and testing experiment with EF was similar with the experiment with NF and VF, but the subject was asked to close eyes and could only tell the grasping force according to the electrotactile stimulation levels.

The whole experiment for each subject lasted for about 2 hours. Subjects might experience muscle fatigue during the training and evaluation process due to the attempts of contracting arm muscles and the electrotactile stimulation. To avoid discomfort and the interference of muscle fatigue, subjects were free to take a rest at any time during the experiment. For both training process and testing process, the attempt result (success/failure), grasping force and time consumption in each attempt for every object were recoded for the evaluation of different feedback conditions.

5.3.5 Data Analysis Criteria

The rehabilitation performance was evaluated by the following criteria. An initial data processing such as the elimination of the maximum value and the minimum value was conducted before the result analysis.

- **Number of attempts (NoA)**

  The number of attempts is the number of grasping trials before the subject successfully grasped an object twice in a row. This also includes the total number of attempts which were required during the training stage. The number of attempts is used to evaluate how fast the subject could learn the fine control of force in different feedback conditions, and how long the training process took.

- **Duration of training (DoT)**

  The duration of training is the sum of each attempt's duration time for each object in the training process. As a complementary value to the number of attempts, the duration of training also aims at the quickness of the training progress.

- **Duration of an attempt (DoaA)**

  The duration of an attempt is the average time consumed on each attempt during the testing stage. It is used to evaluate the subject's operation speed of the virtual grasp.

- **Success rate (SR)**

  The success rate is the percentage of the successful grasps (without slip or breaking) during the testing stage. The success rate was to evaluate the rehabilitation performance.

5.4 Results

5.4.1 Stimulation Parameter Modulation

The transient upper limit of the sEMG signal's intensity varied with individuals from approximate 400 to 600. Considering that the subject was required to hold muscle

contraction for several seconds, the long-lasting upper limits of subjects were also tested, and they presented little difference with an average of 210.

In contrast, there was a significantly individual difference of the settings on electrotactile stimulation parameters because of a different sensitivity to electrical stimulation among subjects. Table 5.1 demonstrates two typical coding schemes tested in the experiment. The values to the left of slashes belong to a subject who was sensitive to electrotactile stimulations of lower intensity, while the bold values to the right of the slashes belong to another subject who could recognise electrotactile stimulations of higher intensity. The preparation and testing of suitable parameters cost about 30-40 minutes on each subject to ensure a comfortable and effortless perception of the 9 stimulation levels.

Table 5.1: Coding scheme of electrotactile feedback

Stimulation parameter		Amplitude (mA)	Frequency (Hz)	Pulse width (us)
Channel 1	Level 1	3 / 3	10 / 10	50 / 180
	Level 2	2 / 2	30 / 61	50 / 50
	Level 3	2 / 2	45 / 62	70 / 50
Channel 2	Level 4	2 / 3	10 / 10	40 / 180
	Level 5	2 / 2	25 / 60	40 / 50
	Level 6	3 / 2	35 / 61	60 / 45
Channel 3	Level 7	1 / 3	10 / 10	20 / 160
	Level 8	1 / 2	20 / 56	20 / 60
	Level 9	1 / 2	35 / 58	20 / 100

5.4.2 Number of Attempts

The average number of attempts (NoA) per object in different conditions are shown in Figure. 5.5(a). When grasping the lightest object, the subjects' learning performance in different feedback conditions are similar. Across the objects, subjects spent comparable NoA in VF and EF conditions. However, it took approximately twice NoA to grasp heavier object (medium, heavy) in NF condition compared with the NoAs of the other two conditions. The overall average NoAs across conditions as shown in Figure.

5.5(b) also indicate the same information that the VF and EF help to save about half NoA compared with the training in NF condition.

5.4.3 Duration of Training and Duration of an Attempt

The average duration of training (DoT) as shown in Fig. 5.6 presents a similar trend with the NoAs in Fig. 5.5(a). It is reasonable that the DoT is positively correlated with the NoA. The DoT of three feedback conditions were similar when grasping the light object. The VF and EF conditions spent less than 60% of the training time of the NF condition when grasping the medium object and the heavy object. Additionally, the VF and EF showed a more consistent performance than the NF condition given the smaller standard deviations.

Fig. 5.7 presents the average duration of an attempt (DoaA) in different feedback conditions during the testing process. The conditions with feedback (VF and EF) took longer duration to accomplish one attempt than the condition of NF. The condition with EF shows the longest DoaA and the largest standard deviation, while the condition with NF shows the least.

5.4.4 Success Rate

The average SR across different objects and feedback conditions are shown in Fig. 5.8(a). It can be seen that the SR of both EF and VF outperforms that of NF. The SR in EF condition is comparable with that in VF condition when grasping object 1 (light) and object 2 (medium), and is even observably higher than the SR in the condition of VF when grasping object 3 (heavy). Fig. 5.8(b) presents the overall average SR of each condition. Grasping with EF shows the higherst SR, and the standard deviations in different feedback conditions are comparable. It indicates that the percentage of standard deviation out of the average SR in EF condition is lower than those of VF and NF.

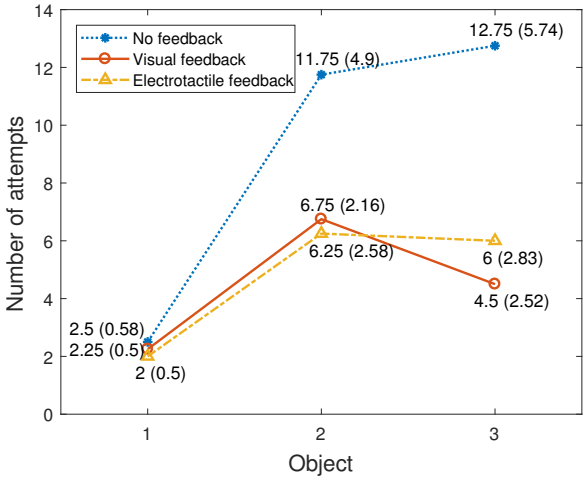

(a) Average number of attempts with the standard deviation of each object in different feedback conditions

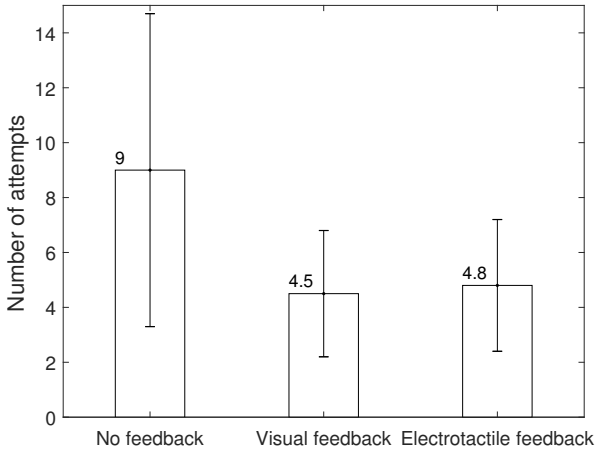

(b) Average number of attempts of all objects in different feedback conditions

Figure 5.5: Average number of attempts of training

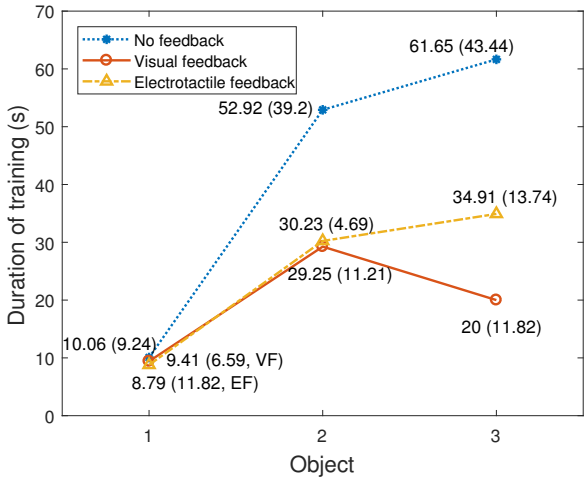

Figure 5.6: Average duration of training with the standard deviation of each object in different feedback conditions

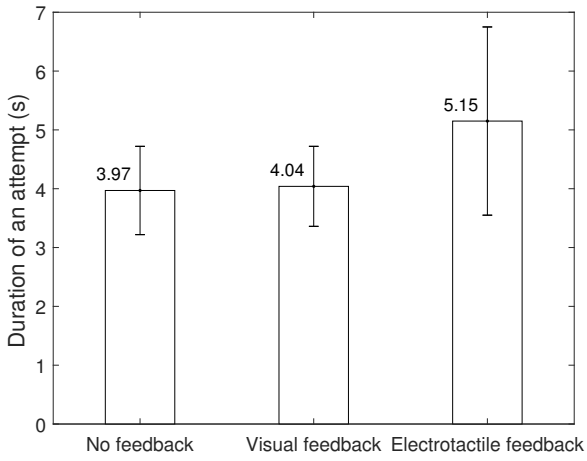

Figure 5.7: Average duration of an attempt in different feedback conditions

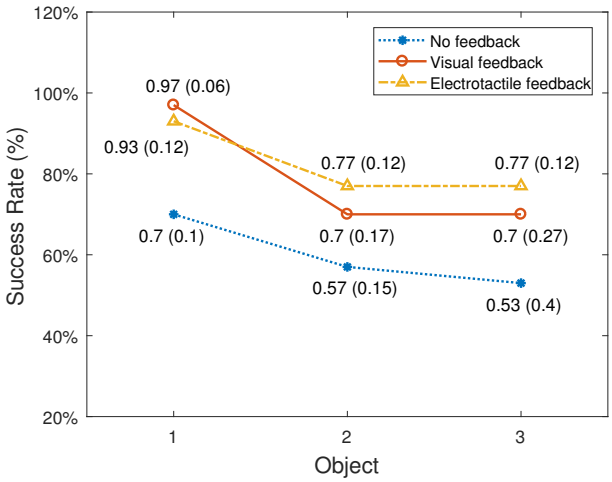

(a) Average success rate with the standard deviation of per object in different feedback conditions

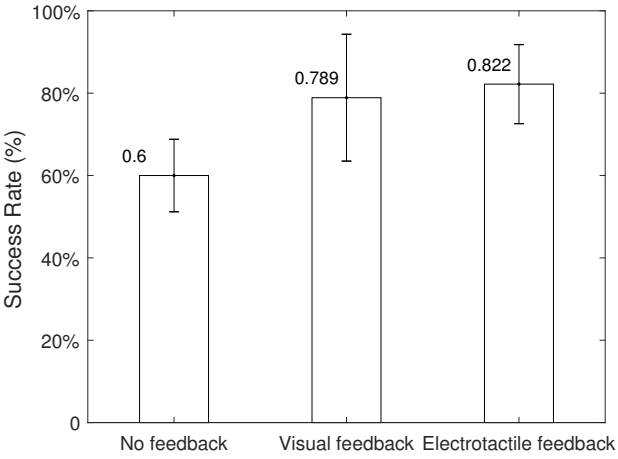

(b) Average success rate in different feedback conditions

Figure 5.8: Average success rate during testing process

5.5 Discussion

The numerical results acquired from the experiments on ten subjects indicate that both VF and EF contribute to an improved training efficiency and grasp control performance. A plausible explanation is that the incorporation of a feedback module provides a reference for users to adjust their voluntary effort of grasp in comparison with the open-loop control, and results in an improved hand grasp in virtual environment for rehabilitation in terms of number of attempts, duration of training and success rate. The average number of attempts is the trials required for a success of grasp in the training process, which reflects the learning rate of the users when equipped with different feedback strategies. The absence of a proper feedback module brings about the need of a large amount of attempts in training. The heavy training burden without a proper feedback is also revealed by the duration of training when compared to settings with the other two strategies adopted. Both VF and EF reduce the required trials by half of the requirements in an open-loop control. Thus the burden of user training is largely reduced, which potentially contributes to a favourable choice by users and the rehabilitation therapists. For example, an average of 2.5 hours is demanded in the experiments for each subject, most of which is occupied by the training without feedback modules. A replacement of the absent feedback module by either VF or EF is capable of alleviating the time-consuming training burden.

It can be seen from the experiments that the average time of an attempt with feedback is longer than that of an open-loop control, although an improved efficiency is provided by the incorporated feedback. This phenomenon is in accordance with the intuitive understanding that users would conduct straightforward hand grasps without adjustment of their force exertion, which in turn leads to an inferior adaptation to the inevitable variation of muscle contraction during a maintained grasp. As a result, the lack of such a process in conventional grasp control leads to a reduced delay yet with a compromised performance. The increase of the average time of an attempt in a closed-loop control is possibly due to the guided self-correcting process, which is perceptive and involves the users' voluntary effort in accommodating the dynamic difference between exerted grasp force and desired force. Moreover, despite the negligible delay introduced by the self-correcting process, the usability of the control process is largely improved together with the implicitly improved efficacy, which is partially reflected

by a better success rate. A significant improvement of the success rate of grasping 3 objects is seen by an average increase of nearly 15% and 17% for the VF and EF, respectively. The improved success rate is in line with supporting and shortening the pathway to grasp control in real life. In summary, both VF and EF outperform the open-loop control according to the numerical metrics of grasp evaluation in the whole training and testing phases, while the visual one is more favoured. The force can be controlled in a more stable and successful scheme, because of the continuous variation of grasp force according to the numerical hints provided by VF.

Despite that the fact that VF shows a superior performance with the least number of attempts and the least duration of training among three candidate feedbacks together with a relatively small sacrifice in the required duration of each attempt, it is not practical to utilise the visual hints in clinical applications such as a force bar and a deformation bar to indicate the real-time grasping force. Besides, the concentration of users during their prosthesis and virtual hand manipulation is mostly confined to the hand-object interaction without spare capacity left for the visual hint observation. As a result, the application of VF is strongly restricted to a laboratory environment for its non-perceptive nature. Regardless of some degraded metrics in comparison with VF, the EF remains a promising and effective way to provide proper feedback, considering its feasibility in reality and the comparable performance with VF. Let alone the clinical feasibility, an even better success rate is observed on EF in the experiments, which is possibly attributed to a more effective self-correcting process with the prioperception of hand involved.

In this research, not only the average performance across multiple subjects is concerned, the variation that resides within grasping different objects is also depicted in the experiment results. An intuitive conclusion is that the control of grasping a light object is easier for the users with less training time required yet better success rate. An exception is observed in the EF incorporated heavy object grasp. A better control of grasping the heavy object instead of the medium weighted object is captured as shown in Fig. 5.8(a). A potential cause of this result could be the perceptive nature of electrotactile stimulation rather than the numerical hint given by VF. The adjustment of hand grasp force between a certain interval with quantitative feedback allows the control without abrupt changes. A large grasp force tends to require more intense muscle contraction, which is not as stable as the light contraction to exert small grasp force. As

a result, the prioperception based EF control of grasping a heavy object with a larger force shows an improvement in terms of success rate.

In addition to the time-consuming process of user training, the testing of suitable stimulation parameters in preparation stage cost quite long time of almost 1/3 of the whole experiment duration, which is due to the large variation of individual of sensitivity to electrotactile stimulation. For example, during the experiment, it was found that subjects seem to be much more sensitive to the change of frequency than amplitude and pulse width. A modulation method is expected to simplify the preparation process to save time. Besides, the intensity of perceived sensation is not linearly mapped to the stimulation intensity. When the stimulation intensity exceeded a certain level, several subjects reported a less intensive perception.

5.6 Summary

This chapter proposed the virtual hand rehabilitation platform which integrated the sEMG acquisition module to extract the subject's muscle contraction information, the virtual grasping environment to simulate a hand grasping process and act as an operating interface of the platform, and the electrotactile stimulation module proposed in Chapter 4. Based on this platform, the training and evaluation of hand grasping tasks were conducted and compared in different conditions with no feedback, visual feedback, and electrotactile feedback. Experiment results confirmed that the electrotactile feedback is feasible and effective in reducing the burden of user training and improving the rehabilitation performance. Furthermore, the flexibility of the virtual environment allows the expanding of the current platform into a broader spectrum of motor function rehabilitation applications.

Chapter 6

Conclusions and Future work

Electrotactile stimulation is a dominant tactile feedback method to restore the tactile perception, i.e. "sense of touch", for prosthesis users. This thesis focuses on the implementation of electrotactile feedback in hand rehabilitation.

To investigate the mechanism of the human sensory system, a description of the skin architecture and mechanoreceptors is provided to have a general view of the human tactile-related sensory system. When a physical contact deforms the skin surface, it may activate the underlying mechanoreceptors and generate a corresponding tactile sensation. Given that most hand-object contacts happen on fingertips, a haptics model of the relation between the contact force and the skin deformation is proposed to further characterise the mechanical behaviour of the human fingertip. Based on the human-side knowledge, an electrotactile stimulator is designed as an artificial tool for tactile sensation restoration. Furthermore, a virtual hand rehabilitation platform is established by integrating the haptics model, electrotactile stimulator and other functional modules. The feasibility and effectiveness of electrotactile stimulation on the hand rehabilitation are investigated based on the platform.

This research aimed to provide a fundamental investigation of electrotactile feedback for clinical use and presented related theoretical model and experimental results that may benefit the future practical implementation. The achievements for main chapters and the conclusions of the thesis are summarized in Section 6.1. Future research topics are discussed in Section 6.2.

6.1 Conclusions

6.1.1 Summary of the Results in Main Chapters

- **Chapter 3: Probability-based Haptics Model**

  In this chapter, a probabilistic haptics model was proposed to characterise the relation of the contact force and the fingertip deformation. Experiments were conducted to collect the contact forces at discrete indentation depth (0, 0.5, 1, ..., 4.5, 5 mm) on the fingertip from ten subjects. There is a non-linear and monotonically increasing relation between the contact force and the fingertip deformation. The force dispersion extended with the increase of the indentation depth. Despite the common features, individual differences can be observed in the force variation range and slope. Based on the collected data, a haptics model, which includes a prediction model to estimate the contact force according to the fingertip indentation depth and a force-deformation distribution model based on Gaussian distribution to characterise the force uncertainty, was established to describe the biomechanics of the human fingertip. The parameters of the haptics model were regulated individually. Four common-used fitting methods, Fourier series model, Gaussian distribution model, polynomial model and exponential model were applied and compared for the estimation of parameters. After model training, validating and testing, Fourier series model and exponential model were chosen to fit Gaussian distribution's mean and standard deviation which were the expressions of force and depth, respectively. The former was also the prediction model which output the most possible contact force under a certain indentation depth, and the probabilistic force variation model could be obtained by introducing the fitted expressions of the mean and standard deviation into the Gaussian distribution.

- **Chapter 4: Design of the Electrotactile Stimulation System**

  In this chapter, a multi-channel electrotactile stimulation (ETS) system was designed for the provision of electrotactile feedback. A general theoretical background of an electrical stimulator's design was introduced, including a typical

design structure, output modes, and output waveforms. Then, a detailed description of the framework and main functional modules of the proposed ETS system was given. The hardware of the ETS system was powered by a +12 V DC battery, which was boosted to +120 V to ensure a stable and constant output. The micro controller unit (MCU) communicated with the host computer via a Bluetooth module and decoded commands to control the output stimulation pulses. The constant-current output mode was employed to ensure a stable current output regardless of load variation. The electrical stimulation output module (ESOM) consisted of the constant-current source circuit (CCSC) to generate stimulation current, amplifying circuit (AC) to boost voltage to drive the CCSC, and the bridge circuit (BC) to regulate biphasic square pulses whose timing sequence was controlled by the pulse width modulation (PWM) signals generated by four timers. The stimulation parameters, including the amplitude, frequency and pulse width, were adjusted by the ESOM. Output capability tests were conducted to test the stimulation waveforms and the output stability with the load resistance variation. According to the preliminary tests, a short interval time (IT) and a dead time (DT) were inserted among the PWM signals to prevent logic errors and reduce the pulse fluctuation. The optimised stimulator was capable to output stable and comfortable stimulations with monophasic pulses, symmetric biphasic square pulses, and asymmetric biphasic square pulses. The stimulation current could maintain constant when it was less than 30 mA.

- **Chapter 5: Evaluation of Electrotactile Feedback on a Virtual Hand Rehabilitation Platform**

  In this chapter, a virtual hand rehabilitation platform was established to conduct hand-related rehabilitation tasks and experiments. A graphical interface was provided to act as an operating panel of the integral platform and display a human-like hand which was driven by an sEMG acquisition module. The virtual hand was equipped with a deformable thumb due to a built-in deformation model which was derived from the haptics model proposed in Chapter 3. An object with adjustable weight and rigidity was set for the control of the virtual grasping force which could be estimated by the subject's sEMG signals generated by muscle contraction. The hand rehabilitation platform could be utilised

for tasks with no feedback, visual feedback and electrotactile feedback. In the condition with visual feedback, the deformable virtual hand, a force bar, a deformation bar and related statistics were presented to subjects as visual hints for the grasping force control. As for the electrotactile feedback, the intensity of the virtual grasping force was coded to 9 levels of electrical stimulation provided by the electrotactile stimulator designed in Chapter 4. Three stimulation channels were employed and a mixed coding strategy was applied to the coding scheme. In this condition, subjects could only rely on the identification of stimulation levels to modulate their muscle contraction. Grasping Experiments in three feedback conditions were conducted on ten able-bodied subjects based on the rehabilitation platform. Four criteria were adopted to evaluate the user training and testing grasp performance, including the number of attempts (NoA), duration of an attempt (DoaA), duration of training (DoT) and success rate (SR). Results showed that the NoA, DoT and SR of tasks with feedback observable outperformed those with no feedback, while the DoaA of non-feedback condition was the shortest compared with the other two. Given the increase of SR, the NoA and DoT of the visual feedback and electrotactile feedback conditions were only half of those in the non-feedback condition which indicated a large reduction of the training time and training burden. The slight increase of DoaA with feedback was in accordance with the intuitive understanding that it was a process for subjects to adjust applied force based on some prompt information compared with a straight-forward grasp without any feedback. The overall performance of electrotactile feedback was comparable with visual feedback, although the visual feedback achieved a slightly better result. However, it was not practical to utilise the visual hints, such as the force bar in reality and pay spare attention to observe skin deformation. Thus, the electrotactile was evaluated to be a promising and effective way to provide tactile feedback, considering its feasibility in reality and the comparable performance with visual feedback

6.1.2 Summary of the Conclusions

The main contributions of the thesis come from three aspects, proposing the biomechanical model of human fingertip, establishing the hardware and software platform

for the implementation of electrotactile stimulation in practice, verifying the effectiveness of elelctrotactile feedback on rehabilitation duration reduction and performance improvement.

For the first aspect, the haptics model was proposed to reflect the non-linear relation between the force and the fingertip deformation depth when the physical contact happened. Different from previous studies, the force uncertainty/variation was also characterised by introducing Gaussian distribution.

With regards to the system design, firstly, the multi-channel electrotactile stimulator was proposed as a prototype of portable electrotactile devices which can be applied to not only prostheses but also a wide range of applications, such as virtual reality, robotics and remote operation. The stimulator's multiple output channels and adjustable stimulation parameters enable the application of spatial coding and mixed coding strategy and make it flexible to be applied for clinical use. The electrotactile stimulator also has an advantage of wireless communication mode via Bluetooth, which makes it suitable to be worn and integrated with hand prostheses. Furthermore, the stimulator with a stable output capability up to 30 mA can also be used for functional electrical stimulation which aims at motor recovery by activating the skeletal muscle of the paralyzed patients to complete desired motions. Secondly, the extensible virtual hand rehabilitation platform was established to implement various feedback modes and hand-related tasks. Its interactive and enjoyable display together with the electrotactile feedback can provide an enriched training environment and encourage the subject's involvement. Additionally, not limited to the virtual grasp, the proposed platform is a promising therapeutic tool to be utilised in a broader spectrum of motor function rehabilitation applications because of the flexibility of virtual environments.

Finally, based on the above work, electrotactile feedback was evaluated and compared with visual feedback and no feedback in the virtual grasping task. Compared with no feedback, electrotactile feedback was confirmed to be effective on reducing the user training burden and shortening half of the rehabilitation duration with a comparable or even improved manipulating performance, despite a negligible delay in each grasping attempt introduced by the self-correcting process. Regarding the visual feedback, visual hints, such as the force/deformation bar, are not practical in reality, despite the fact that it shows a superior performance among three candidate feedbacks. Thus,

electrotactile feedback is an effective way to provide tactile feedback in hand rehabilitation and hand prostheses, considering its satisfactory performance and feasibility in practice.

6.2 Future Work

The description of electrotactile feedback and the presentation of related results in the thesis indicate that the tactile feedback techniques, especially electrotactile stimulation, can benefit prosthesis users and has a wide range of potential applications. However, there remain lots of open challenges and emerging topics in this area which can be investigated in the future. This section presents a list of potential research topics in this area.

The first direction of the future research is the theoretical extension of the current work from the following areas.

- The proposed haptics model characterises the fingertip's biomechanics under a single-point load. To achieve a more comprehensive and deeper understanding of the fingertip's haptics-related behaviour, further studies can be expanded to a multi-point model, a skin surface deformation model, or even a 3D fingertip model. The achievements can be applied to a series of applications, such as the artificial skin development and visual monitored environments for force measurement and prediction.
- It is found in the experiments that the modulation of suitable stimulation parameters for each subject is very time-consuming. On one hand, this is due to the huge individual differences in the sensitivity to electrotactile stimulation. On the other hand, how different stimulation parameters have an effect on the subject's sensory system is still unclear. Thus, an investigation of the action mechanism of electrical stimulation parameters on the human neural system should be considered in the future. Accordingly, a scientific modulation method will be formulated.

The second direction of the future research is experimental research.

- Electrotactile feedback is only employed for grasping force feedback in this research. However, other sensory/functional properties, such as the softness, texture and joint position, are also important clues for hand manipulation and can be fed back by tactile stimulation. Thus, the proposed virtual platform can be further expanded into a multifunctional system covering a large spectrum of sensory/motor functional rehabilitation applications, by incorporating more constraint properties in hand motion tasks.
- In this research, the proposed model, systems and methods were only tested on able-bodied subjects, although the satisfactory results preliminarily verified the feasibility and effectiveness of electrotactile feedback in hand rehabilitation. A discrepancy of physiological conditions may lead to different performance between the able-bodied subjects and limb-impaired subjects. The difference between a virtual hand platform and the practical tests with a real hand prosthesis will also bring new challenges. Thus, a further exploration of electrotactile feedback on targeted subjects with amputation or motor function impairment with hand prostheses should be considered to validate its clinical usability.

References

ABOSERIA, M., CLEMENTE, F., ENGELS, L.F. & CIPRIANI, C. (2018). Discrete vibro-tactile feedback prevents object slippage in hand prostheses more intuitively than other modalities. *IEEE Transactions on Neural Systems and Rehabilitation Engineering*, **26**, 1577–1584.

ACKERLEY, R. & KAVOUNOUDIAS, A. (2015). The role of tactile afference in shaping motor behaviour and implications for prosthetic innovation. *Neuropsychologia*, **79**, 192–205.

AHMED, M., CHITTEBOYINA, M.M., BUTLER, D.P. & ÇELIK-BUTLER, Z. (2013). MEMS force sensor in a flexible substrate using nichrome piezoresistors. *IEEE Sensors Journal*, **13**, 4081–4089.

AKHLAGHI, N., BAKER, C., LAHLOU, M., ZAFAR, H., MURTHY, K., RANGWALA, H., KOSECKA, J., JOINER, W., PANCRAZIO, J. & SIKDAR, S. (2016). Real-time classification of hand motions using ultrasound imaging of forearm muscles. *IEEE Trans. Biomedical Engineering*, **63**, 1687–1698.

ALON, G., LEVITT, A.F. & MCCARTHY, P.A. (2007). Functional electrical stimulation enhancement of upper extremity functional recovery during stroke rehabilitation: a pilot study. *Neurorehabilitation and neural repair*, **21**, 207–215.

ANTFOLK, C., DALONZO, M., ROSÉN, B., LUNDBORG, G., SEBELIUS, F. & CIPRIANI, C. (2013). Sensory feedback in upper limb prosthetics. *Expert review of medical devices*, **10**, 45–54.

AOYAGI, S., TANAKA, T. & MINAMI, M. (2006). Recognition of contact state of four layers arrayed type tactile sensor by using neural network. In *2006 IEEE International Conference on Information Acquisition*, 393–397, IEEE.

ARAFSHA, F., ZHANG, L., DONG, H. & EL SADDIK, A. (2015). Contactless haptic feedback: state of the art. In *Haptic, Audio and Visual Environments and Games (HAVE), 2015 IEEE International Symposium on*, 1–6, IEEE.

ARIETA, A.H., YOKOI, H., ARAI, T. & WENWEI, Y. (2005). FES as biofeedback for an EMG controlled prosthetic hand. In *TENCON 2005-2005 IEEE Region 10 Conference*, 1–6, IEEE.

ASCARI, L., CORRADI, P., BECCAI, L. & LASCHI, C. (2007). A miniaturized and flexible optoelectronic sensing system for tactile skin. *Journal of Micromechanics and Microengineering*, **17**, 2288.

ATAOLLAHI, A., POLYGERINOS, P., PUANGMALI, P., SENEVIRATNE, L.D. & ALTHOEFER, K. (2010). Tactile sensor array using prismatic-tip optical fibers for dexterous robotic hands. In *Intelligent Robots and Systems (IROS), 2010 IEEE/RSJ International Conference on*, 910–915, IEEE.

BAKER, L., MCNEAL, D., BENTON, L., BOWMAN, B. & WATERS, R. (1993). Neuromuscular electrical stimulation: A practical guide. downey, ca: Los amigos research and education institute.

BEBIONIC (2018). Bebionic hand features. http://bebionic.com/the_hand/features.

BHATTACHARYYA, S., CLERC, M. & HAYASHIBE, M. (2016a). A study on the effect of electrical stimulation as a user stimuli for motor imagery classification in brain-machine interface. *European Journal of Translational Myology*, **26**, 165–168.

BHATTACHARYYA, S., CLERC, M. & HAYASHIBE, M. (2016b). A study on the effect of electrical stimulation during motor imagery learning in brain-computer interfacing. In *IEEE International Conference on Systems, Man, and Cybernetics*, Budapest.

BIONICS, T. (2018). Touch bionics products. http://www.touchbionics.com/products.

BIOPAC (2018). STMISOLA constant current and constant voltage isolated linear stimulator. https://www.biopac.com/product/current-or-voltage-linear-isolated-stimulator/.

BRODERICK, B.J., BREEN, P.P. & ÓLAIGHIN, G. (2008). Electronic stimulators for surface neural prosthesis. *Journal of automatic control*, **18**, 25–33.

CALINON, S., GUENTER, F. & BILLARD, A. (2007). On learning, representing, and generalizing a task in a humanoid robot. *IEEE Transactions on Systems, Man, and Cybernetics, Part B (Cybernetics)*, **37**, 286–298.

CARROZZA, M.C., DARIO, P., VECCHI, F., ROCCELLA, S., ZECCA, M. & SEBASTIANI, F. (2003). The cyberhand: on the design of a cybernetic prosthetic hand intended to be interfaced to the peripheral nervous system. In *Intelligent Robots and Systems, 2003.(IROS 2003). Proceedings. 2003 IEEE/RSJ International Conference on*, vol. 3, 2642–2647, IEEE.

CASINI, S., MORVIDONI, M., BIANCHI, M., CATALANO, M., GRIOLI, G. & BICCHI, A. (2015). Design and realization of the cuff-clenching upper-limb force feedback wearable device for distributed mechano-tactile stimulation of normal and tangential skin forces. In *Intelligent Robots and Systems (IROS), 2015 IEEE/RSJ International Conference on*, 1186–1193, IEEE.

CHAI, G., SUI, X., LI, S., HE, L. & LAN, N. (2015). Characterization of evoked tactile sensation in forearm amputees with transcutaneous electrical nerve stimulation. *Journal of Neural Engineering*, **12**, 066002.

CHAI, G.H., SUI, X.H., LI, P., LIU, X.X. & LAN, N. (2014). Review on tactile sensory feedback of prosthetic hands for the upper-limb amputees by sensory afferent stimulation. *Journal of Shanghai Jiaotong University (Science)*, **19**, 587–591.

CHANG, A., O'MODHRAIN, S., JACOB, R., GUNTHER, E. & ISHII, H. (2002). Comtouch: design of a vibrotactile communication device. In *Proceedings of the*

4th conference on Designing interactive systems: processes, practices, methods, and techniques, 312–320, ACM.

CHANG, G.C., LUB, J.J., LIAO, G.D., LAI, J.S., CHENG, C.K., KUO, B.L. & KUO, T.S. (1997). A neuro-control system for the knee joint position control with quadriceps stimulation. *IEEE transactions on rehabilitation engineering*, **5**, 2–11.

CHATTERJEE, A., AGGARWAL, V., RAMOS, A., ACHARYA, S. & THAKOR, N.V. (2007). A brain-computer interface with vibrotactile biofeedback for haptic information. *J. Neuroeng. Rehabil.*, **4**, 40.

CHATTERJEE, A., CHAUBEY, P., MARTIN, J. & THAKOR, N. (2008). Testing a prosthetic haptic feedback simulator with an interactive force matching task. *JPO: Journal of Prosthetics and Orthotics*, **20**, 27–34.

CHEESBOROUGH, J.E., SMITH, L.H., KUIKEN, T.A. & DUMANIAN, G.A. (2015). Targeted muscle reinnervation and advanced prosthetic arms. In *Seminars in plastic surgery*, vol. 29, 62, Thieme Medical Publishers.

CINCOTTI, F., KAUHANEN, L., ALOISE, F., PALOMÄKI, T., CAPORUSSO, N., JYLÄNKI, P., MATTIA, D., BABILONI, F., VANACKER, G., NUTTIN, M. *et al.* (2007). Vibrotactile feedback for brain-computer interface operation. *Computational intelligence and neuroscience*, **2007**, 48937.

CIOCARLIE, M., LACKNER, C. & ALLEN, P. (2007). Soft finger model with adaptive contact geometry for grasping and manipulation tasks. In *EuroHaptics Conference, 2007 and Symposium on Haptic Interfaces for Virtual Environment and Teleoperator Systems. World Haptics 2007. Second Joint*, 219–224, IEEE.

CIPRIANI, C., ZACCONE, F., MICERA, S. & CARROZZA, M.C. (2008). On the shared control of an EMG-controlled prosthetic hand: analysis of user–prosthesis interaction. *IEEE Transactions on Robotics*, **24**, 170–184.

COLES, T.R., MEGLAN, D. & JOHN, N.W. (2011). The role of haptics in medical training simulators: A survey of the state of the art. *IEEE Trans. Haptics*, **4**, 51–66.

CONZELMAN JR JOHN, E., O'BRIEN CLAYTON, W. *et al.* (1953). Prosthetic device sensory attachment. US Patent 2,656,545.

CORDELLA, F., CIANCIO, A.L., SACCHETTI, R., DAVALLI, A., CUTTI, A.G., GUGLIELMELLI, E. & ZOLLO, L. (2016). Literature review on needs of upper limb prosthesis users. *Frontiers in neuroscience*, **10**, 209.

CORNMAN, J., AKHTAR, A. & BRETL, T. (2017). A portable, arbitrary waveform, multichannel constant current electrotactile stimulator. In *Neural Engineering (NER), 2017 8th International IEEE/EMBS Conference on*, 300–303, IEEE.

COTTON, D.P., CHAPPELL, P.H., CRANNY, A., WHITE, N.M. & BEEBY, S.P. (2007). A novel thick-film piezoelectric slip sensor for a prosthetic hand. *IEEE sensors journal*, **7**, 752–761.

CRANNY, A., COTTON, D., CHAPPELL, P., BEEBY, S. & WHITE, N. (2005). Thick-film force and slip sensors for a prosthetic hand. *Sensors and Actuators A: Physical*, **123**, 162–171.

DA ROCHA, J.G.V., DA ROCHA, P.F.A. & LANCEROS-MENDEZ, S. (2009). Capacitive sensor for three-axis force measurements and its readout electronics. *IEEE Trans. Instrumentation and Measurement*, **58**, 2830–2836.

DA SILVA, J.G., DE CARVALHO, A.A. & DA SILVA, D.D. (2002). A strain gauge tactile sensor for finger-mounted applications. *IEEE Trans. Instrumentation and measurement*, **51**, 18–22.

DAHIYA, R.S., METTA, G., VALLE, M. & SANDINI, G. (2010). Tactile sensingfrom humans to humanoids. *IEEE Trans. Robotics*, **26**, 1–20.

DAKUA, I. & AFZULPURKAR, N. (2013). Piezoelectric energy generation and harvesting at the nano-scale: materials and devices. *Nanomaterials and Nanotechnology*, **3**, 21.

D'ALONZO, M., DOSEN, S., CIPRIANI, C. & FARINA, D. (2014a). HyVE: hybrid vibro-electrotactile stimulation for sensory feedback and substitution in rehabilitation. *IEEE Trans. Neural Systems and Rehabilitation Engineering*, **22**, 290–301.

D'ALONZO, M., DOSEN, S., CIPRIANI, C. & FARINA, D. (2014b). HyVEhybrid vibro-electrotactile stimulationis an efficient approach to multi-channel sensory feedback. *IEEE Trans. haptics*, **7**, 181–190.

DANDEKAR, K., RAJU, B.I. & SRINIVASAN, M.A. (2003a). 3-d finite-element models of human and monkey fingertips to investigate the mechanics of tactile sense. *Journal of biomechanical engineering*, **125**, 682–691.

DANDEKAR, K., RAJU, B.I. & SRINIVASAN, M.A. (2003b). 3-d finite-element models of human and monkey fingertips to investigate the mechanics of tactile sense. *Journal of biomechanical engineering*, **125**, 682–691.

D'ANGELO, M.L., CANNELLA, F., BIANCHI, M., D'IMPERIO, M., BATTAGLIA, E., POGGIANI, M., ROSSI, G., BICCHI, A. & CALDWELL, D.G. (2017). An integrated approach to characterize the behavior of a human fingertip in contact with a silica window. *IEEE transactions on haptics*, **10**, 123–129.

DARGAHI, J. (2000). A piezoelectric tactile sensor with three sensing elements for robotic, endoscopic and prosthetic applications. *Sensors and Actuators A: Physical*, **80**, 23–30.

DARGAHI, J. & NAJARIAN, S. (2004). Human tactile perception as a standard for artificial tactile sensinga review. *The International Journal of Medical Robotics and Computer Assisted Surgery*, **1**, 23–35.

DEDE, M.I.C., SELVI, O., BILGINCAN, T. & KANT, Y. (2009). Design of a haptic device for teleoperation and virtual reality systems. In *Systems, Man and Cybernetics, 2009. SMC 2009. IEEE International Conference on*, 3623–3628, IEEE.

DIETRICH, C., WALTER-WALSH, K., PREISSLER, S., HOFMANN, G.O., WITTE, O.W., MILTNER, W.H. & WEISS, T. (2012). Sensory feedback prosthesis reduces phantom limb pain: proof of a principle. *Neuroscience letters*, **507**, 97–100.

DLR (2018). DLR-HIT Hand. https://www.dlr.de/rm/en/Portaldata/52/Resources/Roboter_und_Systeme/Hand/HIT_I_SAH/9DLR-HIT-HAND2006Handout.pdf.

DONALDSON, N., PERKINS, T., FITZWATER, R., WOOD, D. & MIDDLETON, F. (2000). Fes cycling may promote recovery of leg function after incomplete spinal cord injury. *Spinal Cord*, **38**, 680.

DOSEN, S., SCHAEFFER, M.C. & FARINA, D. (2014). Time-division multiplexing for myoelectric closed-loop control using electrotactile feedback. *Journal of neuroengineering and rehabilitation*, **11**, 1.

DOSEN, S., MARKOVIC, M., WILLE, N., HENKEL, M., KOPPE, M., NINU, A., FRÖMMEL, C. & FARINA, D. (2015). Building an internal model of a myoelectric prosthesis via closed-loop control for consistent and routine grasping. *Experimental brain research*, **233**, 1855–1865.

DOSEN, S., MARKOVIC, M., STRBAC, M., PEROVIĆ, M., KOJIĆ, V., BIJELIĆ, G., KELLER, T. & FARINA, D. (2016). Multichannel electrotactile feedback with spatial and mixed coding for closed-loop control of grasping force in hand prostheses. *IEEE Trans. Neural Systems and Rehabilitation Engineering*.

DUCHEMIN, G., MAILLET, P., POIGNET, P., DOMBRE, E. & PIERROT, F. (2005). A hybrid position/force control approach for identification of deformation models of skin and underlying tissues. *IEEE Transactions on Biomedical Engineering*, **52**, 160–170.

ENGEL, J., CHEN, J. & LIU, C. (2003). Development of polyimide flexible tactile sensor skin. *Journal of Micromechanics and Microengineering*, **13**, 359.

FANG, Y., HETTIARACHCHI, N., ZHOU, D. & LIU, H. (2015a). Multi-modal sensing techniques for interfacing hand prostheses: A review. *IEEE Sensors Journal*, **15**, 6065–6076.

FANG, Y., LIU, H., LI, G. & ZHU, X. (2015b). A multichannel surface emg system for hand motion recognition. *International Journal of Humanoid Robotics*, **12**, 1550011.

FANG, Y., ZHOU, D., LI, K. & LIU, H. (2017). Interface prostheses with classifier-feedback-based user training. *IEEE transactions on biomedical engineering*, **64**, 2575–2583.

FARINA, D., JIANG, N., REHBAUM, H., HOLOBAR, A., GRAIMANN, B., DIETL, H. & ASZMANN, O.C. (2014). The extraction of neural information from the surface emg for the control of upper-limb prostheses: emerging avenues and challenges. *IEEE Transactions on Neural Systems and Rehabilitation Engineering*, **22**, 797–809.

GASSON, M., HUTT, B., GOODHEW, I., KYBERD, P. & WARWICK, K. (2005). Invasive neural prosthesis for neural signal detection and nerve stimulation. *International Journal of Adaptive Control and Signal Processing*, **19**, 365–375.

GIRÃO, P.S., RAMOS, P.M.P., POSTOLACHE, O. & PEREIRA, J.M.D. (2013). Tactile sensors for robotic applications. *Measurement*, **46**, 1257–1271.

GONZALEZ, F., GOSSELIN, F. & BACHTA, W. (2014). Analysis of hand contact areas and interaction capabilities during manipulation and exploration. *IEEE transactions on haptics*, **7**, 415–429.

GUPTA, A. & O'MALLEY, M.K. (2006). Design of a haptic arm exoskeleton for training and rehabilitation. *Mechatronics, IEEE/ASME Transactions on*, **11**, 280–289.

HARMON, L.D. (1980). Touch-sensing technology: A review. *Society of Manufacturing Engineers, 1980. 58.*

HARTMANN, C., DOŠEN, S., AMSUESS, S. & FARINA, D. (2015). Closed-loop control of myoelectric prostheses with electrotactile feedback: influence of stimulation artifact and blanking. *IEEE Trans. Neural Systems and Rehabilitation Engineering*, **23**, 807–816.

HEO, J.S., KIM, J.Y. & LEE, J.J. (2008). Tactile sensors using the distributed optical fiber sensors. In *2008 3rd International Conference on Sensing Technology*, 486–490, IEEE.

HOLDERBAUM, W., HUNT, K. & GOLLEE, H. (2002). H robust control design for unsupported paraplegic standing: experimental evaluation. *Control Engineering Practice*, **10**, 1211–1222.

HOLLIS, R.L.J. (2013). Magnetic levitation haptic interface system. U.S. Patent 8 497 767.

HUNT, K.J., STONE, B., NEGARD, N.O., SCHAUER, T., FRASER, M.H., CATHCART, A.J., FERRARIO, C., WARD, S.A. & GRANT, S. (2004). Control strategies for integration of electric motor assist and functional electrical stimulation in paraplegic cycling: utility for exercise testing and mobile cycling. *IEEE Transactions on Neural systems and rehabilitation engineering*, **12**, 89–101.

HWANG, E.S., SEO, J.H. & KIM, Y.J. (2007). A polymer-based flexible tactile sensor for both normal and shear load detections and its application for robotics. *Journal of microelectromechanical systems*, **16**, 556–563.

ILIC, M., VASILJEVIC, D. & POPOVIC, D.B. (1994). A programmable electronic stimulator for fes systems. *IEEE Transactions on rehabilitation engineering*, **2**, 234–239.

ISAKOVIĆ, M., BELIĆ, M., ŠTRBAC, M., POPOVIĆ, I., DOŠEN, S., FARINA, D. & KELLER, T. (2016). Electrotactile feedback improves performance and facilitates learning in the routine grasping task. *European Journal of Translational Myology*, **26**.

JIANG, L., HUANG, Q., ZHAO, J., YANG, D., FAN, S. & LIU, H. (2014). Noise cancellation for electrotactile sensory feedback of myoelectric forearm prostheses. In *Information and Automation (ICIA), 2014 IEEE International Conference on*, 1066–1071, IEEE.

JINDRICH, D.L., ZHOU, Y., BECKER, T. & DENNERLEIN, J.T. (2003). Non-linear viscoelastic models predict fingertip pulp force-displacement characteristics during voluntary tapping. *Journal of biomechanics*, **36**, 497–503.

JOBIN, M., FOSCHIA, R., GRANGE, S., BAUR, C., GREMAUD, G., LEE, K., FORRÓ, L. & KULIK, A. (2005). Versatile force–feedback manipulator for nanotechnology applications. *Review of scientific instruments*, **76**, 053701.

JORGOVANOVIC, N., DOSEN, S., DJOZIC, D.J., KRAJOSKI, G. & FARINA, D. (2014). Virtual grasping: closed-loop force control using electrotactile feedback. *Computational and mathematical methods in medicine*, **2014**, 120357.

KACZMAREK, K.A., WEBSTER, J.G., BACH-Y RITA, P. & TOMPKINS, W.J. (1991). Electrotactile and vibrotactile displays for sensory substitution systems. *IEEE Trans. Biomedical Engineering*, **38**, 1–16.

KALANTARI, M., RAMEZANIFARD, M., AHMADI, R., DARGAHI, J. & KÖVECSES, J. (2011). A piezoresistive tactile sensor for tissue characterization during catheter-based cardiac surgery. *The International Journal of Medical Robotics and Computer Assisted Surgery*, **7**, 431–440.

KANE, B.J., CUTKOSKY, M.R. & KOVACS, G.T. (2000). A traction stress sensor array for use in high-resolution robotic tactile imaging. *Journal of microelectromechanical systems*, **9**, 425–434.

KAO, I. & YANG, F. (2004). Stiffness and contact mechanics for soft fingers in grasping and manipulation. *IEEE Transactions on Robotics and Automation*, **20**, 132–135.

KIM, H.K., LEE, S. & YUN, K.S. (2011). Capacitive tactile sensor array for touch screen application. *Sensors and Actuators A: Physical*, **165**, 2–7.

KIM, J., LEE, M., SHIM, H.J., GHAFFARI, R., CHO, H.R., SON, D., JUNG, Y.H., SOH, M., CHOI, C., JUNG, S. *et al.* (2014). Stretchable silicon nanoribbon electronics for skin prosthesis. *Nature communications*, **5**.

KINETICS, J. (2018). TacWave ETS driver. www.jk-labs.com/ETS.html.

KOIVA, R., ZENKER, M., SCHÜRMANN, C., HASCHKE, R. & RITTER, H.J. (2013). A highly sensitive 3d-shaped tactile sensor. In *2013 IEEE/ASME International Conference on Advanced Intelligent Mechatronics*, 1084–1089, IEEE.

KUIKEN, T.A., LI, G., LOCK, B.A., LIPSCHUTZ, R.D., MILLER, L.A., STUBBLEFIELD, K.A. & ENGLEHART, K.B. (2009). Targeted muscle reinnervation for real-time myoelectric control of multifunction artificial arms. *Jama*, **301**, 619–628.

KUMAR, S., LIU, G., SCHLOERB, D.W. & SRINIVASAN, M.A. (2015). Viscoelastic characterization of the primate finger pad in vivo by microstep indentation and three-dimensional finite element models for tactile sensation studies. *Journal of biomechanical engineering*, **137**, 061002.

KUTILEK, P., HYBL, J., KAULER, J. & VITECKOVA, S. (2012). Prosthetic 6-DOF arm controlled by EMG signals and multi-sensor system. In *MECHATRONIKA, 2012 15th International Symposium*, 1–5, IEEE.

KYBERD, P.J., LIGHT, C., CHAPPELL, P.H., NIGHTINGALE, J.M., WHATLEY, D. & EVANS, M. (2001). The design of anthropomorphic prosthetic hands: A study of the southampton hand. *Robotica*, **19**, 593–600.

KYBERD, P.J., MURGIA, A., GASSON, M., TJERKS, T., METCALF, C., CHAPPELL, P.H., WARWICK, K., LAWSON, S.E. & BARNHILL, T. (2009). Case studies to demonstrate the range of applications of the southampton hand assessment procedure. *The British Journal of Occupational Therapy*, **72**, 212–218.

LANG, S. & MUENSIT, S. (2006). Review of some lesser-known applications of piezoelectric and pyroelectric polymers. *Applied Physics A*, **85**, 125–134.

LEBLANC, S., PAQUIN, K., CARR, K. & HORTON, S. (2013). Non-immersive virtual reality for fine motor rehabilitation of functional activities in individuals with chronic stroke: a review. *Aging Sci*, **1**, 2.

LEE, K.H., SIM, M., RYU, M., JEONG, H.S., JANG, J.E., SOHN, J.I. & CHA, S.N. (2015). Zinc oxide nanowire-based pressure and temperature sensor. In *Proc. 15th IEEE Int. Conf. Nanotechnol.*, 901–904, Rome.

LEE, M.H. (2000). Tactile sensing: new directions, new challenges. *The International Journal of Robotics Research*, **19**, 636–643.

LEE, M.H. & NICHOLLS, H.R. (1999). Review article tactile sensing for mechatronics-a state of the art survey. *Mechatronics*, **9**, 1–31.

LEVIN, M.F., WEISS, P.L. & KESHNER, E.A. (2015). Emergence of virtual reality as a tool for upper limb rehabilitation: incorporation of motor control and motor learning principles. *Physical therapy*, **95**, 415–425.

LI, C., WU, P.M., LEE, S., GORTON, A., SCHULZ, M.J. & AHN, C.H. (2008). Flexible dome and bump shape piezoelectric tactile sensors using pvdf-trfe copolymer. *Journal of Microelectromechanical Systems*, **17**, 334–341.

LI, K., FANG, Y., ZHOU, Y. & LIU, H. (2017). Non-invasive stimulation-based tactile sensation for upper-extremity prosthesis: a review. *IEEE Sensors Journal*, **17**, 2625–2635.

LIBERSON, W. (1961). Functional electrotherapy: stimulation of the peroneal nerve synchronized with the swing phase of the gait of hemiplegic patients. *Arch Phys Med*, **42**, 101–105.

LIU, H. (2011). Exploring human hand capabilities into embedded multifingered object manipulation. *IEEE Trans. Industrial Informatics*, **7**, 389–398.

LUCAROTTI, C., ODDO, C.M., VITIELLO, N. & CARROZZA, M.C. (2013). Synthetic and bio-artificial tactile sensing: A review. *Sensors*, **13**, 1435–1466.

LYNCH, C.L. & POPOVIC, M.R. (2008). Functional electrical stimulation. *IEEE control systems*, **28**, 40–50.

MAEKAWA, H., TANIE, K. & KOMORIYA, K. (1993). A finger-shaped tactile sensor using an optical waveguide. In *Systems, Man and Cybernetics, 1993.'Systems Engineering in the Service of Humans', Conference Proceedings., International Conference on*, 403–408, IEEE.

MARINO, A., GENCHI, G.G., MATTOLI, V. & CIOFANI, G. (2016). Piezoelectric nanotransducers: the future of neural stimulation. *Nano Today*, **Dec**.

MASSARO, A., SPANO, F., LAY-EKUAKILLE, A., CAZZATO, P., CINGOLANI, R. & ATHANASSIOU, A. (2011). Design and characterization of a nanocomposite pressure sensor implemented in a tactile robotic system. *IEEE Trans. Instrumentation and Measurement*, **60**, 2967–2975.

MATJACIC, Z. & BAJD, T. (1998). Arm-free paraplegic standing. ii. experimental results. *IEEE Transactions on Rehabilitation Engineering*, **6**, 139–150.

MEEK, S.G., JACOBSEN, S.C. & GOULDING, P.P. (1989). Extended physiologic taction: design and evaluation of a proportional force feedback system. *J Rehabil Res Dev*, **26**, 53–62.

MEI, T., LI, W.J., GE, Y., CHEN, Y., NI, L. & CHAN, M.H. (2000). An integrated mems three-dimensional tactile sensor with large force range. *Sensors and Actuators A: Physical*, **80**, 155–162.

MILLER, L.A., STUBBLEFIELD, K.A., LIPSCHUTZ, R.D., LOCK, B.A. & KUIKEN, T.A. (2008). Improved myoelectric prosthesis control using targeted reinnervation surgery: a case series. *IEEE Transactions on Neural Systems and Rehabilitation Engineering*, **16**, 46–50.

MOBIUSBIONICS (2018). LUKE arm details. http://www.mobiusbionics.com/luke-arm/.

MUHAMMAD, H., RECCHIUTO, C., ODDO, C., BECCAI, L., ANTHONY, C., ADAMS, M., CARROZZA, M. & WARD, M. (2011). A capacitive tactile sensor array for surface texture discrimination. *Microelectronic Engineering*, **88**, 1811–1813.

MULVEY, M., FAWKNER, H., RADFORD, H. & JOHNSON, M. (2009). The use of transcutaneous electrical nerve stimulation (TENS) to aid perceptual embodiment of prosthetic limbs. *Medical hypotheses*, **72**, 140–142.

MULVEY, M., FAWKNER, H. & JOHNSON, M.I. (2014). An investigation into the perceptual embodiment of an artificial hand using transcutaneous electrical nerve stimulation (TENS) in intact-limbed individuals. *Technology and Health Care*, **22**, 157–166.

MULVEY, M.R., BAGNALL, A.M., JOHNSON, M.I. & MARCHANT, P.R. (2010). Transcutaneous electrical nerve stimulation (TENS) for phantom pain and stump pain following amputation in adults. *The Cochrane Library*.

MULVEY, M.R., FAWKNER, H.J., RADFORD, H.E. & JOHNSON, M.I. (2012). Perceptual embodiment of prosthetic limbs by transcutaneous electrical nerve stimulation. *Neuromodulation: Technology at the Neural Interface*, **15**, 42–47.

NAFARI, A., GHAVANINI, F.A., BRING, M., SVENSSON, K. & ENOKSSON, P. (2007). Calibration methods of force sensors in the micro-newton range. *Journal of Micromechanics and Microengineering*, **17**, 2102.

NAJARIAN, S., DARGAHI, J. & MEHRIZI, A. (2009). *Artificial tactile sensing in biomedical engineering*. McGraw Hill Professional.

NGHIEM, B.T., SANDO, I.C., GILLESPIE, R.B., MCLAUGHLIN, B.L., GERLING, G.J., LANGHALS, N.B., URBANCHEK, M.G. & CEDERNA, P.S. (2015). Providing a sense of touch to prosthetic hands. *Plastic and reconstructive surgery*, **135**, 1652–1663.

NINU, A., DOSEN, S., MUCELI, S., RATTAY, F., DIETL, H. & FARINA, D. (2014). Closed-loop control of grasping with a myoelectric hand prosthesis: Which are the relevant feedback variables for force control? *IEEE transactions on neural systems and rehabilitation engineering*, **22**, 1041–1052.

NODA, K., HOSHINO, K., MATSUMOTO, K. & SHIMOYAMA, I. (2006). A shear stress sensor for tactile sensing with the piezoresistive cantilever standing in elastic material. *Sensors and Actuators A: physical*, **127**, 295–301.

OHKA, M., MITSUYA, Y., TAKEUCHI, S., ISHIHARA, H. & KAMEKAWA, O. (1995). A three-axis optical tactile sensor (FEM contact analyses and sensing experiments using a large-sized tactile sensor). In *Robotics and Automation, 1995. Proceedings., 1995 IEEE International Conference on*, vol. 1, 817–824, IEEE.

OHMURA, Y., KUNIYOSHI, Y. & NAGAKUBO, A. (2006). Conformable and scalable tactile sensor skin for curved surfaces. In *Proceedings 2006 IEEE International Conference on Robotics and Automation, 2006. ICRA 2006.*, 1348–1353, IEEE.

OMATA, S. & TERUNUMA, Y. (1992). New tactile sensor like the human hand and its applications. *Sensors and Actuators A: Physical*, **35**, 9–15.

ONESTI, R.J., TOMPKINS, W., WEBSTER, J. & WERTSCH, J. (1989). Design of a portable electrotactile stimulator for sensory substitution applications. In *Engineering in Medicine and Biology Society, 1989. Images of the Twenty-First Century.,*

Proceedings of the Annual International Conference of the IEEE Engineering in, 1439–1440, IEEE.

ORENGO, G., GIOVANNINI, L., LATESSA, G., SAGGIO, G. & GIANNINI, F. (2009). Characterization of piezoresistive sensors for goniometric glove in hand prostheses. In *Wireless Communication, Vehicular Technology, Information Theory and Aerospace & Electronic Systems Technology, 2009. Wireless VITAE 2009. 1st International Conference on*, 684–687, IEEE.

OSBORN, L., LEE, W.W., KALIKI, R. & THAKOR, N. (2014). Tactile feedback in upper limb prosthetic devices using flexible textile force sensors. In *5th IEEE RAS/EMBS International Conference on Biomedical Robotics and Biomechatronics*, 114–119, IEEE.

ØSTLIE, K., LESJØ, I.M., FRANKLIN, R.J., GARFELT, B., SKJELDAL, O.H. & MAGNUS, P. (2012). Prosthesis rejection in acquired major upper-limb amputees: a population-based survey. *Disability and Rehabilitation: Assistive Technology*, **7**, 294–303.

OTTOBOCK (2018a). Body-powered hand. https://www.ottobock-export.com/en/prosthetics/upper-limb/solution-overview/arm-prostheses-body-powered/.

OTTOBOCK (2018b). Hook hand. https://professionals.ottobockus.com/Prosthetics/Upper-Limb-Prosthetics/Myo-Hands-and-Components/Myo-Terminal-Devices/System-Electric-Hand-DMC-plus/p/8E38~56-L7.

OTTOBOCK (2018c). How the michelangelo works. http://www.ottobockus.com/prosthetics/upper-limb-prosthetics/solution-overview/michelangelo-prosthetic-hand/.

PAMUNGKAS, D. & WARD, K. (2016). Electro-tactile feedback system to enhance virtual reality experience. *International Journal of Computer Theory and Engineering*, **8**, 465–470.

PANG, C., LEE, G.Y., KIM, T.I., KIM, S.M., KIM, H.N., AHN, S.H. & SUH, K.Y. (2012). A flexible and highly sensitive strain-gauge sensor using reversible interlocking of nanofibres. *Nature materials*, **11**, 795–801.

PAREDES, L.P., DOSEN, S., RATTAY, F., GRAIMANN, B. & FARINA, D. (2015). The impact of the stimulation frequency on closed-loop control with electrotactile feedback. *Journal of neuroengineering and rehabilitation*, **12**, 1–16.

PARK, C.S., PARK, J. & LEE, D.W. (2009). A piezoresistive tactile sensor based on carbon fibers and polymer substrates. *Microelectronic Engineering*, **86**, 1250–1253.

PAWLUK, D.T. & HOWE, R.D. (1999). Dynamic lumped element response of the human fingerpad. *Journal of biomechanical engineering*, **121**, 178–183.

PAYANDEH, S. & LI, T. (2003). Toward new designs of haptic devices for minimally invasive surgery. In *International Congress Series*, vol. 1256, 775–781, Elsevier.

PEERDEMAN, B., BOERE, D., WITTEVEEN, H., HUIS IN 'T VELD, R., HERMENS, H., STRAMIGIOLI, S., RIETMAN, H., VELTINK, P. & MISRA, S. (2011). Myoelectric forearm prostheses: State of the art from a user-centered perspective. *Journal of Rehabilitation Research & Development*, **48**, 719–738.

PERUZZINI, M., GERMANI, M. & MENGONI, M. (2012). Electro-tactile device for texture simulation. In *Mechatronics and Embedded Systems and Applications (MESA), 2012 IEEE/ASME International Conference on*, 178–183, IEEE.

POPOVIC, D., STEIN, R.B., OGUZTORELI, M.N., LEBIEDOWSKA, M. & JONIC, S. (1999). Optimal control of walking with functional electrical stimulation: a computer simulation study. *IEEE Transactions on Rehabilitation Engineering*, **7**, 69–79.

POPOVIĆ, D.B. (2014). Advances in functional electrical stimulation (fes). *Journal of Electromyography and Kinesiology*, **24**, 795–802.

PRITCHARD, E., MAHFOUZ, M., EVANS, B., ELIZA, S. & HAIDER, M. (2008). Flexible capacitive sensors for high resolution pressure measurement. In *Sensors, 2008 IEEE*, 1484–1487, IEEE.

PUANGMALI, P., ALTHOEFER, K., SENEVIRATNE, L.D., MURPHY, D. & DASGUPTA, P. (2008). State-of-the-art in force and tactile sensing for minimally invasive surgery. *IEEE Sensors Journal*, **8**, 371–381.

QUANDT, F. & HUMMEL, F.C. (2014). The influence of functional electrical stimulation on hand motor recovery in stroke patients: a review. *Experimental & Translational Stroke Medicine*, **6**, 9.

RASPOPOVIC, S., CAPOGROSSO, M., PETRINI, F.M., BONIZZATO, M., RIGOSA, J., DI PINO, G., CARPANETO, J., CONTROZZI, M., BORETIUS, T., FERNANDEZ, E. *et al.* (2014). Restoring natural sensory feedback in real-time bidirectional hand prostheses. *Science translational medicine*, **6**, 222ra19–222ra19.

ROBERT, C. (2014). Machine learning, a probabilistic perspective.

ROMANO, J.M., HSIAO, K., NIEMEYER, G., CHITTA, S. & KUCHENBECKER, K.J. (2011). Human-inspired robotic grasp control with tactile sensing. *IEEE Trans. Robotics*, **27**, 1067–1079.

ROMBOKAS, E., STEPP, C.E., CHANG, C., MALHOTRA, M. & MATSUOKA, Y. (2013). Vibrotactile sensory substitution for electromyographic control of object manipulation. *IEEE Transactions on Biomedical Engineering*, **60**, 2226–2232.

ROSSITER, J. & MUKAI, T. (2005). A novel tactile sensor using a matrix of leds operating in both photoemitter and photodetector modes. In *IEEE Sensors, 2005.*, 994–997, IEEE.

RUBIO-SIERRA, F.J., STARK, R.W., THALHAMMER, S. & HECKL, W.M. (2003). Force-feedback joystick as a low-cost haptic interface for an atomic-force-microscopy nanomanipulator. *Applied Physics A*, **76**, 903–906.

SANI, H.N. & MEEK, S.G. (2011). Characterizing the performance of an optical slip sensor for grip control in a prosthesis. In *2011 IEEE/RSJ International Conference on Intelligent Robots and Systems*, 1927–1932, IEEE.

SAUNDERS, I. & VIJAYAKUMAR, S. (2011). The role of feed-forward and feedback processes for closed-loop prosthesis control. *Journal of neuroengineering and rehabilitation*, **8**, 60.

SCHÄTZLE, S. & WEBER, B. (2015). Towards vibrotactile direction and distance information for virtual reality and workstations for blind people. In *International Conference on Universal Access in Human-Computer Interaction*, 148–160, Springer.

SCHMITZ, A., MAGGIALI, M., RANDAZZO, M., NATALE, L. & METTA, G. (2008). A prototype fingertip with high spatial resolution pressure sensing for the robot iCub. In *Humanoids 2008-8th IEEE-RAS International Conference on Humanoid Robots*, 423–428, IEEE.

SCHOFIELD, J.S., EVANS, K.R., CAREY, J.P. & HEBERT, J.S. (2014). Applications of sensory feedback in motorized upper extremity prosthesis: A review. *Expert review of medical devices*, **11**, 499–511.

SEMINARA, L., CAPURRO, M., CIRILLO, P., CANNATA, G. & VALLE, M. (2011). Electromechanical characterization of piezoelectric PVDF polymer films for tactile sensors in robotics applications. *Sensors and Actuators A: Physical*, **169**, 49–58.

SERINA, E.R., MOTE, C. & REMPEL, D. (1997). Force response of the fingertip pulp to repeated compressioneffects of loading rate, loading angle and anthropometry. *Journal of biomechanics*, **30**, 1035–1040.

SERINA, E.R., MOCKENSTURM, E., MOTE, C. & REMPEL, D. (1998). A structural model of the forced compression of the fingertip pulp. *Journal of biomechanics*, **31**, 639–646.

SHADOW (2018). Shadow hand: key features. https://www.shadowrobot.com/products/dexterous-hand/.

SHAO, F., CHILDS, T.H. & HENSON, B. (2009). Developing an artificial fingertip with human friction properties. *Tribology international*, **42**, 1575–1581.

SHEFFLER, L.R. & CHAE, J. (2007). Neuromuscular electrical stimulation in neurorehabilitation. *Muscle & Nerve: Official Journal of the American Association of Electrodiagnostic Medicine*, **35**, 562–590.

SILVERA-TAWIL, D., RYE, D. & VELONAKI, M. (2015). Artificial skin and tactile sensing for socially interactive robots: A review. *Robotics and Autonomous Systems*, **63**, 230–243.

SNYDER-MACKLER, L., DELITTO, A., BAILEY, S.L. & STRALKA, S.W. (1995). Strength of the quadriceps femoris muscle and functional recovery after reconstruction of the anterior cruciate ligament. a prospective, randomized clinical trial of electrical stimulation. *JBJS*, **77**, 1166–1173.

SRINIVASAN, M.A. (1989). Surface deflection of primate fingertip under line load. *Journal of biomechanics*, **22**, 343–349.

STASSI, S., CAUDA, V., CANAVESE, G. & PIRRI, C.F. (2014). Flexible tactile sensing based on piezoresistive composites: a review. *Sensors*, **14**, 5296–5332.

TAKAMUKU, S., GOMEZ, G., HOSODA, K. & PFEIFER, R. (2007). Haptic discrimination of material properties by a robotic hand. In *2007 IEEE 6th International Conference on Development and Learning*, 1–6, IEEE.

TAKEDA, K., TANINO, G. & MIYASAKA, H. (2017). Review of devices used in neuromuscular electrical stimulation for stroke rehabilitation. *Medical devices (Auckland, NZ)*, **10**, 207.

TAN, D.W., SCHIEFER, M.A., KEITH, M.W., ANDERSON, J.R., TYLER, J. & TYLER, D.J. (2014). A neural interface provides long-term stable natural touch perception. *Science Translational Medicine*, **6**, 257ra138.

TEE, B.C.K., CHORTOS, A., BERNDT, A., NGUYEN, A.K., TOM, A., MCGUIRE, A., LIN, Z.C., TIEN, K., BAE, W.G., WANG, H., MEI, P., CHOU, H.H., CUI, B., DEISSEROTH, K., NG, T.N. & BAO, Z. (2015). A skin-inspired organic digital mechanoreceptor. *Science*, **350**, 313–316.

TENS+, T. (2018). TENS machines and muscle stimulators. http://www.med-fit.co.uk/tens-and-stimulation.html.

TENSPROS (2018). Quattro 2.5 clinical electrotherapy unit with TENS. https://www.tenspros.com/quattro-25-clinical-electrotherapy-unit-dq8450.html.

THRASHER, T., FLETT, H. & POPOVIC, M. (2006). Gait training regimen for incomplete spinal cord injury using functional electrical stimulation. *Spinal Cord*, **44**, 357.

TIWANA, M.I., SHASHANK, A., REDMOND, S.J. & LOVELL, N.H. (2011). Characterization of a capacitive tactile shear sensor for application in robotic and upper limb prostheses. *Sensors and Actuators A: Physical*, **165**, 164–172.

TIWANA, M.I., REDMOND, S.J. & LOVELL, N.H. (2012). A review of tactile sensing technologies with applications in biomedical engineering. *Sensors and Actuators A: physical*, **179**, 17–31.

TYLER, D.J. (2016). Restoring the human touch: Prosthetics imbued with haptics give their wearers fine motor control and a sense of connection. *IEEE Spectrum*, **53**, 28–33.

UEBERSCHLAG, P. (2001). PVDF piezoelectric polymer. *Sensor Review*, **21**, 118–126.

ULMEN, J. & CUTKOSKY, M.R. (2010). A robust, low-cost and low-noise artificial skin for human-friendly robots. In *ICRA*, 4836–4841.

UNITYASSETSTORE (2018). Hand physics controller. https://assetstore.unity.com/packages/tools/physics/hand-physics-controller-21105.

VINCENTSYSTEMS (2018). The touch sensing hand prosthesis of the next generation: VINCENTevolution 2. https://vincentsystems.de/en/prosthetics/vincent-evolution-2/.

WALKER, J.M., BLANK, A.A., SHEWOKIS, P.A. & OMALLEY, M.K. (2015). Tactile feedback of object slip facilitates virtual object manipulation. *IEEE transactions on haptics*, **8**, 454–466.

WANG, P., BECKER, A., JONES, I., GLOVER, A., BENFORD, S., GREENHALGH, C. & VLOEBERGHS, M. (2006). A virtual reality surgery simulation of cutting and retraction in neurosurgery with force-feedback. *Computer methods and programs in biomedicine*, **84**, 11–18.

WANG, Y., XI, K., LIANG, G., MEI, M. & CHEN, Z. (2014). A flexible capacitive tactile sensor array for prosthetic hand real-time contact force measurement. In *Information and Automation (ICIA), 2014 IEEE International Conference on*, 937–942, IEEE.

WANG, Z., WANG, L., MORIKAWA, S., HIRAI, S. *et al.* (2012). A 3-d nonhomogeneous fe model of human fingertip based on mri measurements. *IEEE Transactions on Instrumentation and Measurement*, **61**, 3147–3157.

WIDJAJA, F., SHEE, C.Y., POIGNET, P. & ANG, W.T. (2009). FES artifact suppression for real-time tremor compensation. In *2009 IEEE International Conference on Rehabilitation Robotics*, 53–58, IEEE.

WIERTLEWSKI, M. & HAYWARD, V. (2012). Mechanical behavior of the fingertip in the range of frequencies and displacements relevant to touch. *Journal of biomechanics*, **45**, 1869–1874.

WIJK, U. & CARLSSON, I. (2015). Forearm amputees' views of prosthesis use and sensory feedback. *Journal of Hand Therapy*, **28**, 269–278.

WISITSORAAT, A., PATTHANASETAKUL, V., LOMAS, T. & TUANTRANONT, A. (2007). Low cost thin film based piezoresistive MEMS tactile sensor. *Sensors and Actuators A: Physical*, **139**, 17–22.

WITTEVEEN, H.J., RIETMAN, H.S. & VELTINK, P.H. (2014). Vibrotactile grasping force and hand aperture feedback for myoelectric forearm prosthesis users. *Prosthetics and orthotics international*, 204–212.

WU, J.Z., DONG, R.G., RAKHEJA, S., SCHOPPER, A. & SMUTZ, W. (2004). A structural fingertip model for simulating of the biomechanics of tactile sensation. *Medical engineering & physics*, **26**, 165–175.

WU, J.Z., WELCOME, D.E. & DONG, R.G. (2006). Three-dimensional finite element simulations of the mechanical response of the fingertip to static and dynamic compressions. *Computer methods in biomechanics and biomedical engineering*, **9**, 55–63.

XU, H., ZHANG, D., HUEGEL, J.C., XU, W. & ZHU, X. (2016). Effects of different tactile feedback on myoelectric closed-loop control for grasping based on electrotactile stimulation. *IEEE Transactions on Neural Systems and Rehabilitation Engineering*, **24**, 827–836.

XYDAS, N. & KAO, I. (1999). Modeling of contact mechanics and friction limit surfaces for soft fingers in robotics, with experimental results. *The International Journal of Robotics Research*, **18**, 941–950.

YAMADA, Y., MORIZONO, T., UMETANI, Y. & TAKAHASHI, H. (2005). Highly soft viscoelastic robot skin with a contact object-location-sensing capability. *IEEE Trans. Industrial electronics*, **52**, 960–968.

YANG, D., ZHAO, J., GU, Y., JIANG, L. & LIU, H. (2009). Estimation of hand grasp force based on forearm surface emg. In *Mechatronics and Automation, 2009. ICMA 2009. International Conference on*, 1795–1799, IEEE.

YOUSEF, H., BOUKALLEL, M. & ALTHOEFER, K. (2011). Tactile sensing for dexterous in-hand manipulation in roboticsa review. *Sensors and Actuators A: physical*, **167**, 171–187.

ZHAO, H., OBRIEN, K., LI, S. & SHEPHERD, R.F. (2016). Optoelectronically innervated soft prosthetic hand via stretchable optical waveguides. *Science Robotics*, **1**, 1–10.

ZIEGLER-GRAHAM, K., MACKENZIE, E.J., EPHRAIM, P.L., TRAVISON, T.G. & BROOKMEYER, R. (2008). Estimating the prevalence of limb loss in the united states: 2005 to 2050. *Archives of physical medicine and rehabilitation*, **89**, 422–429.

Appendix A

Publications

A.1 Journal Papers

1. **Li, K.**, BOYD, P., Y., ZHOU, ZHAO, J. & LIU, H. (2018). Electrotactile Feedback in a Virtual Hand Rehabilitation Platform: Evaluation and Implementation. *IEEE Transactions on Automation Science and Engineering*. (Accepted, DOI: 10.1109/TASE.2018.2882465)

2. **Li, K.**, FANG, Y., ZHOU, ZHAO, J. & LIU, H. (2018). Haptics Model for Human Fingertips Based on Gaussian Distribution. *Journal of Intelligent & Fuzzy Systems*. (Accepted)

3. **Li, K.**, FANG, Y., ZHOU, Y. & LIU, H. (2017). Non-invasive stimulation-based tactile sensation for upper-extremity prosthesis: a review. *IEEE Sensors Journal*, 17(9), 2625-2635.

4. ZHOU, Y., FANG, Y., GUI, K., **Li, K.**, ZHANG, D. & LIU, H. (2018). sEMG Bias-driven functional electrical stimulation system for upper-limb stroke rehabilitation. *IEEE Sensors Journal*, 18(16), 6812-6821.

5. ZHOU, Y., LIU, J., ZENG, J., **Li, K.** & LIU, H. (2018). sEMG Bias-driven functional electrical stimulation system for upper-limb stroke rehabilitation. *Science China-Technological Sciences*. (Accepted)

6. FANG, Y., ZHOU, D., **Li, K.** & LIU, H. (2017). Interface prostheses with classifierfeedback-based user training. *IEEE transactions on biomedical engineering*, 64(11), 2575-2583.

A.2 Conference Papers

1. Zhou, Y., Fang, Y., Zeng, J., **Li, K.** & Liu, H. (2018).A Multi-channel EMG-Driven FES Solution for Stroke Rehabilitation. *11th International Conference Intelligent Robotics and Applications (ICIRA)*, 235-243.

2. FANG, Y., ZHOU, D., **Li, K.**, JU, Z. & LIU, H. (2017). A force-driven granular model for EMG based grasp recognition. *IEEE International Conference on Systems, Man, and Cybernetics (SMC)*, 2939-2944.

Appendix B

Research Ethics

FORM UPR16

Research Ethics Review Checklist

Please include this completed form as an appendix to your thesis (see the Research Degrees Operational Handbook for more information

Postgraduate Research Student (PGRS) Information		**Student ID:**	794182
PGRS Name:	Kairu Li		
Department:	School of Computing	**First Supervisor:**	Prof. Honghai Liu
Start Date: (or progression date for Prof Doc students)	**1 Oct 2015**		
Study Mode and Route:	Part-time ☐ Full-time ☒	MPhil ☐ PhD ☒	MD ☐ Professional Doctorate ☐

Title of Thesis:	Electrotactile Feedback for Sensory Restoration: Modelling and Application
Thesis Word Count: (excluding ancillary data)	31453

If you are unsure about any of the following, please contact the local representative on your Faculty Ethics Committee for advice. Please note that it is your responsibility to follow the University's Ethics Policy and any relevant University, academic or professional guidelines in the conduct of your study

Although the Ethics Committee may have given your study a favourable opinion, the final responsibility for the ethical conduct of this work lies with the researcher(s).

UKRIO Finished Research Checklist:
(If you would like to know more about the checklist, please see your Faculty or Departmental Ethics Committee rep or see the online version of the full checklist at: http://www.ukrio.org/what-we-do/code-of-practice-for-research/)

a) Have all of your research and findings been reported accurately, honestly and within a reasonable time frame?	YES ☒ NO ☐
b) Have all contributions to knowledge been acknowledged?	YES ☒ NO ☐
c) Have you complied with all agreements relating to intellectual property, publication and authorship?	YES ☒ NO ☐
d) Has your research data been retained in a secure and accessible form and will it remain so for the required duration?	YES ☒ NO ☐
e) Does your research comply with all legal, ethical, and contractual requirements?	YES ☒ NO ☐

Candidate Statement:

I have considered the ethical dimensions of the above named research project, and have successfully obtained the necessary ethical approval(s)

Ethical review number(s) from Faculty Ethics Committee (or from NRES/SCREC):	TECH 2018 - K.L. - 01

If you have *not* submitted your work for ethical review, and/or you have answered 'No' to one or more of questions a) to e), please explain below why this is so:

Signed *(PGRS)*:	Kairu Li	**Date:** 7 Sep 2018

Technology Faculty Ethics Committee

ethics-tech@port.ac.uk

Date 26/04/18

Kairu Li
School of Computing

Dear Kairu,

Study Title:	Multi-channel electrotactile stimulation for sensory feedback in upper-extremity prosthesis
Ethics Committee reference:	TECH 2018 - K.L. - 01

The Ethics Committee reviewed the above application by an email discussion between the dates of 13/04/18 and 25/04/18.

Ethical opinion

The members of the Committee present gave a favourable ethical opinion of the survey on the basis described in the application and supporting documentation.

Conditions of the favourable opinion

Conditions

In the participant information sheet, the information on The Head of Department and the University Complaints officer needs to be included as in the template. Also the funding information needs to be included.

Recommendations: (You should give these due consideration but there is no obligation to comply or respond)

The applicant is encouraged to check the templates and confirm that there is any other missing information that needs to be provided in the forms.

The favourable opinion of the EC does not grant permission or approval to undertake the research. Management permission or approval must be obtained from any host organisation, including University of Portsmouth, prior to the start of the study.

Summary of discussion at the meeting

The application was given a favourable opinion by the reviewers. The reviewers were complimentary about the clarity and comprehensiveness of the application form.

Documents reviewed

The documents reviewed at the meeting were:

Document	*Version*	*Date*
Application	V1	26/3/18
Participant Information Sheet	None identified	26/3/18
Invitation Letter	None identified	26/3/18
Debrief Sheet	None identified	26/3/18
Consent Form	None identified	26/3/18

Statement of compliance

The Committee is constituted in accordance with the Governance Arrangements set out by the University of Portsmouth

After ethical review

Reporting requirements

The attached document acts as a reminder that research should be conducted with integrity and gives detailed guidance on reporting requirements for studies with a favourable opinion, including:

- Notifying substantial amendments
- Notification of serious breaches of the protocol
- Progress reports
- Notifying the end of the study

Feedback

You are invited to give your view of the service that you have received from the Faculty Ethics Committee. If you wish to make your views known please contact the administrator ethics-tech@port.ac.uk

University of Portsmouth
Faculty of Technology

Please quote this number on all correspondence: TECH 2018 - K.L. - 01

Yours sincerely and wishing you every success in your research

Professor John Williams

Chair Technology FEC

Email: ethics-tech@port.ac.uk